Recombinant Production of Aβ$_{1\text{-}42}$ Peptide and Analysis of Interactions between Aβ$_{1\text{-}42}$ and Peptide Inhibitor NanoParticles (PINPs) Developed as a Potential Novel Treatment for Alzheimer's Disease

By

Michael Sherer

BSc (Hons) Biological Sciences

A thesis presented for the degree of

Master of Science (By Research)

In

The Division of Biomedical and Life Sciences

Lancaster University

August 2015

Table of Contents

Acknowledgements

There are a number of people that I would like to thank for enabling me to undertake and complete this project.

Firstly, I would like to thank my family for their consistant support throughout the duration of this project. Their unwavering support ensured that I was able to complete this project and it is something that I appreciate and I am hugely grateful for.

Secondly I would like to thank David Allsop, Nigel Fullwood and Mark Taylor for their advice and assistance throughout this project. The input from these individuals has been greatly appreciated and has enabled me to develop a range of skills and overcome numerous challenges whilst undertaking this project.

Abbreviations Used

α2M	α2-macroglobulin
Aβ	Amyloid β peptide
Aβ$_{1-40}$	40 amino acid form of the Aβ peptide
Aβ$_{1-42}$	42 amino acid form of the Aβ peptide
A280	Absorbance reading measured using a wavelength of 280 nm
a7nAChRs	α7 class of Nicotinic Acetylcholine Receptors
Ach	Acetylcholine
AD	Alzheimer's Disease
ADAM	A Disintegrin and Metalloproteinase
ADE	Amyloid Degrading Enzyme
AMPAR	α-amino-3-hydroxy-5-methyl-4-isoxazole Receptor
APH1	Anterior Pharynx Defective 1
ApoE	Apolipoprotein E
APP	Amyloid Precursor Protein
APP$_s$	Shortened form of the Amyloid Precursor Protein produced following cleavage of APP during the amyloidogenic pathway of APP cleavage.
APP$_s$-α	Shortened form of the Amyloid Precursor Protein produced following cleavage of APP during the non-amyloidogenic pathway of APP cleavage.
BBB	Blood Brain Barrier
BDNF	Brain Derived Neurotrophic Factor
CamKII	Calcium/Calmodulin dependent Kinase II
CI	Cholinesterase Inhibitor
CREB	cAMP Response Element Binding protein

CSF	Cerebrospinal Fluid
dH₂O	Distilled water
DSPE	1,2-Distearoyl-*sn*-glycero-3-phosphoethanolamine
DMT	Disease Modifying Therapy
EAAT	Glutamate Amino Acid Transporter
ELISA	Enzyme-Linked Immunosorbent Assay
EM	Electron Microscope
ERK	Extracellular signal Related Kinase
FBD	Familial British Dementia
FDD	Familial Danish Dementia
FDG	Fluorodeoxyglucose
GABA	Gamma-Aminobutyric-Acid
GLAST	Glutamate-Aspartate Transporter
GLT-1	Glutamate Transporter 1
H₂O₂	Hydrogen Peroxide
HFIP	Hexafluoroisopropanol
HPLC	High Performance Liquid Chromatography
HRP	Horseradish Peroxidase
IMAC	Immobilized Metal-ion Affinity Chromatography
IPTG	Isopropyl β-D-1-thiogalactopyranoside
KPI	Kunitz Protease Inhibitory (domain)
KPI-APP	APP containing a KPI domain
LRP	Lipoprotein Receptor-related Protein
LTP	Long Term Potentiation
MAP	Microtubule Associated Protein
MCI	Mild Cognitive Impairment

MLV	Multilamellar Vesicle
MMP-9	Matrix Metalloproteinase 9
MPS	Mononuclear Phagocyte System
MW	Molecular Weight
NFT	Neurofibrillary Tangle
Ni-NTA	Nickel-Nitriloacetic Acid
NMDAR	N-methyl-D-aspartate Receptor
NPS	Neuropsychiatric Symptoms
•OH	Hydroxyl Radical
PAGE	Polyacrylamide Gel Electrophoresis
PB	Phosphate Buffer
PB2S	PBS containing twice the salt concentration of standard PBS
PBS	Phosphate Buffered Saline
PBS$^+$	Modified PBS (see methods for details)
PEG	Polyethylene Glycol
PEG-PE	Polyethylene Glycol-Phosphatidylethanolamine
PEN-2	Presenilin Enhancer 2
PET	Positron Emission Tomography
PHF	Paired Helical Filament
PiB	Pittsburgh Compound B
PINPs	Peptide Inhibitor NanoParticles
PTA	Phosphotungstic Acid
rAβ$_{1\text{-}42}$	Recombinant Aβ$_{1\text{-}42}$
RAGE	Receptor for Advanced Glycation End products
ROS	Reactive Oxygen Species
SDS	Sodium-Dodecyl Sulphate

SGL	Second Generation Liposome
SSRI	Selective Serotonin Reuptake Inhibitor
T2DM	Type 2 Diabetes Mellitus
TAT	Trans-acting Activator of Transcription
TEM	Transmission Electron Microscopy
TEV	Tobacco Etch Virus
ThT	Thioflavin T
UCH	Ubiquitin C-terminal Hydrolase
ULV	Unilamellar Vesicle
ZnT3	Zinc Transporter 3 protein

List of Figures

List of Tables

Name: **Michael Sherer**

Degree: **BSc (Hons)**

Title of thesis: **Recombinant Production of Aβ$_{1\text{-}42}$ Peptide and Analysis of Interactions between Aβ$_{1\text{-}42}$ and Peptide Inhibitor NanoParticles (PINPs) Developed as a Potential Novel Treatment for Alzheimer's Disease**

A thesis presented for the degree of: **Master of Science (By Research)**

In The Division of Biomedical and Life Sciences, Lancaster University, August 2015

Abstract

This study addressed two main aims relating to the Aβ$_{1\text{-}42}$ peptide – widely demonstrated to play a key role in the pathogenesis of Alzheimer's Disease (AD). Aβ$_{1\text{-}42}$ is an amyloid peptide that readily self-associates forming neurotoxic aggregates. With the primary risk factor for AD being age, and ageing populations increasing, the need for research into methods of reducing the levels of Aβ$_{1\text{-}42}$ aggregates has never been greater. The first aim of this study was to recombinantly produce the Aβ$_{1\text{-}42}$ peptide using a previously published protocol in order to produce stocks for future experimental use. Producing Aβ$_{1\text{-}42}$ recombinantly results in less peptide variability than occurs via peptide synthesis, and is a much cheaper source of the peptide than commercial procurement. The peptide was expressed by induction of *Escherichia coli* to express a fusion protein encoding the Aβ$_{1\text{-}42}$ peptide in addition to specific regions necessary for purification. Analysis of the purified Aβ$_{1\text{-}42}$ peptide by transmission electron microscopy demonstrated that the peptide was able to self-associate forming a variety of structures characteristic of Aβ$_{1\text{-}42}$ aggregation as illustrated in the literature. The second aim of the study was to evalauate the effect of Peptide Inhibitor NanoParticles (PINPs) upon Aβ$_{1\text{-}42}$ aggregation. PINPs are second-generation liposomes with the RI-OR2-TAT peptide attached to the surface. RI-OR2-TAT has been found previously to reduce Aβ$_{1\text{-}42}$ aggregation in mouse models of AD. Analysis of the effect of PINPs upon Aβ$_{1\text{-}42}$ aggregation

was performed using transmission electron microscopy and fluorescence based assays with PINPs being found to directly bind early and late stage $A\beta_{1\text{-}42}$ aggregates and reduce levels of aggregation. Based on the findings of this study, amendments to the $A\beta_{1\text{-}42}$ production protocol are proposed and it is recommended that PINPs be carried forward into clinical trials as a potential treatment option for AD.

Chapter 1 – Introduction

1.1 - Introduction to AD

1.1.1 - The First Recognised Case of AD

In 1907, Alois Alzheimer reported the case of Auguste Deter - a 51-year-old female patient at an asylum for the insane in Frankfurt who suffered from deliriousness, disorientation and impaired memory. He noted that her condition did not exhibit symptoms which would enable classification into other known mental illnesses and that her condition had resulted in progressive deterioration from normal health to her delirious and helpless state (Alzheimer, 1907; Stelzmann et al., 1995). Another key observation made by Alzheimer was that the patient suffered substantial memory loss in a short space of time. In spite of these profound mental symptoms, Alzheimer reported that Deter's ability to walk or use her hands had been unaffected by her condition (Alzheimer, 1907). Following her death, Alzheimer performed a histological analysis of Deter's brain finding evenly spread brain atrophy. Further examination of specimens of the subject's brain showed profound abnormalities of the neurofilaments in comparison with what he had previously encountered as well as 'miliary foci' (now referred to as senile plaques) located extracellularly (Alzheimer, 1907; Tanzi & Bertram, 2005). Deter was suffering from what is now referred to as AD.

1.1.2 - Clinical Features of AD

AD is the leading cause of dementia, responsible for up to 80% of all cases. Dementia refers to a set of symptoms which accompany the loss of neuronal cells or when such cells function abnormally (Thies & Bleiler, 2013). The major risk factor for AD is age and increasingly ageing populations in many contries around the world has increased the need for research into effectives treatments for this disease. Data from the 2010 United States consensus indicated that 5.2 million Americans suffered from AD (Thies & Bleiler, 2013), with only 4% (0.2

million) under the age of 65 (early onset) (Alzheimer's Association, 2006), meaning that the remaining 5 million sufferers (96%) were over the age of 65 (late onset) (Hebert et al., 2013). AD causes multiple symptoms such as impaired memory, cognitive decline, changes in behaviour and difficulty communicating. Neuropsychiatric symptoms such as hallucinations and depression are also common features of AD (Yiannopoulou & Papageorgiou, 2013). An example of an instance of impaired memory resulting from AD is reported in Alois Alzheimer's 1907 paper where he notes that during assessment his patient – Auguste Deter – was unable to remember the word 'cup' and instead referred to the item as a 'milk-pourer' (Alzheimer, 1907; Stelzmann et al., 1995). AD is a chronic, progressive disease and therefore eventually leads to death of the individual. The rate of progression of the disease varies between individuals although during the latter stages of the disease, many sufferers require assistance with 'activities of daily living' such as dressing, preparing meals and washing (Thies & Bleiler, 2013). During the final stages of disease sufferers often have difficulty walking and memory has deteriorated so severely that they are unable to remember loved ones or perform everyday tasks. At this point the sufferers are usually bedbound and receive constant care (Thies & Bleiler, 2013). This frailty usually results in the contraction of infections such as pneumonia, which is often (along with AD) responsible for the death of the individual (Thies & Bleiler, 2013).

1.1.3 - Pathological Features of AD

In addition to the clinical features of AD that have been identified, there are also characteristic pathological features present in disease sufferers (Figure 1.1). These pathological features include senile (or neuritic) plaques, neurofibrillary tangles with gliosis, inflammation and neuronal loss (Masters et al., 1985). Neuronal loss is particularly apparent in the basal forebrain where many cholinergic neurons are lost due to AD (Yan & Feng, 2004). There is also a substantial deposition of insoluble amyloid in the brain and therefore this disease can be referred to as an amyloidosis. There are multiple types of amyloidosis

that affect humans such as the prion disease Creutzfeldt-Jakob disease, Parkinson's disease, as well as other forms of dementia such as Familial British dementia (FBD) and Familial Danish dementia (FDD) (Ghiso & Frangione, 2002). In addition to the aforementioned amyloidoses that affect the brain, there are also other forms of amyloidosis that affect other regions of the body such as pancreatic islets in Type 2 Diabetes Mellitus (T2DM) (due to accumulation of the amylin peptide) (Westermark et al., 2011). AD is a form of amyloidosis where there is localised deposition of the Amyloid Beta (Aβ) peptide in the brain and central nervous system and can thus be referred to as a cerebral amyloidosis (Ghiso & Frangione, 2002).
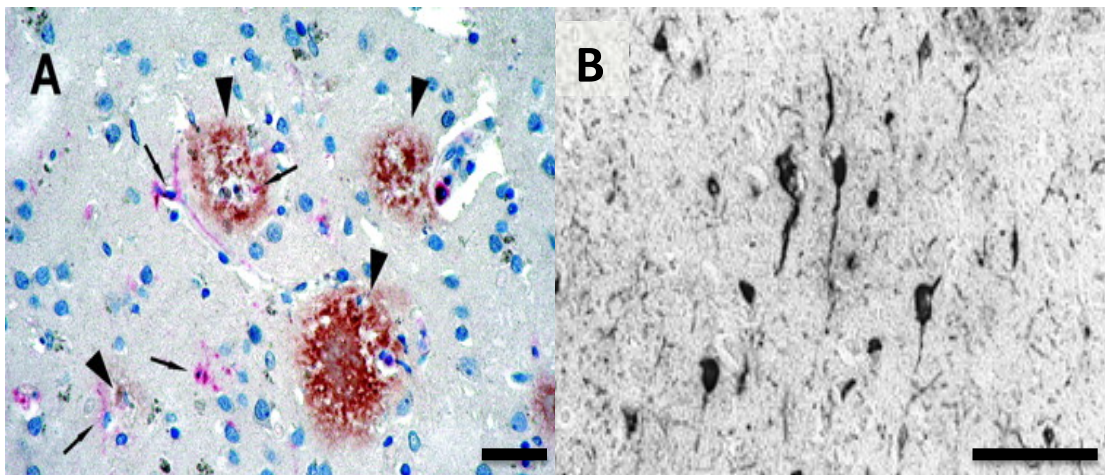
Figure 1.1 – Pathological hallmarks of AD imaged from the brains of AD sufferers. 'A' shows the presence of senile plaques (arrowhead) and activated microglia (thin arrow). 'B' shows a number of neurofibrillary tangles (arrows). Figures adapted from Bennett et al., 2004 and Liu et al., 2005.

Senile plaques (Figure 1.1A) are microscopic focal points of amyloid deposition surrounded by the processes of injured neuronal cells (Selkoe, 2001), with plaques usually spherical in appearance. The Aβ peptides (the amyloid component of the senile plaques) are deposited extracellularly to form these plaques and individual soluble Aβ monomers or oligomers aggregate to form insoluble fibrils of Aβ (Haass & Selkoe, 2007). The neuronal cells possessing these injured processes show marked differences in their ultrastructure in comparison to healthy cells i.e. possessing significantly larger lysosomes and increased

numbers of mitochondria (Selkoe, 2001). The cell processes contributing to the senile

plaques may originate from neurons of multiple neurotransmitter classes and as a result, AD

sufferers show a range of cognitive deficiencies that are a direct consequence of the

interruption or improper functioning of these various neurotransmitter systems (Selkoe,

2001). Surrounding and also embedded within the senile plaques are microglial cells, with

astrocytes usually found situated around the perimeter of the plaques. The activated

microglial cells display characteristic antigens that represent activation such as CD45, with

approximately 70% of these cells located within the neuropil and the remaining 30% located

within the senile plaques (Masliah et al., 1992; Selkoe, 2001).

Neurofibrillary tangles (NFTs) (Figure 1.1B) are also found in numerous brain regions affected

by AD. These tangles are found intracellularly within neuronal cells, in contrast to senile

plaques, which are found extracellularly. Neuronal cells, like many other cells contain

microtubules and their assembly is regulated by the presence of microtubule associated

proteins (MAPs) and their respective level of phosphorylation (Sloboda et al., 1975;

Mandelkow et al., 2007). One of these MAPs is known as 'Tau' (Weingarten et al., 1975),

which plays a role in regulating the stability of microtubules by binding to tubulin and

preventing depolymerisation, particularly in neuronal cell processes such as axons (Drubin &

Kirschner, 1986; Mandelkow et al., 2007). Along with senile plaques, NFTs are characteristic

neuropathological features of AD. In AD, NFTs are present as large bundles of ~10 nm fibres

occupying large volumes of the cytoplasm within neuronal cells (Selkoe, 2001). These fibres

are often found in pairs, associated in a helical manner and are therefore termed paired

helical filaments (PHFs) although straight fibres are also present along with PHFs (Selkoe,

2001). The confirmation of Tau as a component of NFTs came following a series of

investigations where the PHFs were treated with solvents or proteases followed by analysis

of their electrophoretic migration which revealed a higher molecular weight protein than

was found in brains which did not suffer from AD (Lee et al., 1991; Kondo et al., 1988;

Selkoe, 2001). Using in vitro dephosphorylation of the Tau protein, the migration of the protein was very similar to that of Tau from unaffected brains. It is now known that the Tau found in PHFs is abnormal in the senses that it is hyperphosphorylated, aggregated and truncated (Metcalfe & Figueiredo-Pereira, 2010). The affinity of hyperphosphorylated forms of Tau for microtubules is reduced, leading to decreased stability of the microtubules (Anand et al., 2014). Therefore the hyperphosphorylated form of Tau results in aggregation and formation of PHFs with a resulting loss of the ability of the Tau proteins forming the PHFs to bind and stabilize microtubules (Anand et al., 2014). As microtubules have many important cellular functions such as contributing to cellular organisation, establishing appropriate morphology of axons and cellular growth, sufficient stabilization by Tau is critical (Anand et al., 2014). Therefore the decreased stabilization of microtubules within neurons contributes to the neuronal loss associated with AD (Anand et al., 2014).

Oxidative damage and inflammation are also important processes that contribute towards AD pathology. The levels of products resulting from oxidation of macromolecules such as proteins, nucleic acids and lipids has been found to be increased in the brains of individuals suffering from AD (Zhao & Zhao, 2013).

1.2 - Production of Aβ

1.2.1 - What is Aβ?

The amyloid fibrils seen in AD brains are formed from Aβ peptide, which is capable of self-assembly to form filaments (Tycko, 2004). Like other amyloid fibrils, Aβ fibrils consist of many cross β-sheet structures that run perpendicular to the length of the fibril (Glenner & Wong, 1984). The fibrils can range in length from approximately 0.1-10 μm with a width of ~10 nm (Tycko, 2004). In addition to being found within senile plaques, Aβ deposits can also be detected in the walls of cerebral blood vessels and in some cases this can lead to haemorrhage (Selkoe et al., 1987). The Aβ peptide itself consists of between 39 and 43

amino acids and these different isoforms of the peptide result from proteolytic cleavage of the much larger Amyloid Precursor Protein (APP) (Sisodia & Price, 1995). Different species of Aβ are produced known as Aβ40 and $Aβ_{1-42}$ with the number following 'Aβ' corresponding to the number of residues in the peptide. Aβ40 is said to be the major species of Aβ with $Aβ_{1-42}$ referred to as the minor species, usually present at a ratio of 9:1 (Qahwash et al., 1993; Allsop & Mayes, 2014). $Aβ_{1-42}$ is more amyloidogenic than Aβ40 due to the extra 2 hydrophobic C terminal residues in this isoform, which increases its propensity to aggregate. The extra residues in $Aβ_{1-42}$ consist of Isoleucine at position 41 and Alanine and position 42 (Lazo et al., 2005). The highly conserved APP gene is located on the long arm of chromosome 21 at position 21q21.3 and is approximately 400kb in length (Blanquet et al., 1987; Goldgaber et al., 1987; Lamb et al., 1993). APP is a type 1 transmembrane glycoprotein, present in multiple different tissues throughout the body (Kang et al., 1987), with different isoforms produced by alternative splicing of the APP pre-mRNA (Sisodia & Price, 1995). Of the different isoforms of APP produced, those with 695 (Kang et al., 1987), 751 and 770 residues are the most common (Kitaguchi et al., 1988; Ponte et al., 1988; Selkoe, 2001). Although the exact function of APP has not been definitively determined, multiple roles for this protein have been postulated including metal ion homeostasis (Barnham et al., 2003), cell growth regulation (Small et al., 1994), intracellular calcium regulation (Mattson et al., 1993) and the axonal transport of intracellular vesicles (Gunawardena & Goldstein, 2001; Allsop & Mayes, 2014).

1.2.2 - APP Cleavage

Cleavage of APP can occur down one of two pathways (Figure 1.2), which either lead to production of Aβ (amyloidogenic cleavage pathway), or do not lead to the production of Aβ (non-amyloidogenic cleavage pathway) (Allsop & Mayes, 2014). The Aβ peptide region of APP consists of 12-14 residues in the transmembrane domain and 28 residues of the extracellular side of the protein (Blennow et al., 2006). The difference in products of the two

pathways is a result of cleavage at different APP sites. Both pathways consist of consecutive cleavage events, with the second cleavage carried out by γ-secretase. It is therefore the initial cleavage event that determines whether Aβ will be produced. In the amyloidogenic pathway, the initial cleavage is performed by β-secretase which cleaves APP outside of the Aβ region, forming the N-terminus of Aβ and a shortened form of APP (APP_s) known as APP_s-β (Selkoe, 1998; Seubert et al., 1993). The second cleavage event in this pathway (performed by γ-secretase) separates the Aβ peptide and a 99 residue C terminal fragment, thus releasing Aβ (Selkoe, 1998). The non-amyloidogenic pathway begins with cleavage of APP by α-secretase between the Lys_{16} and Leu_{17} residues in the Aβ region, thus preventing the formation of Aβ (Allinson et al., 2003). This cleavage releases another shortened version of APP (APP_s-α). A recent study using mouse models of AD has reported that the release of APP_s-α following α-secretase cleavage exerts a neuro-protective effect and that Aβ oligomers act to oppose this effect (Jimenez et al., 2011). This neuroprotective action is initiated by the activation of insulin and/or IGF-1 receptors and the subsequent action of the PI3-Kinase pathway (Jimenez et al., 2011). The Aβ oligomers opposed this effect by inhibiting downstream phosphorylation in the PI3-Kinase pathway, which is essential for the neuroprotective effect induced by APP_s-α (Jimenez et al., 2011). Additionally α-secretase cleavage of APP results in the generation of the p3 N-terminal domain, with the subsequent cleavage by γ-secretase generating the p3 C terminal and an 83 residue C terminal fragment (Selkoe, 1998).
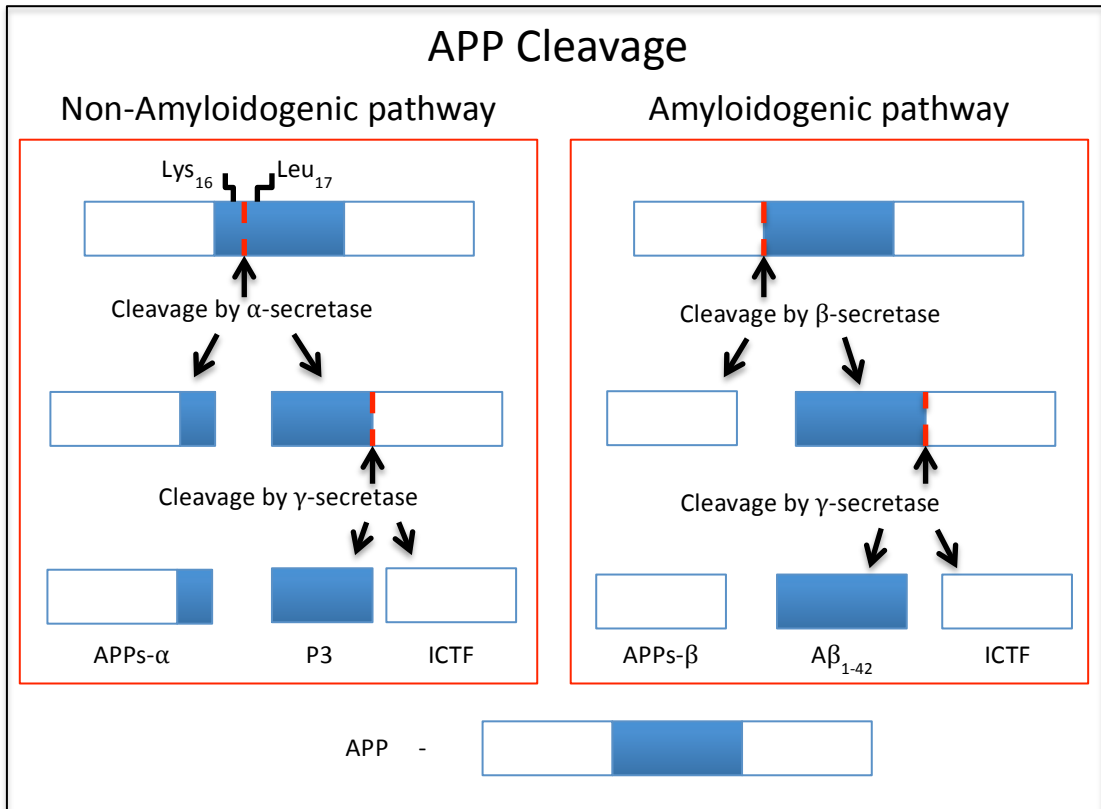
Figure 1.2 – APP Cleavage. Cleavage of APP can occur down the amyloidogenic pathway or the non-amyloidogenic pathway. The non-amyloidogenic pathway begins with cleavage of APP by α-secretase between Lys_{16} and Leu_{17} of the Aβ region of APP. This cleavage produces a shortened form of APP (APPs-α) and produces a C-terminal fragment which contains the N-terminal of the P3 protein. Cleavage of the C terminal fragment by γ-secretase forms the C-terminal of the P3 protein, resulting in formation of the P3 protein and a separate 83 residue intracellular C-terminal fragment (ICTF). The amyloidogenic pathway begins with cleavage of APP by β-secretase, which cleaves at the N terminal of the Aβ region of APP, forming the N terminal of the peptide and a shortened version of APP (APPs-β). Further cleavage by γ-secretase at the C terminal of the Aβ region releases the Aβ peptide in addition to an ICTF. ICTFs produced via both pathways are identical.

1.2.2.1 - APP cleavage by α-Secretase

The α-secretase(s) responsible for precluding the release of Aβ via the non-amyloidogenic pathway have not been definitively deduced. It is likely that rather than one enzyme being responsible for this activity, multiple enzymes may perform a similar catalytic function upon

APP at the α-secretase site exhibiting a degree of redundancy in their actions (Allinson et al., 2003). The enzymes responsible for the α-secretase cleavage event are thought to be members of the ADAM (a disintegrin and metalloproteinase) family such as ADAM9, ADAM10 and TACE although current evidence suggests that in regard to AD, ADAM10 is predominantly involved in α-secretase activity (Allsop & Mayes, 2014; Allinson et al., 2003).

1.2.2.2 - APP cleavage by β-Secretase

β-secretase (aka BACE1 (Vassar et al., 1999), memapsin 2 (Lin et al., 2000)) is a transmembrane protein consisting of 501 amino acids and is primarily expressed in neurons (Sinha et al., 1999; Vassar et al., 2009). β-secretase exhibits greatest activity at low pH and is resultantly located within acidic cellular compartments, with luminal exposure of the enzyme active site (Vassar et al., 2009). It has also been found that in AD brains, the levels and activity of β-secretase can be much greater than in non-AD brains, therefore promoting the release of Aβ (Fukumoto et al., 2002; Vassar et al., 2009). Various studies have attributed this increase in β-secretase activity to a stress response triggered by factors such as neuronal injury, increased levels of reactive oxygen species and apoptosis (Vassar et al., 2009). A number of studies investigating β-secretase activity have found that in addition to cleaving APP, this enzyme also has a number of other substrates, which like APP, are all transmembrane proteins (Vassar et al., 2009).

1.2.2.3 - APP cleavage by γ-Secretase

γ-secretase is a transmembrane protein complex consisting of multiple subunits which function to facilitate proteolysis within the hydrophobic lipid bilayer of the plasma membrane (Smolarkiewicz et al., 2013). The γ-secretase multi-pass transmembrane complex consists of nicastrin, presenilin, APH1 (anterior pharynx defective-1), PEN2 (presenilin enhancer-2) and is part of a family of proteins referred to as intramembrane cleaving proteases (Allsop & Mayes, 2014; Smolarkiewicz et al., 2013; Kimberly et al., 2003). These

subunits are produced and assembled in the endoplasmic reticulum (Smolarkiewicz et al., 2013).The γ-secretase complex has over 60 substrates and in addition to cleaving APP, the γ-secretase complex is also capable of cleaving the notch protein, releasing the notch intracellular domain which acts a signalling molecule in multiple different processes (De Strooper et al., 1999; Smolarkiewicz et al., 2013). Of the four subunits which comprise the γ-secretase complex, presenilin is the only catalytic subunit, representing a difference to other members of the intramembrane cleaving proteases (Smolarkiewicz et al., 2013). A key difference between the cleavage process of the γ-secretase complex compared with α- and β-secretase cleavage is that γ-secretase cleavage is dependent on recognition of the conformation of the juxtamembrane region rather than a specific amino acid sequence as is the case with α- and β–secretase cleavage (Smolarkiewicz et al., 2013).

1.3 – Aβ aggregation

Following cleavage of the APP protein by the β- and γ-secretases – resulting in the formation of Aβ monomers – self-association between monomers leads to the formation of higher order aggregations of Aβ peptide. Binding of the Aβ peptides occurs via residues 16-22 of the peptide, which consists of the amino acid sequence KLVFFAE (Tjernberg et al., 1996). This self-association of Aβ produces aggregates of varying sizes, from monomers through to oligomers, protofibrils and insoluble amyloid fibrils. The importance of accurately understanding the aggregation characteristics of the Aβ peptide is clear, as disease modifying treatments that target this peptide must interfere with the toxicity that results from Aβ aggregation. In order to determine the mechanisms of Aβ aggregation that results in the formation of various Aβ aggregates, a substantial amount of resources have been invested in such investigations in numerous laboratories worldwide. Although the exact nature of the formation of different Aβ aggregates has not yet been definitively determined, current evidence suggests that there are at least two pathways responsible for the formation of higher order Aβ aggregations (Allsop & Mayes, 2014). These two pathways that are

thought to be responsible for the different sized Aβ aggregations are termed 'on-pathway' and the 'off-pathway'. These pathways are named based on the formation of the elongated insoluble Aβ fibrils, with 'on-pathway' resulting in fibril formation and 'off-pathway' leading to alternative aggregations (Schnabel, 2011). The 'off-pathway' route proceeds following the cleavage of APP, which produces monomeric Aβ that begins to aggregate, forming oligomers stable oligomers that will not go on to produce fibrils (Allsop & Mayes, 2014). The 'on-pathway' route on the other hand, follows a different path than the 'off-pathway'. Following monomer formation, Aβ aggregates form oligomers ranging from dimers and trimers to higher order oligomers, which are able to form a nucleus for further aggregation. Formation of this nucleus then enables other Aβ monomers to aggregate leading to the growth of protofibrils and ultimately the mature insoluble Aβ fibrils which comprise a key component of senile plaques found in the brain of AD sufferers (Schnabel, 2011, Allsop & Mayes, 2014). The process of aggregation of monomers into mature fibrils can be split into 3 phases, at which different levels of Aβ aggregates will be present – lag, growth and plateau phases (Figure 1.3).
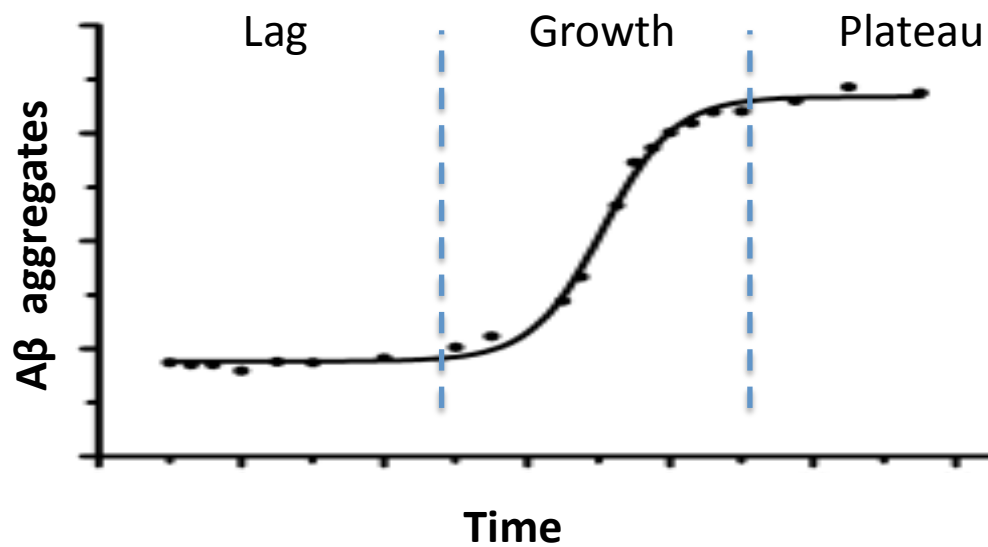
Figure 1.3 – Kinetics of Aβ aggregation. Graphical representation of Aβ aggregation over time typically produces a sigmoidal curve. The curve can be split into 3 phases: lag, growth and plateau (Arosio et al., 2013). Figure adapted from Bartolini et al., 2007.

The aggregation of the Aβ monomers into higher order structures occurs over 3 different phases with different rates of aggregation. Initially when a solution contains solely monomers, primary nucleation is the only possible method of growth (Arosio et al., 2013). This is the process of binding of monomers and elongation of the aggregate. This stage is termed primary nucleation and is a slow process as monomers contributing to the primary nuclei can also dissociate (Arosio et al., 2013). Another method is termed secondary nucleation and occurs where elongated aggregates formed from multiple monomers are able to act as a nucleus for new Aβ aggregates. Secondary nucleation is a more rapid process than primary nucleation and therefore levels of amyloid structures increase greatly by this method of formation (Arosio et al., 2013). This is partly as a result of the positive feedback loop that is generated as levels of aggregates increase, providing yet more surfaces for secondary nucleation to occur (Arosio et al., 2013).

Whether a particular Aβ early aggregate will form a stable oligomer or will progress to form part of an insoluble mature fibril can be influenced by the interaction of the Aβ aggregate

with metal ions such as copper and zinc (Hane & Leonenko, 2014). Aβ aggregation in the presence of either of these metal ions has been found to occur at a faster rate than in their absence. This is due to the shortened (in the presence of zinc) or abolished (in the presence of copper) lag phase in which nucleation usually occurs prior to the formation of larger aggregates such as protofibrils and mature fibrils (Pedersen et al., 2011; Hane & Leonenko, 2014). Although different phases of Aβ aggregation may represent different nucleation methods, in reality the different nucleation methods are active throughout all phases of aggregation although in each phase a particular nucleation method may dominate.

1.4 - Aβ Removal

Just as levels of Aβ in the brain may increase following cleavage of the peptide from APP, Aβ can also be cleared, therefore Aβ levels begin to increase when formation of the peptide surpasses its clearance. Aβ can be cleared from the brain via the blood-brain-barrier (BBB) or by turnover of cerebrospinal fluid (CSF)(Shibata et al., 2000; Silverberg et al., 2003). However, clearance of Aβ via CSF turnover is thought to only account for between 10-15% of Aβ clearance, with the remaining removal being attributed to clearance via the BBB (Shibata et al., 2000; Zlokovic, 2004). There are two methods of clearance via the BBB; receptor mediated clearance of Aβ and degradation of Aβ (Tanzi et al., 2004).

1.4.1 - Receptor Mediated Removal - LRP

Receptor mediated removal occurs via the low-density lipoprotein receptor-related protein (LRP) which acts to transfer Aβ from the brain across the BBB and into the peripheral circulation (Tanzi et al., 2004). The LRP is a scavenger and signalling receptor, possessing a 515 kDa heavy chain capable of binding a number of ligands such as apolipoprotein E (apoE), APP, lactoferrin and α2-macroglobulin (α2M) among others (Tanzi et al., 2004; Zlokovic, 2004). The 85 kDa light chain of the LRP receptor is involved in intracellular signalling following phosphorylation on serine and tyrosine residues (Zlokovic, 2004). Shibata and

colleagues demonstrated the importance of LRP in facilitating Aβ efflux by treating mice with LRP antagonists, with a reduction in radiolabelled Aβ40 efflux as high as 90% compared to controls (Shibata et al., 2000; Tanzi et al., 2004). There is evidence to show that the Aβ peptide is able to bind directly to LRP and undergo efflux (Deane et al., 2004). However Aβ is able to form complexes with other LRP ligands such as α2M or apoE, which in turn bind LRP facilitating passage across the BBB (Tanzi et al., 2004). Building on the evidence of the direct interaction between Aβ and LRP, Deane et al. also reported findings that showed LRP bound Aβ40 with a higher affinity than the more toxic $Aβ_{1-42}$ and that Aβ concentrations >1 μM trigger proteasomal degradation of LRP (Deane et al., 2004). This reduction in LRP therefore results in greater concentrations of Aβ in brain interstitial fluid, thus contributing to the pathogenesis of Aβ (Shibata et al., 2000).

1.4.2 - Receptor Mediated Entry - RAGE

Another important receptor implicated in the pathogenesis of AD is the receptor for advanced glycation end products (RAGE). Unlike LRP, the activity of RAGE facilitates movement of Aβ from cerebral blood vessels into the brain (Makic et al., 1998; Deane et al., 2003). RAGE belongs to the immunoglobulin superfamily of receptors capable of binding multiple different ligands, including soluble Aβ, and acts to elicit cellular responses following ligand binding (Du Yan et al., 1996; Deane et al., 2003). RAGE is thought to be the main effector involved in transport of circulating Aβ into the brain, and the expression of this receptor is affected by its ligands (e.g. Aβ)(Zlokovic, 2004). As concentrations of RAGE ligands increase, there is greater expression of the receptor on endothelial cells of cerebral blood vessels. Therefore as Aβ levels in circulation increase, so too do levels of RAGE, resulting in increased transport of Aβ from circulation into brain interstitial fluid (Zlokovic, 2004).

1.4.3 - Proteolytic Degradation of Aβ

Another method of Aβ removal from the brain interstitial fluid via the BBB is by proteolytic degradation. The enzymes capable of degrading Aβ are known as amyloid degrading enzymes (ADEs) and the number of ADEs currently known has increased markedly over the past 15 years. Initially, the peptidolytic degradation of Aβ was attributed to 2 metalloendopeptidases known as isulysin and neprilysin, but now almost 20 ADEs have been identified with many (but not all) being members of the zinc metalloproteinases (Tanzi et al., 2004; Nalivaeva et al., 2012).

1.5 -The Amyloid Cascade Hypothesis

The amyloid cascade hypothesis has been the basis of research into AD for over 20 years. The hypothesis originally implicated the deposition of fibrillar Aβ as the initiating factor in AD, which initiated a cascade of events that ultimately lead to the characteristic features of AD such as senile plaques, neurofibrillary tangles and cognitive deficits (dementia) (Hardy & Allsop, 1991). Over the years the hypothesis has been modified as knowledge around AD has increased, but this model continues to drive research in this field to this day. At the most basic level, the hypothesis states that an imbalance between the production and removal of Aβ enables concentrations of this peptide to increase, thus leading to AD.

Aβ is a peptide cleaved from the APP protein and is found within human CSF and brains throughout the lifetime of every individual, showing that the mere presence of the peptide is not responsible for neuronal injury (Walsh & Selkoe, 2007). Monomeric Aβ (as it is produced) is not toxic, however the peptide has the ability to self-aggregate into larger structures that do exhibit toxic effects. Aβ is known to self-aggregate into soluble oligomers of various sizes and also into larger complexes such as fibrils, which are insoluble. Early research into the AD disease process confirmed that higher order structures than monomers were required for toxicity (Walsh & Selkoe, 2007). Aβ fibrils are components of senile plaques observed both

microscopically and macroscopically in human brains. As individuals with AD tend to have greater plaque counts than non-AD sufferers, the amyloid fibrils that formed these plaques were presumed as the toxic substance driving the disease process. However, as research into AD progressed, it was noticed that the correlation between the numbers of plaques in AD brains correlated poorly with the extent of cognitive deficits (Haas & Selkoe, 2007). These findings questioned the role of the Aβ fibrils in the disease process. As the use of more modern biochemical methods became available to study Aβ, the levels of smaller Aβ aggregates such as oligomers could be determined. These techniques were employed to investigate the correlation between levels of soluble oligomers and cognitive deficits in AD sufferers. The correlation of soluble oligomer levels and cognitive impairment was substantially improved compared with using plaque count (McLean et al., 1999), shifting the emphasis from fibrillar forms of Aβ to soluble oligomeric forms as the pathogenic agent in AD. Other complementary evidence exists which shows oligomers as having a greater combined surface area to induce neuronal damage than plaques and the ability of these oligomers to diffuse into synaptic clefts (Haas & Selkoe, 2007). Recently, further significant evidence of the role of Aβ in the AD disease process has been illustrated by the outcomes of phase 3 clinical trials using Solanezumab. Solanezumab is an antibody that recognises a portion of the Aβ peptide (epitope lies in the mid-domain of the peptide) and is thought to facilitate removal of the Aβ peptide from the brain (Liu-Seifert et al., 2015). Individuals treated with this immunotherapy experienced significantly less cognitive decline than their counterparts that received a placebo. This demonstrates that targeting the Aβ peptide enables significant modification of the disease process and therefore that the Aβ peptide is likely to be a significant causative factor in the development of symptoms associated with AD.

1.5.1 - Aβ associated memory loss

1.5.1.1 - Aβ affects long-term potentiation

Long-term potentiation (LTP) is the change in synaptic plasticity due to repeated stimulation of the postsynaptic neuron. LTP is involved in learning and memory and processes that affect LTP therefore affect an individual's capacity for learning and memory. Aβ oligomers have been found to inhibit the maintenance of LTP in the hippocampal region of the brain, which is primarily involved in the storage and maintenance of memory (Walsh et al., 2002). These oligomers have also been neutralized by anti-Aβ antibodies (which did not bind to monomeric of fibrillar forms of Aβ) and subsequently prevented their detrimental effects on LTP (Klyubin et al., 2005). These lines of evidence show that Aβ oligomers affect LTP and when they are neutralized their effect upon LTP is removed, proving that monomeric or fibrillar forms of Aβ are not responsible for memory loss. Aβ oligomers have also been shown to cause loss of synapses, which in turn is known to cause cognitive defects such as loss of memory and mood alterations - characteristic symptoms of AD. Shankar et al. demonstrated that at normal physiological concentrations, Aβ oligomers were sufficient to cause synaptic loss, which is a fundamental characteristic of AD brains along with senile plaques and neurofibrillary tangles (Shankar et al., 2007). In a study that investigated the hippocampal synapse to neuron ratio in non-AD individuals and AD sufferers, it was found that this ratio was reduced by 50% in AD sufferers compared with healthy individuals (Bertoni-Freddari et al., 1990).

1.5.1.2 - Synaptic action of Aβ

Elucidating the series of events leading to Aβ induced loss of synapses has been the subject of substantial research effort. It has been found that the electrical activity of neurons is able to induce greater levels of Aβ production (Kamenetz et al., 2003). The production of both $A\beta_{40}$ and $A\beta_{1-42}$ is under the control of neuronal electrical activity. This increase in electrical

activity has been found to affect β-secretase in such a way that the enzyme enhances the levels of Aβ produced. These increased levels of Aβ in turn caused a reduction in excitatory synaptic transmission (Kamenetz et al., 2003; Haas & Selkoe, 2007). These results were complemented by the finding that levels of Aβ in interstitial fluid correlated with synaptic activity (Cirrito et al., 2005; Haas & Selkoe, 2007). Aβ is able to reduce excitatory synaptic transmission by reducing the levels of NMDA (N-methyl-D-aspartate) or AMPA (α-amino-3-hydroxy-5-methyl-4-isoxazole) receptors present at the cell surface of neurons by binding to the α7 class of nicotinic acetylcholine receptors (a7nAChRs) (Haas & Selkoe, 2007; Palop & Mucke, 2010; Wang et al., 2013).

NMDA receptors (NMDARs) are ligand gated glutamate receptors which following activation open ion channels in the plasma membrane, facilitating the influx of Ca^{2+} (Wang et al., 2013). The downstream effect of the Aβ binding to a7nAChRs enables a LTP response but prevents maintenance of LTP (Haas & Selkoe, 2007). Binding of Aβ to a7nAChRs results in the internalisation of NMDARs and thus results in a reduction in Ca^{2+} uptake (Snyder et al., 2005; Wang et al., 2010). As well as reducing Ca^{2+} uptake, the binding of Aβ to the a7nAChRs has also been shown to induce the formation of NFTs and stimulate aggregation of intraneuronal Aβ (Nagele et al., 2002; Wang et al., 2003; Wang et al., 2013).
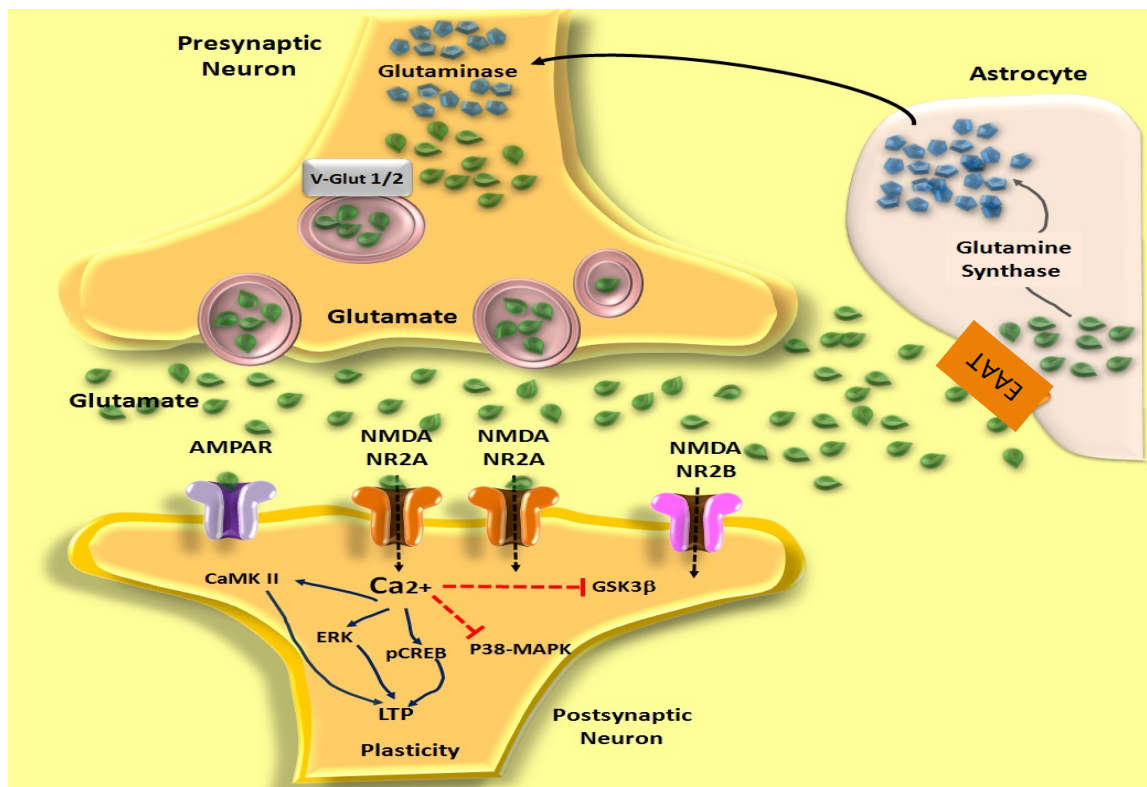
Figure 1.4 – Functioning of the glutamatergic system in a healthy brain. Glutamate stored in vesicles (V-Gluts) is released from the presynaptic neuron into the synaptic cleft where it binds to AMPA receptors (AMPAR) and NMDARs. Binding to NMDARs stimulates Ca^{2+} influx which activates downstream signalling pathways via Calcium/Calmodulin dependent kinase II (CaMKII), ERK and CREB which function in the establishment of long term potentiation and activation of anti-apoptotic mechanisms. Excess glutamate is taken up by astrocytes via glutamate amino acid transporters (EAAT) where it is converted to glutamine via glutamine synthase. Figure adapted from Campos-Peña & Meraz-Ríos, 2014.

In addition to affecting LTP, the action of Aβ is able to cause neuronal loss. NMDARs can be classified as either synaptic or extra-synaptic with regard to their location. As the name suggests, the synaptic NMDARs are located at the synapse whereas extra-synaptic NMDARs are located in different regions of the cell such as the cell body (Wang et al., 2013). The downstream activity following activation of NMDARs depends on the location of the NMDARs that are activated, with synaptic and extra-synaptic NDMARs having opposite effects with regard to cell survival (Wang et al., 2013). Additionally, activation of NMDARs has an effect upon Aβ production.

Activation of synaptic NDMARs occurs following release of presynaptic vesicles containing

the neurotransmitter glutamate, which bind NDMARs on the postsynaptic membrane,

enabling influx of Ca^{2+}. Following Ca^{2+} influx via synaptic NDMAR activation, a

neuroprotective signalling process occurs whereby activation of NMDARs increases signalling

to cAMP response element binding protein (CREB) which in turn up regulates production of

brain derived neurotrophic factor (BDNF) (Hardingham et al., 2002; Wang et al., 2013). BDNF

then stimulates extracellular signal regulated kinases (ERK) and thus promote cell survival

(Ivanov et al., 2006). The activation of extra-synaptic NMDARs activates a general CREB shut-

off pathway that prevents the up-regulation of BDNF production (Hardingham et al., 2002).

Thus overall, synaptic NMDARs promote neuronal survival by activating an anti-apoptotic

pathway (Figure 1.4), whereas extra-synaptic NMDARs promote neuronal death due to the

loss of mitochondrial membrane potential caused by glutamate toxicity (Figure 1.5)

(Hardingham et al., 2002). However, excitotoxicity can occur due to overstimulation of the

NMDAR receptors by glutamate, resulting in neuronal loss (Shah et al., 2008).

Figure 1.5 – Effect of Aβ at the synapse. The presence of Aβ at the synapase has the effect of inducing the endocytosis of NMDARs as well as inhibiting the uptake of glutamate by the astrocytes. This reduction in synaptic uptake of Aβ due to lower concentrationf of NMDARs and reduced uptake by astrocyes results in glutamate spillover. This occurs when glutamate diffuses from the synaptic clef and binds to extra-synaptic NMDARs, resulting in neuronal death (excitotoxicity). Abbreviations: Glutamate-Aspartate Transporter (GLAST), Glutamate Transporter 1 (GLT-1). Image adapted from Campos-Peña & Meraz-Ríos, 2014 and Wang et al., 2013.

Investigations into the levels of Aβ produced following activation of synaptic and extra-synaptic NMDARs found that stimulation of the synaptic NMDARs was associated with lower levels of Aβ production, in contrast to extra-synaptic NMDAR stimulation which increased Aβ levels (Wang et al., 2013). The activation of synaptic NMDARs has been found to decrease

the levels of Aβ produced by increasing the cleavage of APP by α-secretases (Hoey et al., 2009). These findings are supported by increases in Aβ production when α-secretase inhibitors or NMDAR antagonists are present (Hoey et al., 2009). These findings also indicate that basal level stimulation of the NMDARs acts to prevent the formation of Aβ (Verges et al., 2011). The activation of extra-synaptic NMDARs results in increased production of APP isoforms which possess a specific domain known as a Kunitz Protease Inhibitory (KPI) domain (KPI-APP), compared with APP isoforms which do not possess a KPI domain which are produced following synaptic NMDAR stimulation (Wang et al., 2013). Further studies have found that selective stimulation of synaptic NMDARs did not result in an increased level of ERK phosphorylation and Aβ in interstitial fluid, and no KPI-APP was detected (Bordji et al., 2010). This was not the case when extra-synaptic NMDARs were selectively stimulated as ERK phosphorylation does not occur (Hoey et al., 2009), and Aβ and KPI-APP levels are increased (Bordji et al, 2010). Interestingly, the increase in Aβ production following extra-synaptic NMDARs is not due to increased production of total APP mRNAs, rather a switch in production of APP to KPI-APP (Bordji et al., 2010). During synaptic NMDAR activation, downstream pathways increase the production of ADAM10, which as mentioned earlier is an α-secretase and therefore precludes the production of Aβ (Wan et al., 2012; Wang et al., 2013).

Furthermore, Aβ is able to inhibit a ubiquitin c-terminal hydrolase (UCH) enzyme which functions in labelling proteins for proteasomal degradation, and in doing so Aβ inhibits LTP (Haas & Selkoe, 2007). This inhibition of LTP contributes to the characteristic cognitive decline associated with AD.

1.5.2 - Metal ions and ROS in AD

Reactive oxygen species (ROS) are oxygen-containing molecules produced by aerobic cells (Pimentel et al., 2012). ROS are chemically reactive and can cause oxidative stress when their

production exceeds removal. Some species of ROS possess free electrons and are therefore referred to as free radicals. In 1999 Huang and colleagues found that the Aβ peptide was able to directly produce hydrogen peroxide (H_2O_2) and hydroxyl radicals ($\bullet OH$), which are both important ROS (Huang et al., 1999). ROS can damage macromolecules such as nucleic acids, proteins and lipids (Mayes et al., 2014), and the oxidation of these groups of macromolecules is increased in the brains of AD sufferers (Kontush, 2001). Both $Aβ_{1-40}$ and $Aβ_{1-42}$ are able to reduce metals however the increased ability of $Aβ_{1-42}$ compared with $Aβ_{1-40}$ to chelate metals means that $Aβ_{1-42}$ is more effective at reducing particular metals and leading to the production of ROS (Atwood et al., 2000a; Huang et al., 1999). This reducing ability is however also dependent on the efficiency of binding of a particular metal to the peptide (Kontush, 2001). As mentioned earlier, elevated ROS production may contribute to increased activity of the β-secretase enzyme, leading to increased production of Aβ (Vassar et al., 2009).

1.6 – Current methods of diagnosis and treatments

As mentioned, AD is a chronic progressive disease which results in neurodegeneration and decline in a range of cognitive functions. The nature of disease onset is insidious and it is estimated that the pathophysiological features of the disease such as amyloid deposition and Tau pathologies begin to develop decades before the onset of clinical symptoms that can be recognised as AD (Morris, 2004; Sperling et al., 2011). The time between the onset of AD pathophysiology and the onset of clinical symptoms is known as the preclinical phase of AD. Confirmation of AD can only currently be definitively determined by post-mortem identification of senile plaques and NFTs thus diagnosis during an individual's lifetime is regarded as 'suspected AD' with confirmation coming after the death of the individual (Judd, 2007).

Once an individual has been diagnosed with AD, there are a limited number of therapeutic options available to an individual. Treatments for AD can be split into two main classes; the first being 'symptomatic treatments' which aim to address the symptoms associated with the disease such as those caused by altered neurotransmitter signalling (e.g. ACh), with the second class being 'disease modifying treatments' which aim to impact upon disease progression such as stopping any further damage due to AD (Yiannopoulou & Papageorgiou. 2013). Currently there are no disease-modifying treatments available to AD sufferers, although there are some in various stages of clinical trials. It is hoped that future disease modifying treatments will be able to interact with the pathological features of AD brains e.g. NFTs and senile plaques, in order to modify the outcome of the disease.

1.6.1 – Diagnosis

1.6.1.1 – Mild cognitive impairment

Current criteria used to assist in the diagnosis of AD are based on significant cognitive decline of an individual. The initial decline is usually brought to the clinician's attention by the patient themselves, or an informant. This is the stage where the decline in cognitive ability is explained to the clinician and is the reason behind testing and diagnosis of mild cognitive impairment (MCI) (Albert et al., 2011). It is believed that if the diagnosis is made much earlier in disease progression, such as in the preclinical phase, therapeutic intervention may yield better results than is currently observed in individuals who have increased levels of cognitive decline (Petersen, 2004). A decline in cognitive function is a part of normal healthy ageing and therefore distinguishing the early stages of AD from normal ageing can be difficult. MCI is used to describe a condition in which individuals have a decline in cognition that is greater than expected for a person of their age, and is associated with the preclinical phase of AD. However it is important to note that with MCI the changes are much more subtle than those seen following diagnosis of AD, where the rate of decline is much

greater. Individuals diagnosed with MCI therefore have greater cognitive decline than healthy individuals but the decline is not severe enough to diagnose early AD (Petersen, 2004). Not all individuals diagnosed with MCI will go on to develop AD, and therefore different criteria are used to distinguish between standard age related cognitive decline and MCI, as well as between MCI and dementia (Petersen, 2004). An issue with the various criteria used in diagnosis of AD (e.g. criteria found in the Diagnostic and Statistical Manual of Mental Disorders 4th edition) is that there are no defined cut off points with regard to the criteria and that whether a person meets each criterion or not is down to the judgement of the investigating clinician (American Psychiatric Association, 1994; Petersen, 2004). The fundamental features of these criteria involve memory impairment and executive function and diagnosis based on these criteria by clinicians are generally accurate (Petersen, 2004). The most common form of memory impairment in MCI to AD converters is that of episodic memory (Albert et al., 2011). If a person meets the criteria from such a test to be diagnosed with AD, the clinician must also determine whether the level of cognitive decline observed affects either the social or occupational activities of the patient. In order for AD to be diagnosed the test criteria must be met in addition to the condition affecting the individual in a social or occupational capacity (Petersen, 2004).

A range of cognitive assessments can be performed to investigate the likelihood of an individual with MCI converting to AD in the near future. Due to the number of people with MCI and issues with episodic memory that convert to AD, the cognitive assessments are largely designed to investigate the episodic memory of MCI sufferers (Albert et al., 2011). As memory is not the only cognitive function affected by MCI further tests are employed to investigate individual competencies in areas such as visuospatial skills, language and executive functions (Albert et al., 2011).

Thus by using a combination of diagnostic criteria and a range of cognitive assessments (although a combination of these methods is not essential), clinicians can investigate with substantial accuracy, whether a person suffers from MCI and whether that individual is likely to convert to AD.

1.6.1.2 - Using Biomarkers to Assist in Diagnosis of AD

In addition to diagnosis based upon set criteria and cognitive assessments, biomarkers can also be used to aid determination of individuals in the preclinical or clinical phases of AD. Multiple different biomarkers can shed light on individuals with MCI who are likely to convert to AD. Biomarkers can be specific or non-specific with regards to diagnosing likely conversion to AD. For example one possible specific biomarker that can be used to investigate the chance of individuals with MCI converting to AD is the level of $A\beta_{1-42}$ in CSF. Investigation of this biomarker in CSF is based on determining whether the level of $A\beta_{1-42}$ in CSF is decreased compared to normal levels, which would signify that $A\beta_{1-42}$ is being deposited in the brain (Albert et al., 2011). It has been established that individuals with mild AD and also MCI converters to AD have decreased levels of CSF $A\beta_{1-42}$ (Andreasen et al., 1999; Lautenschlager et al., 2001). Another method used to detect signs that an individual with MCI will convert to AD also detects $A\beta$ using positron emission tomography (PET) scans to detect the presence of fibrillar $A\beta$. This molecular imaging technique can be performed using a variety of tracers such as Pittsburgh compound B (PiB) which binds fibrillar $A\beta$ such as that located in senile plaques and is then imaged using PET (Klunk et al., 2004). As this technique is an imaging technique, the brain regions where PiB is retained (due to binding $A\beta$) can be visualised in addition to determining how much of the tracer was retained (i.e. levels of fibrillar $A\beta$ present to bind PiB) (Albert et al., 2011). Thus PiB retention in brain regions mainly affected in AD points towards AD conversion.

In addition to biomarkers that indicate the levels of Aβ in the brain, biomarkers related to neuronal injury – non-specific biomarkers – are also useful for investigating the likelihood of MCI to AD conversion (Albert et al., 2011). Although the Tau protein is responsible for the NFTs that are characteristic of AD, tau elevation is used as a non-specific biomarker. Elevated levels of total Tau in the CSF represent neuronal injury but do not attribute the cause of the injury directly to AD (Albert et al., 2011). However in a study of MCI individuals where total Tau was found to be elevated in conjunction with decreased levels of CSF $Aβ_{1-42}$, 90% of the individuals with MCI later converted to AD whilst 10% did not convert (Riemenschneider et al., 2002). Additionally using elevated levels of the phosphorylated form of Tau as a biomarker is useful in detecting the likelihood of MCI to AD conversion. It has been found that MCI to AD converters have increased levels of phosphorylated tau compared with individuals with stable MCI (Buerger et al., 2002; Blennow & Hempel, 2003). Functional imaging is also a useful technique to assess the performance of cells in the brain. Techniques such as fluorodeoxyglucose PET (FDG-PET) measure the uptake of glucose by neuronal cells. Thus regions where there is reduced FDG uptake signify glucose hypometabolism and therefore neuronal injury. This hypometabolism is commonly found in the temporal and parietal lobes of AD sufferers (Sperling et al., 2011). Reduced FDG uptake has been closely associated with the atrophy that occurs during AD but is non-specific and therefore alone cannot be used to identify AD (Albert et al., 2011). However the level of hypometabolism identified using FDG-PET can be used alongside specific AD biomarkers indicating that MCI to AD conversion is likely, in order to gauge the staging of the disease (Albert et al., 2011).

As mentioned, AD causes multiple pathologies including brain atrophy. By using structural imaging - for example magnetic resonance imaging - brain changes associated with AD such as the enlargement of the ventricles and atrophy of the hippocampus can be detected, aiding in the diagnosis of AD (Apostolova et al., 2012).

1.6.1.3 - Why is there a delay between the onset of pathophysiological symptoms and the clinical symptoms of AD?

Due to the nature of AD, there is a preclinical stage of the disease whereby disease pathology begins but without the emergence of clinical symptoms sufficient to diagnose AD. In 1986, it was suggested that the educational or socio-economic status of an individual may affect their likelihood of developing AD (Berkman, 1986), whilst other researchers claimed that level of education must be taken into account when investigating possible dementia (Kittner et al., 1986). Soon after these claims, it was found that levels of AD were decreased among individuals with a high level of education (Zhang et al., 1990). As mentioned, certain biomarkers or clinical features associated with AD such as senile plaques, correlate poorly with severity of disease. For example, Ince reported that 25% of elderly individuals which following cognitive assessments were judged to be normal, were found at post mortem to fulfil the pathological criteria for diagnosis of AD (Ince, 2001). To account for the individual differences between level of pathology and clinical features, the concept of 'reserve' was formulated. Reserve refers to the way in which clinical features are affected by pathology and can be split into two forms - brain reserve and cognitive reserve (Stern, 2012).

Brain reserve refers to the ability of the brain to deal with the insults caused by the pathologies associated with AD and is attributed to the physical size of the brain. The incidence of dementia has been found to be lower in individuals with larger brains (Schofield et al., 1997). Therefore individuals with larger brains have an increased brain reserve, which is thought to be due to them possessing an increased number of neurons and synapses. This in turn enables a greater number of neurons to be lost (by AD pathologies) before the emergence of clinical symptoms compared with individuals with smaller brains who have fewer neurons and synapses (Stern, 2012).

Cognitive reserve differs from brain reserve as it does not rely on the physical dimensions of the brain, but rather cognitive reserve is based on the ability of the brain to employ coping mechanisms to deal with the pathology (i.e. compensatory mechanisms)(Stern, 2012). Cognitive reserve has been found to be increased dependent upon the activities, education or occupation of an individual (See Table 2). Therefore individuals with increased cognitive reserve should be more resistant to the cognitive effects of AD pathology. This should mean that such individuals develop the dementia associated with AD at a later point in disease progression than those with a smaller cognitive reserve.

Factor	Increase in Risk of Developing Dementia	Reference
Under 8 years of education (compared with over 8 years of education)	2.2 Times Greater	(Stern et al., 1994)
Low Occupational attainment (Compared with high occupational attainment)	2.25 Times Greater	(Stern et al., 1994)
Number of Activities Undertaken by Over 65s – Less than 6 (Compared with greater than 6)	1.38 Times Greater	(Scarmeas et al., 2001)

Table 1.2 - Effect of activity, education and occupational attainment on incidence of dementia.

1.6.2 – Therapeutic options for AD sufferers

1.6.2.1 – Symptomatic treatments

There exists a range of symptomatic drugs available for the treatment of AD, which fall into two classes based on the systems/pathways targeted by the drug. One such class of drugs are the cholinesterase inhibitors (CI) with the other class targeting the NMDARs. In addition to treatment of an AD sufferer with these symptomatic treatments, antidepressant and antipsychotic medication may also be administered to reduce the neuropsychiatric effects of AD (Yiannopoulou & Papageorgiou, 2013).

1.6.2.1 - Cholinesterase inhibitors (CIs)

AD is associated with neuronal loss and this loss is particularly evident in the basal forebrain at a relatively early stage of disease progression (Yiannopoulou & Papageorgiou, 2013). This degeneration of the basal forebrain has profound detrimental effects upon the cholinergic systems located within this region such as loss of the ability to synthesise and degrade ACh. In turn this results in increased loss of both cognitive and non-cognitive functions (Yiannopoulou & Papageorgiou, 2013). For the treatment of AD, CIs are widely regarded as the first line of treatment (Birks, 2006). Although CIs may benefit AD suffers, the alleviation of symptoms is only a short term fix as they aim to reduce the symptoms, without providing a treatment for the underlying pathologic manifestations of AD which are ultimately responsible for the clinical effects of the disease.

There are multiple different CIs available manufactured by different pharmaceutical companies (Donepezil, Rivastigmine, Galantamine), although there are no data that indicate a significant difference in efficacy between the different drugs (Birks, 2006). However all of these drugs have been shown to improve cognition following 6 months of treatment – on average of 2.7 points on the ADAS-Cog scale – compared with placebo (Birks, 2006). Also, the effects of these CIs extend to improvements in activities of daily living and behaviours of

sufferers (Birks et al., 2006). Donepezil does however have a marginally increased effect upon global cognition than Rivastigmine and Galantamine (Hansen et al., 2008).

Donepezil is a reversible inhibitor which is specific and selective for the acetylcholinesterase enzyme, Rivastigmine is an inhibitor of both acetylcholinesterase and butylcholinesterase, and Galantamine inhibits acetylcholinesterase but additionally has the ability to trigger acetylcholine release by stimulating nicotinic receptors (Lanctôt et al., 2009; Tayeb et al., 2012). Although CIs are regarded as the first line treatment given to AD sufferers, their efficacy has been proved from mild to severe AD, meaning that they can be beneficial to an individual no matter how advanced disease progression in that individual is (Birks, 2006). Whilst CIs have been shown to be effective from mild to severe AD, the earlier in disease progression that an individual receives treatment with CIs, the greater the effects of the drug. For example a study investigating the effects of Rivastigmine on individuals with mild to moderately severe AD found that individuals starting the treatment 6 months earlier showed greater cognitive performance than those who were administered the drug 6 months later (Farlow et al., 2000; Yiannopoulou & Papageorgiou, 2013). This level of performance was also found to be preserved over a period of 12 months, whereas performance of individuals receiving no treatment showed significant decline (Almkvist et al., 2004). In addition to the reported effect of CIs on cognition, they were also observed to improve AD related behavioural changes in individuals suffering from mild to severe AD (Birks, 2006).

As the ability of AD sufferers to produce ACh is reduced, CIs are used to prevent the breakdown of ACh at the synaptic cleft (Yiannopoulou & Papageorgiou, 2013). CIs directly enhance cholinergic transmission by inhibiting the enzyme acetylcholinesterase thus increasing the levels of ACh available at the synapse to transmit the presynaptic signal to the postsynaptic neuron (Lasner & Lee, 1998).

It is important to note that whilst the CIs have been shown to benefit cognition in AD sufferers, this effect is only temporary, lasting on average no more than 2 years (Giacobini, 2000). Additionally, these drugs are not able to decelerate, over the long term, the cognitive decline associated with AD (Courtney et al. 2004). As is the case with many drugs, treatment of individuals with CIs can have a range of side effects. The most common side effects are gastrointestinal associated effects such as nausea, diarrhoea and vomiting although in some cases more serious side effects such as bradycardia and syncope can occur (Yiannopoulou & Papageorgiou, 2013). It is therefore important for clinicians to analyse the cost/benefits of a drug for a particular individual before that drug is administered (Yiannopoulou & Papageorgiou, 2013).

1.6.2.2 - NMDAR Antagonists

As mentioned earlier, glutamatergic NMDAR activation can have beneficial effects in terms of neuronal cell survival and also plays a role in LTP. Glutamate excitotoxicity is also an issue in AD as overstimulation of NMDARs can result in cell death (Figure 2), and inhibiting stimulation of NMDARs can protect against this detrimental effect. The excitotoxicity occurs as a result of increased levels of glutamate present in the synaptic cleft following impaired reuptake of glutamate by astrocytes due to Aβ and therefore the glutamate cycle is dysregulated (Figure 2)(Anand et al, 2014). This dysregulation of the glutamatergic system occurs at a later point in disease progression than damage to the cholinergic system, which in contrast occurs early in AD (Anand et al., 2014).

Multiple NMDARs have been developed however their ability to be used as a treatment for neurodegenerative diseases such as AD has been poor due to serious side effects such as impaired memory formation and reduced synaptic transmission (Johnson & Kotermanski, 2006). As mentioned, glutamate is an essential neurotransmitter due to its involvement in multiple processes such as learning and memory, however excess glutamate is neurotoxic.

NMDAR antagonists act to bind NMDARs, thus preventing excitotoxicity and preventing cell death. Memantine is currently the only approved NMDAR antagonist licenced to treat AD. It is believed that the beneficial effect of memantine is not solely attributable to its ability to reduce excitotoxicity. It has been shown that this drug is also able to reduce the level of Tau phosphorylation and improve LTP (Frankiewicz & Parsons, 1999; Li et al., 2004; Tayeb et al., 2012)

Memantine is an NMDAR antagonist and binds these receptors in an uncompetitive manner via interaction with the NR1 and NR2 subunits of NMDARs (which are quaternary structures) (Johnson & Kotermanski, 2006; Yiannopoulou & Papageorgiou, 2013). The proposed reason for the success of memantine as a treatment for AD compared with other NMDARs is that the activity of memantine functions in such a way as to enable stimulation of NMDARs which enables processes that rely on them to continue, whilst also preventing the overstimulation associated with AD pathology (Johnson & Kotermanski, 2006). The overstimulation associated with the AD pathology is attributed to continuous activation of NMDARs even on the absence of presynaptic signalling and therefore memantine administration is able to prevent this constant state of low level stimulation, Ca^{2+} influx and intracellular signalling (Anand et al., 2014). Memantine is not only effective for treatment of AD but also other neurodegenerative diseases such as Huntington's (Beister et al., 2004), Parkinson's (Parsons et al., 1999), as well as other non-neurodegenerative diseases such as epilepsy and glaucoma (Johnson & Kotermanski, 2006). Memantine blocks the ion channels within the NMDARs but is only able to exhibit this action when the channel is open – thus memantine is referred to as an 'open channel blocker' (Johnson & Kotermanski, 2006). Once memantine has blocked the channel, NMDAR agonists can then dissociate from the receptors, resulting in channel closure.

This drug has been proven to be an effective treatment across all severities of AD. For example when comparing the effects of memantine (vs placebo) over a 6-month period, memantine showed a statistically significant improvement in all areas tested – Behaviour, cognition, function and global status (Winblad et al., 2007). Studies have also confirmed that the use of memantine is able to improve patient suffering from aggression in addition to delusions, when compared to a placebo group (Gauthier et al., 2008; Lanctôt et al., 2009)

Memantine can have unwanted side effects in individuals who have been administered the drug, however these side effects are rare and are generally associated with high doses e.g. 40mg/kg (normal dosage of memantine for all disease stages of AD is 20mg/kg) (Lipton, 2004). Reported side effects include dizziness, headaches and agitation (Lipton 2004).

1.6.2.3 - Use of cholinesterase inhibitors and NMDARs in combination

There is evidence to show that the use of a combination therapy whereby memantine and CIs (usually Donepezil) are administered to patients suffering from AD is beneficial compared with treatment solely with CI (Atri et al., 2008). Individuals given the combination therapy had a slower decline in cognitive and functional abilities than those treated with CIs alone (Atri et al., 2008). The effect of the combination therapy was found to increase over time and was therefore sustainable (Atri et al., 2008).

1.6.2.4 - Approaches to treat the behavioural and psychological symptoms of AD

In addition to the cognitive decline associated with AD, the clinical manifestations of the disease also include neuropsychiatric symptoms (NPS) such as depression, hallucinations, apathy and aggression, among a range of others (Yiannopoulou & Papageorgiou, 2013).

One form of approach to improve the NPS (or psychological and behavioural symptoms) of AD is a non-pharmacological approach. This involves a variety of activities such as relaxation techniques, individualisation of care (by caregivers), and reminiscence activities that have all

been shown to improve behaviours and reduce depression (Welden & Yesavage, 1982; Baines et al., 1987; Goldwasser et al., 1987; Bird et al, 1995).

There are also pharmacological approaches that can be taken to deal with NPS associated with AD. Many studies have investigated the efficacy of various drugs to deal with the NPS experienced by AD sufferers with a large amount of these finding no improvement or detrimental effects of drug treatment compared with placebo (Ballard & Howard, 2006). However treatment with risperidone has been found to improve overall behaviour, with the greatest improvements noted in aggression levels (Brodaty et al., 2003; Ballard and Howard, 2006; Ballard et al., 2006). Risperidone has also been found to be effective against the symptoms of psychosis (hallucinations and delusions) that are frequently encountered in AD (Brodaty et al, 2003). Selective serotonin reuptake inhibitors (SSRIs) such as Citalopram can also be administered and are the most effective drugs available to treat the depression associated with AD dementia (Zec & Burkett, 2008; Yiannopoulou & Papageorgiou, 2013).

There is clear evidence to show that particular pharmacological treatments have beneficial effects when used to treat AD dementia however these effects are often small. This is possibly due to the fact that by the time the requirement for the treatment is recognised and the treatment is started, symptoms may have reached a point where they are non-reversible (Yiannopoulou & Papageorgiou, 2013). Therefore increased efforts to target these pharmacological treatments to individuals as early in disease progression as possible may enable an intervention at a time when these symptoms may well be reversible.

1.6.2.5 - Disease modifying therapies

As AD is the leading cause of dementia, with the number of affected individuals expected to rise dramatically as ageing populations increase, it is imperative that treatments that alter the progression of the disease are developed. Currently, the only licenced treatments for AD are symptomatic treatments that aim to reduce the symptoms of the disease over the short

term, without addressing the underlying pathological mechanisms responsible for the clinical effects of the disease.

Multiple disease modifying therapies have been developed which have different targets relating to the progression of the disease e.g. modifying activity of secretases, immunotherapy, inhibition of Aβ plaque formation (Allsop & Mayes, 2014). However none of these disease-modifying therapies have made it past phase 3 trials and thus are not available for the treatment of AD (Allsop & Mayes, 2014). The major problems associated with the development of treatments appear to be a poor bioavailability of the therapeutic agent when administered or undesirable side effects (Allsop & Mayes, 2014). For example inhibiting the BACE1 enzyme (and therefore preventing Aβ production) is difficult as this enzyme has multiple substrates which play critical roles in the nervous system and various organs such as contact dependent communication between cells or may act as receptors (Hemming et al., 2009). For inhibition of BACE1 to be an effective strategy then the ability of BACE1 to cleave APP would need to be reduced whilst enabling the enzyme to interact with other important substrates, which is proving a difficult task for medicinal chemists (Allsop & Mayes, 2014).

As Aβ aggregation is a pathological hallmark of AD, searches for drugs that can prevent this aggregation have been on going for many years. One drug designed to prevent aggregation was Tramiprosate. Following clinical trials, analysis of the effects of the drug showed an improvement in specific cognitive functions such as memory and language (Anand et al., 2014). However, the method of action of this drug is to reduce the binding of proteoglycans to Aβ and thus is unable to prevent aggregation of Aβ into toxic oligomeric forms (Allsop & Mayes, 2014). In addition to the inability of tramiprozate to prevent formation of Aβ oligomers, the drug has been shown to increase tau pathology, which is also a major cause of neuronal loss in AD (Anand et al., 2014).

An alternative form of therapy which initially showed exciting potential was Aβ immunotherapy. Early studies in a mouse model of AD showed that immunization with Aβ was able to improve cognitive functioning whilst also reducing the levels of Aβ plaques (Schenk et al., 1999; Morgan et al., 2000). Following these positive results, clinical trials were set up, finding that the therapy did reduce the number of amyloid plaques (Holmes et al., 2008). However clinical trials of this therapy showed no effect upon cognitive decline of the test subjects and were stopped before completion due to severe side effects such as encephalitis (Iwata & Iwatsubo, 2013). An additional problem stemming from a treatment aiming to reduce the numbers of senile plaques is that breaking up these structures may release smaller, oligomeric forms of Aβ which due to their toxicity may even exacerbate the extent of Aβ toxicity in the individual (Allsop & Mayes, 2014). However, a recent study investigating the effects of a monoclonal IgG1 antibody that recognises a mid-region of Aβ (Solanezumab) found that this antibody represents a promising candidate for a DMT (Liu-Seifert et al., 2015). By using a novel statistical analysis method, it was found that Solanezumab treatment resulted in significant cognitive improvements in individuals with mild AD and the effect of the drug was shown to reduce cognitive decline by 34% over an 80-week period (Liu-Seifert et al., 2015). Importantly, analysis of the safety of Solanezumab did not find treatment with this antibody to result in any statistically significant increases in adverse affects when compared to a placebo group (Liu-Seifert et al., 2015). The benefits of targeting individuals for treatment at an earlier stage of disease was illustrated in this study by the ability of Solanezumab to improve cognition in individuals with mild AD, but not in those with moderate AD. Therefore the reduction in cognitive decline following administration of Solanezumab and the safety of this drug provide hope for future development of Solanezumab as a DMT for AD, whilst clearly demonstrating the need to administration of DMTs at an early stage of AD.

As mentioned earlier, insulin desensitisation is observed in in T2DM and in brains of AD sufferers, and is regarded as a risk factor for the disease. Recently, drugs traditionally used to treat T2DM such as Lixisenatide and Liraglutide have begun to be investigated for their potential use as a disease modifying therapy for the treatment of AD (McClean & Holscher, 2014a; McClean & Holscher 2014b). Investigation into the effects of liraglutide treatment on transgenic mice showed a 33% reduction in plaque load, 30% reduction in inflammation (via reduction in microglial activation), 50% increase in neural stem cells in the dentate gyrus and a reduction in overall levels of Aβ oligomers in the brain (McClean & Holscher, 2014b). This study found that levels of liraglutide much lower than those given to T2DM sufferers were most effective and this drug is currently in clinical trials as the interactions of the drug within humans is already known from its use as a treatment for T2DM.

Therefore to date the results of various drugs that have entered clinical trials have been disappointing and there is a sustained requirement to continue to develop novel therapies. The hope for these therapies is that they can halt and maybe even reverse disease progression, without adverse side effects which have been found when testing previous disease modifying therapies. Additionally, potential drugs successful enough to reach clinical trials should be investigated not just in individuals diagnosed with AD but also in individuals with MCI. Diagnostic tests using biomarkers and brain imaging scans can be used to predict the likelihood of progression of a person with MCI to AD with substantial accuracy (Eckerström et al., 2013). Therefore by including these individuals (with MCI predicted to later convert to AD) in clinical trials, the drugs being tested may have a greater chance of modifying disease progression before a relatively large degree of irreversible damage to the brain is caused.

1.6.2.6 - RI-OR2-TAT

One promising therapy currently still in the early stages of development is a peptide referred to as RI-OR2-TAT (Parthsarathy et al, 2013). Residues 16-22 (KLVFFAE) of the Aβ peptide have been found of be primarily responsible for the aggregation the peptides (Tjernberg et al., 1996; Tjernberg et al., 1999). RI-OR2-TAT is based on the previously developed inhibitor OR2 that binds residues 16-20 (KLVFF) of the Aβ peptide (Austen et al., 2008). Following development of OR2 (amino acid sequence – H_2N-R-G-K-L-V-F-F-G-R-NH_2) it was found that this inhibitor was poorly resistant to proteolytic degradation and therefore a retro-inverted version of the protein was produced which replaced the L-amino acids with D-amino acids whilst also reversing the direction of the peptide bond (Taylor et al., 2010). This retro-inverted peptide was referred to as RI-OR2 (H_2N-r-G-k-l-v-f-f-G-r-Ac - L-amino acids in upper case – with the exception Glycine, D-amino acids in lower case) and was found to maintain the desired effects of OR2 such as inhibiting cell death due to Aβ cytotoxicity and preventing Aβ monomers aggregating into oligomers whilst possessing greatly increased proteolytic stability (Taylor et al., 2010). The RI-OR2 inhibitor was further developed by the addition of TAT (trans-acting activator of transcription) - a protein encoded by the HIV virus - that is able to rapidly pass across the plasma membrane of cells (Frankel & Pabo, 1988; Ziegler & Seelig, 2004). This ability of the TAT protein to pass across plasma membranes was utilised via attachment to RI-OR2 (forming RI-OR2-TAT) to effectively transport the inhibitor across the BBB and into the brain where it could interact with Aβ plaques with the hope of modifying AD progression. The TAT peptide is able to facilitate the movement of conjugates across the BBB due to two main effects of the peptide that act to increase the permeability of the BBB by destabilising the tight junctions between cells (Xu et al., 2012). TAT causes this destabilisation by decreasing the expression of occludins, which are essential proteins involved in establishment and maintenance of tight junctions. Furthermore, TAT also triggers increased expression of matrix metalloproteinase-9 (MMP-9), which acts to cleave the

occludin proteins. Taken together, the increased expression of MMP-9 and reduced

expression of occluding combine to weaken the tight junctions between cells and increase

BBB permeability (Xu et al., 2012). Without the addition of TAT, RI-OR2 is unable to cross the

BBB and therefore the inhibitor cannot reach the brain where senile plaques are found thus

in this form, RI-OR2 would not be a candidate for potential AD therapy (Parthsarathy et al.,

2013).

The ability of RI-OR2-TAT to cross the BBB and exert its beneficial effects by preventing the

aggregation of Aβ peptides was then investigated. Results from these investigations using

transgenic mice that overexpressed APP showed that intraperitoneal injection of RI-OR2-TAT

for 21 days had a substantial effect upon disease progression (Parthsarathy et al., 2013).

Importantly, RI-OR2-TAT was found to cross the BBB and bind to activated microglia and

senile plaques, demonstrating that the TAT domain functioned effectively to facilitate

passage of the inhibitor across the BBB without preventing the interaction of the inhibitor

with Aβ (Parthsarathy et al., 2013). The binding affinity between Aβ and RI-OR2-TAT was

determined to be (k_d = 58-125 nm). RI-OR2-TAT was found to reduce levels of; Aβ oligomers

by 25%, number of senile plaques by 32%, activated microglia by 44% and oxidative damage

by 25% (Parthsarathy et al., 2013). Additionally, RI-OR2-TAT treatment was also found to

increase the number of neurons in the dentate gyrus by 210% (Parthsarathy et al., 2013).

These results suggest that RI-OR2-TAT is an even stronger candidate for a novel disease

modifying therapy for AD than liraglutide. The next steps therefore are to determine the

interactions between Ri-OR2-TAT and Aβ and identify the most effective delivery method for

this drug.

1.6.2.7 - Peptide Inhibitor Nanoparticles (PINPs)

In order to maximise the potential therapeutic effect of a particular drug, the most effective

methods of drug delivery must be determined. This is crucial as drugs may be metabolised

before they reach their desired target, or may elicit strong immune responses resulting in a decreased therapeutic index. One method that has been developed to address the issues of drug delivery has been the use of nanoparticles to administer therapeutic agents. One class of nanoparticles that have been employed to improve drug delivery are liposomes, an artificially produced lipidic vesicle possessing many similarities with biological membranes. This resemblance to natural membranes means that liposomes exhibit extremely low levels of toxicity and immunogenicity (Immordino et al., 2006)

Liposomes were first observed in 1963 by Alec Bangham and have since been the focus of intense research interest for their potential use as drug delivery systems for a wide range of therapeutics (Bangham & Horne, 1964). Liposomes consist of a phospholipid bilayer with an aqueous core and are produced in an extensive range of particle sizes from just 20 nm to as large as 10 µm (Patel, 2006). In addition to size, liposomes vary in composition and structure. These phospholipid vesicles may be unilamellar (ULV) or multilamellar (MLV) and may consist of natural (e.g. sphingomyelin) or synthetic (e.g. Stearylamine) lipids. The characteristics of a lipid bilayer endow liposomes with the capability to transport both hydrophilic and lipophilic cargoes contained within the aqueous core or the lipid bilayer, respectively (Bozzuto & Molinari, 2015). The characteristics of the drug being delivered will dictate the appropriate type of liposome to use. For example MLVs have a greater capacity to transport lipid soluble drugs than ULVs, whilst ULVs release their cargoes at an increased rate (Bozzuto & Molinari, 2015).

A significant advance in the clinical use of liposomes came with the advent of 'second generation' liposomes (SGLs) where properties such as the diameter, charge and physical makeup of these nanoparticles received increased focus (Bozzuto & Molinari, 2015). The addition of cholesterol to SLGs had a significant effect upon their stability following administration. Cholesterol addition has the effect of decreasing membrane fluidity thus

preventing the loss of SGLs to high and low-density lipoproteins (Bozzuto & Molinari, 2015).

A disadvantage of the earlier liposome formations was the binding of opsonins to the

liposome surface, which lead to their removal by the mononuclear phagocyte system (MPS)

(Immordino et al., 2006). The ability to attach molecules such as polyethylene glycol (PEG) to

cholesterol within the membrane enabled increased *in vivo* stability of the liposomes. By

attaching many PEG molecules to the liposome surface, the nanoparticle can be effectively

shielded from recognition from the MPS, which reduces liposome destruction thus

increasing circulation times (Bozzuto & Molinari, 2015).

Following these advances in the production of liposomes with increased *in vivo* stability, the

RI-OR2-TAT peptide has been attached to nanoliposomes to form PINPs (Figure 1.6). As is the

case for the transport of peptides, conjugation of liposomes to a peptide containing the TAT

domain facilitates the movement of such liposomes across the BBB (Wei et al., 2009). The

nanoliposomes are formed from a mixture of sphingomyelin and cholesterol at a 1:1 ratio.

Following this step, 1,2-Distearoyl-*sn*-glycero-3-phosphoethanolamine (DSPE) is added,

which is conjugated to PEG2000 that in turn possesses a maleimide group at its terminus. In

recent years, click chemistry has been increasingly used to conjugate various ligands to

liposomes, enabling liposomes to be targeted to specific cells based on interactions between

the liposome conjugate (i.e. peptide) and cellular features such as specific cell surface

receptors (Said Hassane et al., 2006). Click chemistry is used in the production of PINPs in the

crucial process of RI-OR2-TAT peptide conjugation to the nanoliposomes particles. 'Click'

chemistry occurs between the maleimide group and the sulphydryl group of the cysteine

amino acid at the terminus of RI-OR2-TAT, forming a stable disulphide bond. This is a fast

and non-reversible reaction that ensures strong coupling of the RI-OR2-TAT peptide to the

PEG molecules anchored in the liposomal bilayer.
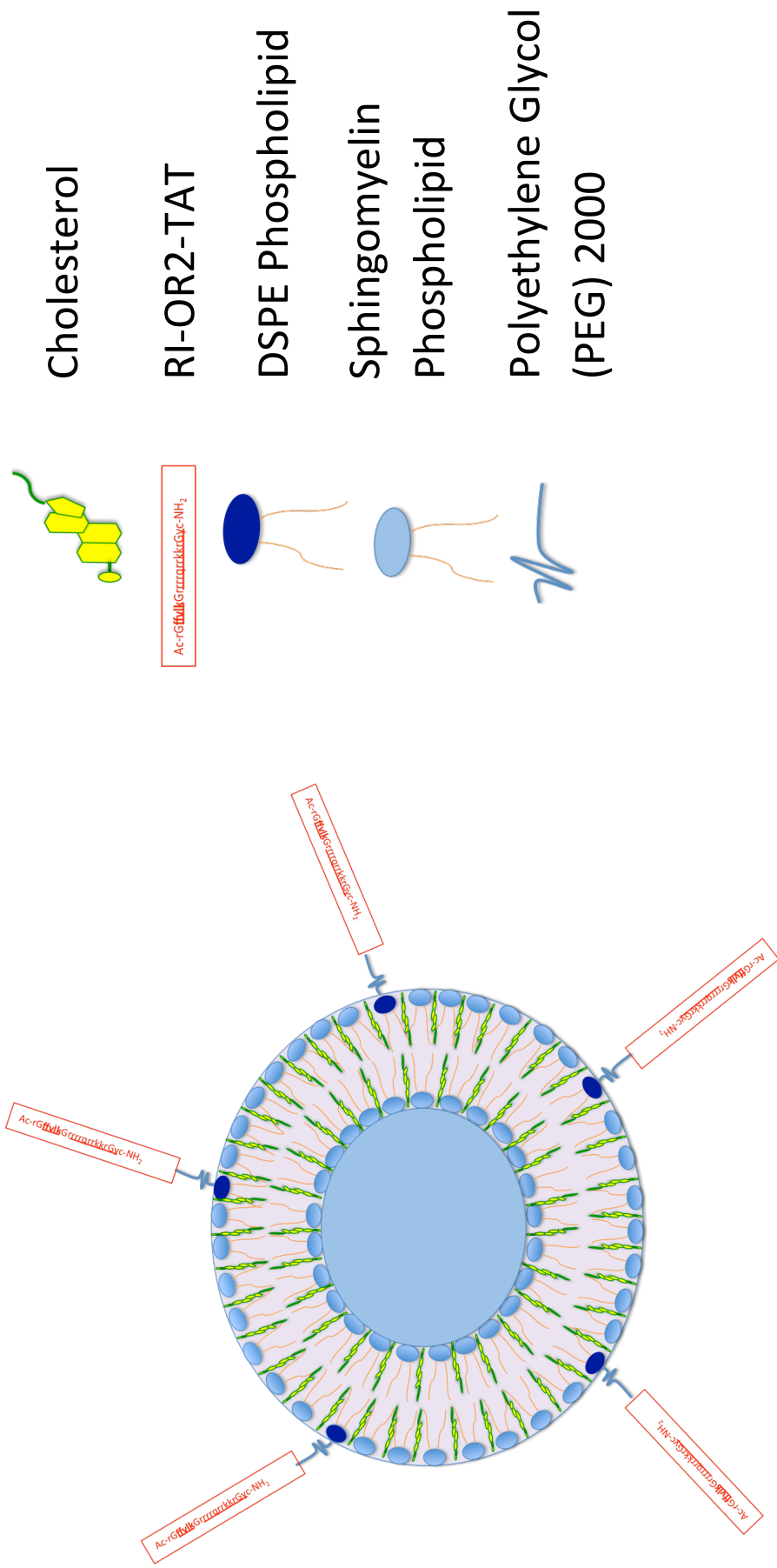
Figure 1.6 – 2D structure of a Peptide Inhibitor NanoParticle (PINP). PINPs consist of liposomes made from 1:1 Cholesterol:Sphingomyelin. DPSE is also incorporated into the lipid bilayer of the liposome and is conjugated to PEG2000, which extends from the outer layer of the bilayer. PEG2000 possesses a maleimide group and by performing click chemistry, RI-OR2-TAT is attached to PEG2000. RI-OR2-TAT is present at approximately 5% of the liposomal surface.

1.7 - Recombinant production of $A\beta_{1-42}$ peptide

The $A\beta$ peptide is an essential aspect of many investigations into AD and potential therapeutic options, however the price of this peptide remains high and expenditure on this peptide alone can account for significant proportions of funds available to individual laboratory groups for their research. Producing the $A\beta_{1-42}$ peptide recombinantly (rather than by peptide synthesis - used by many commercial suppliers) has the potential to enable the production of very large batches of $A\beta_{1-42}$ for use into AD research at a fraction of the cost of procuring the peptide commercially. Additionally, there are limitations to the production of peptides by peptide synthesis such as racemization (the switch from 1 specific enantiomer present in a peptide to the presence of both enantiomers), which is known to alter the aggregation characteristics of the $A\beta$ peptide (Finder et al., 2010). Furthermore, analysis of samples of $A\beta$ from different manufacturers - and even between batches from the same manufacturer - have been found to exhibit substantially different aggregation characteristics (i.e. rate of fibrillization), affecting the ability of researchers to direcly compare results obtained using different batches of $A\beta$ (Soto et al., 1995). Recombinant production of the $A\beta_{1-42}$ peptide therefore provides a method of producing $A\beta_{1-42}$ with the potential to avoid the aforementioned limitations of commercial $A\beta_{1-42}$. In 2010 Finder et al. published a method of producing recombinant $A\beta_{1-42}$ and highlighted the difference in aggregation characteristics between recombinant and synthetic $A\beta_{1-42}$ (Finder et al., 2010). The group demonstrated that the impurities and racemization in commercially produced synthetic $A\beta_{1-42}$ act to slow the rate of $A\beta_{1-42}$ aggregation, meaning that analysis of aggregation of such peptides do not necessarily provide information applicable to naturally produced $A\beta_{1-42}$.

1.8 – Project Aims

This project consisted of two main aims that were designed to increase the knowledge relating to the production of the Aβ peptide whilst investigating the method of action of a potential novel therapeutic option for the treatment of AD.

Due to the limitations of commercially produced $A\beta_{1-42}$, the initial aim of this project aimed to produce recombinant $A\beta_{1-42}$ that could be used for research purposes at a lesser cost than current commercially available options. By using a recombinant approach to the production of Aβ, the need for a expensive equipment such as peptide synthesisers is removed and would allow for relatively fast and low-cost production of the Aβ peptide, as well as greater comparibility between studies undertaken using different batches of $A\beta_{1-42}$. Production of recombinant $A\beta_{1-42}$ involved using a protocol designed by Finder et al. in order to successfully adopt this technique to develop stocks of recombinant $A\beta_{1-42}$ for future experimental use at Lancaster University (Finder et al., 2010). To address this aim, glycerol stocks of *Eschericia coli* transfected with plasmids encoding the $A\beta_{1-42}$ fusion protein DNA construct were provided as part of a material transfer agreement by Professor Rudolph Glockshuber (Swiss Federal Institute of Technology, Zurich). This project therefore involved the performance of all production/purification process for all stages following transfection of the *E. coli* cells with the plasmids.

The second aim of the project was to investigate a potential novel DMT for AD by assessing the effect of peptide (RI-OR2-TAT) conjugated nanoliposomes upon aggregation of the $A\beta_{1-42}$ peptide. RI-OR2-TAT was developed with the ultimate aim of preventing the self-aggregation of Aβ peptide monomers into higher order structures that are thought to be at least partly responsible for the neurodegeneration observed in individuals with AD. By attaching this peptide to second-generation liposomes, PINPs have been created and their effectiveness as a potential therapeutic option for AD was investigated in this project. This investigation was

performed by combining quantitative data analysis from assays such as the Thioflavin T (ThT) Assay, with qualitative methods of investigation such as transmission electron microscopy. By collecting both qualitative and quantitative data surrounding the effects of PINPs upon Aβ aggregation, it was predicted that these methods would yield sufficient insights into the potential effectiveness of PINPs as a therapy for AD.

Produce recombinant $A\beta_{1-42}$ using published protocol (Finder et al., 2010). TEV protease was also recombinantly produced for use in the production of $A\beta_{1-42}$.

Analyse success of $A\beta_{1-42}$ production by investigating the identity and purity of proteins produced.

Investigate effect of PINPs upon $A\beta_{1-42}$ aggregation using transmission electron microscopy.

Investigate effect of PINPs upon $A\beta_{1-42}$ aggregation using fluorescence-based assays.

Figure 1.7 – Project aims.

Chapter 2 - Materials and methods

2.1 – Recombinant Aβ$_{1-42}$ (rAβ$_{1-42}$) production

2.1.1 – Expression and purification of recombinant Tobacco Etch Virus (TEV) protease

Escherichia coli BL21 (DE3) were transfected with the pRK793 plasmid, encoding the TEV protease. *E.coli* were incubated overnight in Terrific Broth containing ampicillin. When the optical density (600 nm) of the cell suspension reached 0.8, cells were induced with 1 mM Isopropyl β-D-1-thiogalactopyranoside (IPTG). Following an induction period of 3h at 37°C cells were harvested, resuspended in HisA buffer and frozen overnight at -20°C. Thawing of the cells was performed at room temperature to avoid causing heat-shock of cells and the suspension was sonicated to lyse cells and release cellular contents. A sample of cell lysate was taken at this stage for later analysis whilst the remaining cell lysate was added to a Nickel-NTA column (Sephacryl S200, GE Healthcare) for purification by immobilised metal-ion affinity chromatography (IMAC). Increasing concentrations of imidazole (20 mM, 50 mM, 500 mM) were then passed through the nickel column. The solution exiting the column following the addition of 500 mM imidazole was then collected in 1 ml aliquots and the protein concentration of each 1 ml sample determined using a Nanodrop 2000c spectrophotometer. Samples then underwent sodium dodecyl sulphate (SDS) polyacrylamide gel electrophoresis (PAGE) – SDS-PAGE – to separate proteins within the sample for later analysis by western blotting and Coomassie blue staining.

2.1.2 – Expression and purification of recombinant Aβ$_{1-42}$

Escherichia coli BL21 (DE3) cells were transfected with PRSET-A expression vector containing an Aβ$_{1-42}$ fusion protein construct. This construct possessed the domain corresponding to the Aβ$_{1-42}$ peptide of interest (in addition to other domains) and cells containing the plasmid

encoding the fusion protein were provided by Professor Rudolph Glockshuber (Swiss Federal Institute of Technology, Zurich) in a material transfer agreement. The *E. coli* stocks were incubated at 37°C in Terrific Broth to an OD of ~2 in a shaking incubator. Once OD ~2 had been reached, the cells were induced with 1 mM IPTG and returned to the incubator for 4 hours. Cells were then centrifuged at 3,900g for 25 mins at 4°C and pelleted cells were then resuspended in Guanidine HCL buffer (pH 8). Cells were lysed by sonication and centrifuged at 149,000g for 1h at 4°C to remove cell debris and the supernatant was loaded onto a Nickel-NTA column equilibrated with Guanidine HCL buffer (pH 8). Guanidine HCL buffers at pH 6 and pH 2 were then passed through the column, with the flow through following addition of Guanidine HCL Buffer (pH 2) being collected in 1ml aliquots. Analysis of $A\beta_{1-42}$ protein concentration (by A280) revealed that the $A\beta_{1-42}$ peptide was not present at a high enough concentration for cleavage (1.4mg/ml) in any single 1 ml aliquot. Therefore in order to obtain a sample of sufficient concentration for cleavage, dialysis using the 3 most concentrated aliquots was performed in ammonium carbonate buffer for 24h. A 3 ml Slide-a-lyzer dialysis cassette with a 2 kDa molecular weight cut-off was used for dialysis. Following dialysis, the ammonium carbonate buffer was removed using Speedvac and resuspended in TEV cleavage buffer (10 mM Tris HCl, 0.5 M EDTA, 1 mM DTT, pH 8). The concentration of this sample was then diluted in TEV buffer to the optimal cleavage concentration of 1.4 mg/ml (Finder et al., 2010).

2.1.3 – Cleavage of $A\beta_{1-42}$ from fusion protein

In order to perform the cleavage of the fusion protein, TEV (from aliquot no. 5) was diluted to a concentration of 0.14 mg/ml and then added to the sample of fusion protein (1.4 mg/ml). The sample was agitated to ensure even distribution of the fusion protein and TEV protease and cleavage was allowed to proceed for 16h at 4°C. Once 16h had elapsed, the sample was centrifuged at 13,000g for 10 mins to pellet the $A\beta_{1-42}$ peptide. Supernatant was

discarded and the cleaved Aβ$_{1\text{-}42}$ was resuspended in HFIP to reduce formation of aggregates by self-aggregation of the peptide as much as possible.

2.1.4 – Measuring Protein Concentration (A280)

Before beginning analysis of any samples of either Aβ$_{1\text{-}42}$ or TEV protease, each time this equipment was used, routine wavelength verification was performed to ensure correct functioning of the apparatus. Protein concentration was determined by measuring light absorbance at a wavelength of 280 nm (A280). In order to accurately measure protein concentration, a 'blank' sample consisting of the buffer of which the protein was suspended in was read on the spectrophotometer each time the equipment was used. The pedestal of the device upon which the samples were placed, was thoroughly cleaned using ethanol and lint free lens tissue. This ensured that any protein detected by the spectrophotometer had originated in the sample being analysed rather than from earlier samples.

2.1.5 – Ethanol precipitation of Aβ$_{1\text{-}42}$

Prior to western blotting and coomassie staining of gels containing Aβ$_{1\text{-}42}$ samples, guanidine was removed from the buffer solution by precipitation of the protein in absolute ethanol. This enabled gel electrophoresis to be performed using the protein samples which would not have been possible whilst solubilised in a solution with high guanidine concentration (6 M). Precipitation of the protein was achieved by addition of the protein sample to absolute ethanol at a ratio of 1:9 (sample:ethanol). This solution was then frozen at -80°C for 2h whilst the protein precipitated from the solution. Following precipitation, washing in absolute ethanol and resolubilisation in SDS-Gel loading buffer, samples were vortexed for 30 secs, sonicated 4 x 5 mins and then heated to 98°C for 3 mins. Following a further 30 sec vortex, samples were loaded into the wells of the polyacrylamide gels. The MW marker used in all analyses was Keleidoscope prestained protein standards (Bio-Rad).

2.1.6 – Protein Analysis by SDS-PAGE and Western Immunoblotting

In order to confirm that the protein detected within samples (as indicated by NanoDrop apparatus) was the protein of interest, and therefore that the expression methods were successful, Coomassie staining and Western blotting were performed. Initially, samples to be analysed were added 1:1 to gel loading buffer, heated to 98°C for 3 mins and then added to their respective well in the polyacrylamide gel (10 µl per well). Proteins were electrophoresed for 45 mins at a voltage of 150v.

Following SDS-PAGE, gels to be stained with Coomassie brilliant blue R-250 (Sigma Aldrich) were placed in a small container and 20ml Coomassie staining solution (0.25% w/v Coomassie brilliant blue, 40% v/v 40% Ethanol, 10% v/v acetic acid, 50% v/v MilliQ water) was added so that the gel was submerged in the stain. The gel was submerged in the stain at room temperature and placed on a rocking platform overnight. Following staining, destaining solution (40% v/v 20% ethanol, 10% v/v Acetic acid, 50% v/v MilliQ) was added and replaced hourly until all excess stain had been removed from the gel.

Western blotting was performed on gels which were not Coomassie stained and instead were used to transfer proteins onto a nitrocellulose membrane. This transfer of proteins from the gel to the nitrocellulose membrane proceeded at 25v for 90 mins. Following protein transfer the membrane was washed by submergence in PBST (10 mM PBS, 0.1% v/v Tween-20) for 5 mins and was then blocked using 2% powdered milk in PBST (blocking solution) for 1h at room temperature on a rocking platform. The blocking solution was poured off the membrane and the primary antibody was added (diluted 1:5000 in blocking solution) and incubated on a rocking platform for 90 mins. Primary antibody was removed and the membrane was washed 4 x 5 mins with PBST. Horseradish peroxidase (HRP) conjugated anti-mouse immunoglobulin secondary antibody was then added (1:5000 dilution in blocking solution) and was incubated under the same conditions as with the primary antibody.

Following incubation with the secondary antibody, the membrane was washed 4 x 5 mins with PBST to remove any unbound secondary antibodies and was exposed to an enhanced chemiluminescent substrate for 1 min to enable detection and localisation of HRP.

Western blots and Coomassie stained gels were visualized and imaged using a Bio-Rad ChemiDoc MP imaging system and Image Lab software.

2.2 - Preparation of rAβ_{1-42} for TEM

Following dilution in either PBS or dH$_2$O to a concentration of 25 µM, the samples were vortexed for 1 min followed by sonication on ice for a further minute to ensure rAβ_{1-42} peptides were not aggregated in the samples. Samples were then negatively stained using the negative staining procedure detailed therein.

2.3 – Sample preparation and staining

2% (w/v) phosphotunstic acid (PTA) was prepared using PTA and distilled water and was centrifuged at 18,400g for 5 mins to pellet any insolublised stain thus avoiding interference by PTA crystals upon TEM examination. 2% PTA had a pH of 7.4. Samples were then added to 300 mesh formvar and carbon coated copper grids (Agar Scientific, UK) for 2 mins. Following this time, grids were blotted with filter paper. The stain was then added to the copper grid for 2 mins after which the stain was blotted off the grid using filter paper.

2.4 - Recording electron micrographs

Negatively stained samples were viewed and recorded using a JEOL JEM-1010 electron microscope (EM) operating at 80kV. Micrographs were recorded onto Kodak 4489 photographic film and upon removal from EM were developed under safe lights. Developing proceeded at 20°C using Ilphord Phenisol developer and water at a ratio of 1:4. Following exposure to the developer solution, the films were washed in water, fixed with Ilphord Hypam fixer – fixer to water ratio 4:1 - and then washed. Before removal from the wash,

Kodak Photo-flo wetting agent was added to reduce drying marks left on the photographic film increasing the clarity of micrographs. Following air drying, digital copies of the films were produced by directly scanning the developed film using an Epson Perfection 4490 flatbed scanner.

2.5 - Nanoliposomes

Nanoliposomes consisted of cholesterol:sphingomyelin 1:1 with 5% maleimide polyethylene glycol-phosphatidylethanolamine (PEG-PE). Liposomes referred to as 'MAL-PEG liposomes' possess the PEG-PE and maleimide group but lack the RI-OR2-TAT peptide.

PINPS consisted of nanoliposomes with the RI-OR2-TAT peptide attached to the PEG-PE. The RI-OR2-TAT attached to the PINP consists of the amino acid sequence Ac-rGffvlkGrrrrqrrkkrGy-NH$_2$ where L-amino acids are represented by upper case letters and D-amino acids by lower case (with the exception of Glycine, which does not possess distinct enantiomers as it lacks a chiral centre). Attachment to the PEG-PE was achieved using click chemistry via an additional cysteine residue on the RI-OR2-TAT peptide. Each PINP was decorated with ~1690 RI-OR2-TAT peptides and they were previously determined via nanoparticle tracking analysis to have a mean diameter of ~130 nm. RI-OR2-TAT decoration of the liposome accounted for approximately 5% of the liposomal surface area.

PINPs were produced by solubilising the appropriate amounts of cholesterol, sphingomyelin and PEG-PE in chloroform. After ensuring even distribution of the lipids by agitation, the chroloform was evaporarted from the solution using a stream of nitrogen gas. PBS was filtered through a 0.2μm filter to remove any large artifacts in the sample (e.g. salt crystals) before being added to the lipid mixture. Following solubilisation in the PBS solution by agitation, liposomes existed as multilammellar vesicles, rather than the desired unilammelar vesicles. To produce a sample containing unilamellar vesicles, a freeze thaw process was performed 3 times. Theis process involved submersion of the vial containing the liposome

solution in liquid nitrogen for 15 seconds, followed by submersion in a 42°C water bath.

Sonication was then performed in a bath sonicator for 5 minutes before liposomes were

extruded 11 times through a whatmann 130nm polycarbonate membrane. This extrusion

process produced liposomes of the desired size (130nm). For production of MAL-PEG

liposomes, this stage marks the end of the process. For production of PINPs there is a further

step that results in attachment of RI-OR2-TAT to the PEG-PE. RI-OR2-TAT is dissolved in PBS

and coincubated with the PEGylated liposomes at 37°C for 2h. Following this incubation

period, RI-OR2-TAT is attached to the PEGylated liposomes, yielding PINPs (Figure 2.1).
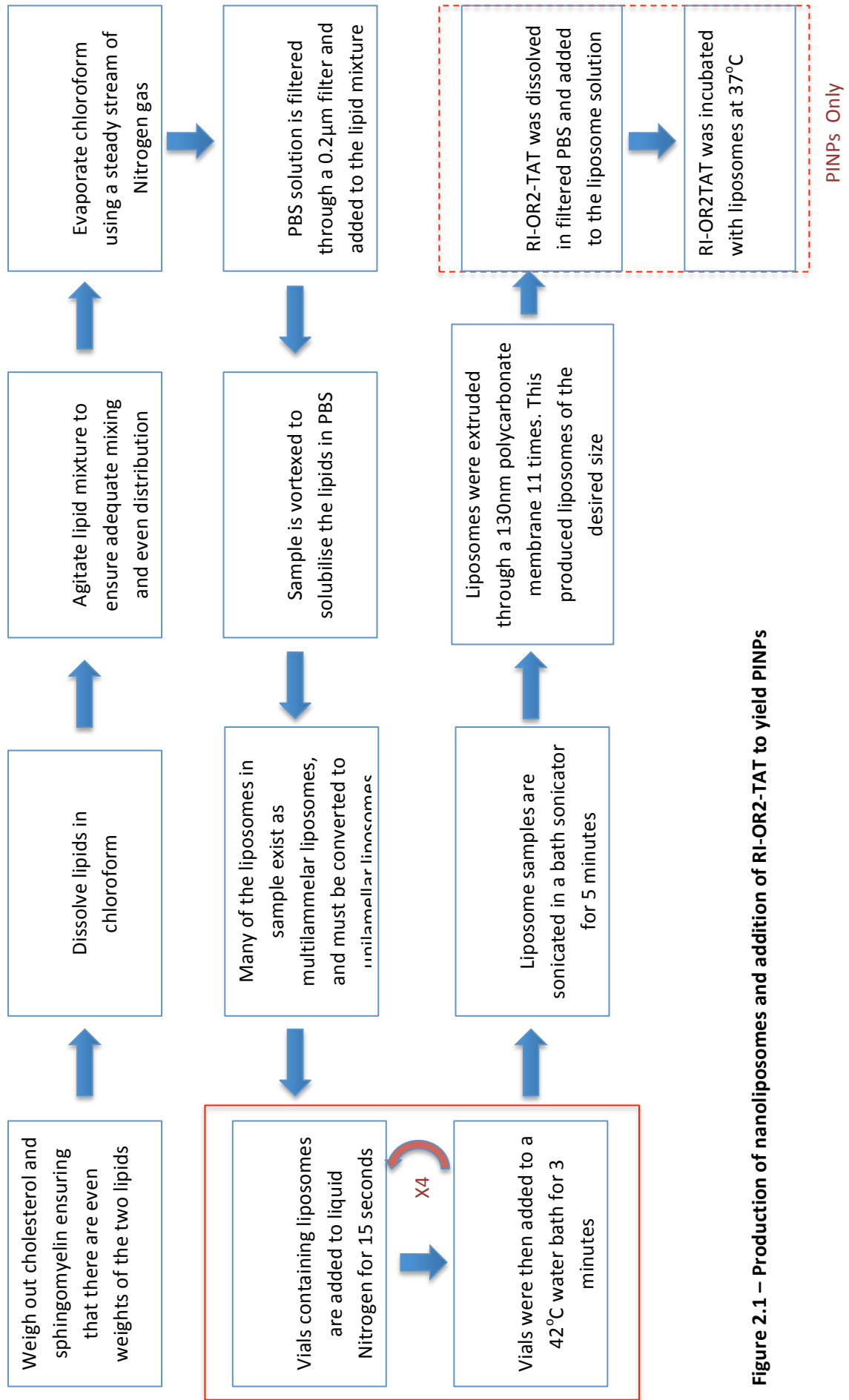
Figure 2.1 – Production of nanoliposomes and addition of RI-OR2-TAT to yield PINPs

Flowchart steps:

- Weigh out cholesterol and sphingomyelin ensuring that there are even weights of the two lipids

- Dissolve lipids in chloroform

- Agitate lipid mixture to ensure adequate mixing and even distribution

- Evaporate chloroform using a steady stream of Nitrogen gas

- PBS solution is filtered through a 0.2μm filter and added to the lipid mixture

- Sample is vortexed to solubilise the lipids in PBS

- Many of the liposomes in sample exist as multilammelar liposomes, and must be converted to unilamellar liposomes

- Vials containing liposomes are added to liquid Nitrogen for 15 seconds

- X4

- Vials were then added to a 42°C water bath for 3 minutes

- Liposome samples are sonicated in a bath sonicator for 5 minutes

- Liposomes were extruded through a 130nm polycarbonate membrane 11 times. This produced liposomes of the desired size

- RI-OR2-TAT was dissolved in filtered PBS and added to the liposome solution

- RI-OR2TAT was incubated with liposomes at 37°C

PINPs Only

2.6 – Determining effect of PINPs upon Aβ$_{1-42}$ aggregation using TEM

2.6.1 – Conventional negative staining

Ultrapure Aβ$_{1-42}$ was purchased solubilised in 1,1,1,3,3,3-hexafluoro-2-propanol (HFIP) (rPeptide LLC), and was frozen for storage. Before use Aβ$_{1-42}$ was removed from the freezer and solubilised in 10 mM phosphate buffer pH 7.4 (PB), diluting the Aβ$_{1-42}$ to a concentration of 25 μM. Samples were vortexed for 1 minute followed by sonication on ice for a further minute to ensure that Aβ$_{1-42}$ peptides were not aggregated at the beginning of the test. Prior to the beginning of the experiment, peptide inhibitor nanoparticles (PINPS) were stored at 4°C. PINPS were solubilised in phosphate buffered saline (PBS) rather than PB as without NaCl, the PINPS would burst in solution. When fully hydrated, PINPS have a diameter of ~130 nm.

The test samples (i.e. Aβ$_{1-42}$ + PB$_2$S + PINPS) were produced so that the ratio of PINPS to Aβ$_{1-42}$ was 1:1. Test samples taken after 0h were vortexed for 30 seconds prior to sample removal for staining, in order to ensure uniform distribution of contents throughout the sample. The control samples (i.e. Aβ$_{1-42}$ + PB$_2$S + PBS) had a ratio of Aβ$_{1-42}$ to PBS of 1:1 and were treated in the same way as test samples. Samples were then negatively stained using the negative staining procedure detailed earlier.

Both test and control samples were stored at 21°C for the duration of the investigation.

2.6.2 – Immunogold labelling

Two different procedures were used for immunogold labelling. The first method was used for figures (6.1.1 and 6.1.2). The second method was used for figures (6.1.3, 6.2.1, 6.3.1). Two different methods were used in order to ensure that the staining protocol employed did not produce inaccurate representations of the samples. By using two different methods, the true appearance of features within the samples could more accurately be determined. The

6E10 primary antibody is a monoclonal anti-Aβ antibody (IgG) raised in mice, with an epitope that lies between the 3rd- 8th amino acids of the Aβ peptide (6E10, Abcam, Cambridge, UK). The secondary antibody used was an anti-mouse IgG antibody raised in goat, conjugated with 10 nm colloidal gold (G7777, Sigma-Aldrich, UK).

The first method used to investigate binding of $Aβ_{1-42}$ oligomer interactions with PINPs was based on a similar method previously used by Al-Hilaly et al. for investigating dityrosine crosslinking of $Aβ_{1-42}$ (Al-Hilaly et al., 2013). Before starting immunolabelling, samples to be labelled had been incubated at $37^{o}C$ for 24 hours. 4 µl of each sample was pipetted onto a 300 mesh formvar and carbon coated copper grid (Agar Scientific, UK) for 1 minute. The sample was then blotted from the grid using filter paper. All further interactions were performed by floating the grids on the solutions mentioned therein. Grids were then blocked for 15 minutes in goat serum:PBS^+ 1:10 to prevent non-specific interactions. PBS^+ consisted of 1% (w/v) bovine serum albumin, 0.05% (v/v) Tween-20, and PBS. Following blocking, grids were incubated at room temperature for 1 hour in the primary antibody 6E10 (0.02 µl/ml). Grids were then washed 3x2 minutes in PBS^+ before being incubated at room temperature with the gold conjugated secondary antibody (diluted 1/50 PBS) for 2 hours. Following incubation with secondary antibody, grids were washed 3x2 minutes in PBS^+ and then 3x2 minutes in distilled water (MilliQ, 0.2 µm filter). Any liquid remaining on the grids was blotted with filter paper and 4 µl 2% PTA was added to grids for 1 minute and then blotted. Grids were left to dry and were examined by TEM.

The second method of immunolabelling did not involve floating the EM grids, but rather the grids were stained in solution. Samples to be stained were removed from the incubator after 24 hours at $37^{o}C$. 10 µl of the sample was added to 10 µl of 6E10 (0.2 µl/ml) and incubated at room temperature for 15 minutes. 10 µl of secondary antibody was then added and incubated for a further 15 minutes. 10 µl of this sample was then pipetted onto a 300 mesh

formvar and carbon coated copper grid (Agar Scientific, UK) for 2 minutes and then blotted. 4 µl of 2% (w/v) PTA was pipetted onto the EM grid, left to stain for 1 minute, and then blotted. Grids were left to dry and then examined by TEM.

2.7 – Determining effect of PINPs upon AB aggregation using the Thioflavin T (ThT) Assay

For this assay, samples were loaded into a black clear-bottomed 384 well microtitre plate. Each well had a total volume of 60 µl and a ThT concentration of 15 µM (ThT solubilised in 10 mM PBS, pH 7.4). For accuracy, each sample was added to the plate in triplicate and space was left between wells containing samples to prevent florescence interference from neighbouring wells. Samples were incubated at 30°C for 48 hours in a Biotek Synergy 2 plate reader, with florescence readings recorded every 10 minutes (excitation wavelength 442 nm, emission wavelength 483 nm). Concentration of $A\beta_{1-42}$ added to wells was 25 µM, with various concentrations of MAL-PEG liposomes, PINPs and RI-OR2-TAT used at relative molar ratios of 1:2, 1:1, 2:1 3:1 (12.5 µM, 25 µM, 50 µM and 75 µM) to $A\beta_{1-42}$.

2.7 - Determining effect of PINPs upon AB aggregation using a sandwich ELISA

To determine $A\beta_{1-42}$ oligomer levels, a sandwich enzyme linked immunosorbent assay (ELISA) approach was employed. The capture antibody was 6E10 and the detetion anytibody was a biotinylated form of 6E10. Briefly, a 96 well plate was incubated with the capture antibody, washed, blocked and then incubated with the samples to be analysed. Any unbound sample was then washed from the plate and biotinylated 6E10 was added (detection antibody). Unbound biotinylated 6E10 was washed from the plate, streptavidin was added and the plate was agitated for 1 hour protected from light. Following a further wash, DELFIA enhancement solution was added and the fluorescence was measured using a Wallac Victor2 multi label plate reader and a time resolved europium detection protocol.

2.8 - Statistics

Data for fibril dimensions are given as average ± standard deviation.

In order to compare the effects of the $A\beta_{1-42}$+PINP coincubations during the sandwhich ELISA to detect $A\beta_{1-42}$ oligomers, triplicate fluorescence values from coincubations were compared with those from the control sample ('Aβ alone') using a one-way ANOVA in IBM SPSS 22. Dunnett's t-tests were performed post-hoc to identify specifically the coincubations with oligomer levels that differed from the control sample. Significance for this test was regarded as a p value less than 0.05.

Chapter 3 – Results I: Production and purification of recombinant Aβ$_{1-42}$

One challenge facing many laboratory groups undertaking research in a variety of fields is the cost of performing research. In the case of research into treatments that aim to prevent aggregation of the Aβ peptide, purchasing this peptide from commercial suppliers comes at a significant cost and therefore developing methods of producing Aβ in-house has the potential to reduce unnecessary expenditure on Aβ. This means that available funds can be made to go further, enabling increased research to be carried out without the need to spend time securing extra funding. Aside from cost, another significant issue with purchasing Aβ$_{1-42}$ from commercial suppliers is that many of these suppliers use peptide synthesizers to produce the peptide, which has been found to result in significant variation between manufacturers and even inter-batch variability from the same manufacturer (Soto et al., 1995). This has a detrimental effect upon the relevance of insights gained using this peptide (as the peptide may not be identical to naturally produced Aβ$_{1-42}$) and may reduce the reproducibility of results. It is also important that any recombinant Aβ$_{1-42}$ that is produced accurately represents naturally produced Aβ$_{1-42}$ as found in the brains of AD sufferers. If this is not the case, investigations into this atypical form of Aβ will bear little relevance in respect to developing further understanding of, and treatments to combat AD.

In order to express Aβ$_{1-42}$ that is soluble and able to be purified, the Aβ$_{1-42}$ peptide is expressed as a ~14 kDa fusion protein that can be cleaved by TEV protease to form the ~4.5 kDa Aβ$_{1-42}$ peptide. The fusion protein consists of multiple different regions, each performing distinct functions which aid the recombinant expression and subsequent purification of this peptide. The regions include a hexa-histidine region for purification, a region enabling solubilisation and reducing aggregation of the peptide, a cleavage site for the TEV protease, and the region encoding the Aβ$_{1-42}$ peptide itself (Figure 3.1) (Finder et al., 2010). The N-

terminal of the fusion protein contains the hexa-histidine tag, followed by a linker region and then the region of the peptide responsible for solubilisation and preventing aggregation. This effect is achieved by incorporating a highly hydrophilic region derived from the circumsporozoite protein found naturally in *Plasmodium falciparum* known as $NANP_{19}$ (as the tetra-peptide sequence Asparagine-Alanine-Asparagine-Proline is repeated 19 times) and its use as a solubilizing partner for $A\beta_{1-42}$ was first reported in 1995 by Dobeli et al. (Dobeli et al., 1995). The hydrophilic nature of this region facilitates solubilisation and this in turn acts to prevent aggregation. The purpose of the TEV protease cleavage site is to enable post-purification cleavage of all regions of the fusion protein from the region consisting of the $A\beta_{1-42}$ peptide and the presence of the $NANP_{19}$ region enables the cleavage process to be performed in solution. Following completion of the peptide expression stages of the experimental protocol, purification is performed to reduce impurities in the sample, before the $A\beta_{1-42}$ peptide domain of interest is cleaved from the larger fusion protein construct.

Figure 3.1 – Structure of recombinant $A\beta_{1-42}$ fusion protein. The fusion protein contains a hexa-histidine (6xHis) sequence at the N-terminal that is used to bind the protein to the IMAC column during purification. L1 is short linker sequence consisting of Glycine-Serine, L2 is a short linker sequence consisting of Arginine-Serine. The purpose of the linker sequences is to join different regions of the fusion protein without interference that would disrupt the structure or the necessary characteristics of each domain. The $NANP_{19}$ region is incorporated into the fusion protein to reduce aggregation of the $A\beta_{1-42}$ peptide and increase solubility. The cleavage sequence (CS) provides an amino acid sequence recognised by the TEV protease so that the $A\beta_{1-42}$ peptide can be cleaved from the fusion protein. The $A\beta_{1-42}$ region contains the $A\beta_{1-42}$ peptide of interest.

3.1 - Expression of $A\beta_{1-42}$

The production of $A\beta_{1-42}$ is achieved by the expression of a ~14 kDa fusion protein which must be cleaved by the TEV protease to yield the ~4.5 kDa $A\beta_{1-42}$ peptide. This study involved performing all production and purification steps following the transfection of the bacterial

cell lines with the plasmids encoding Aβ$_{1-42}$ fusion protein and TEV protease. The *E.coli* cells

encoding the Aβ$_{1-42}$ fusion protein were provided as part of a MTA by Professor Rudolph

Glockshuber.
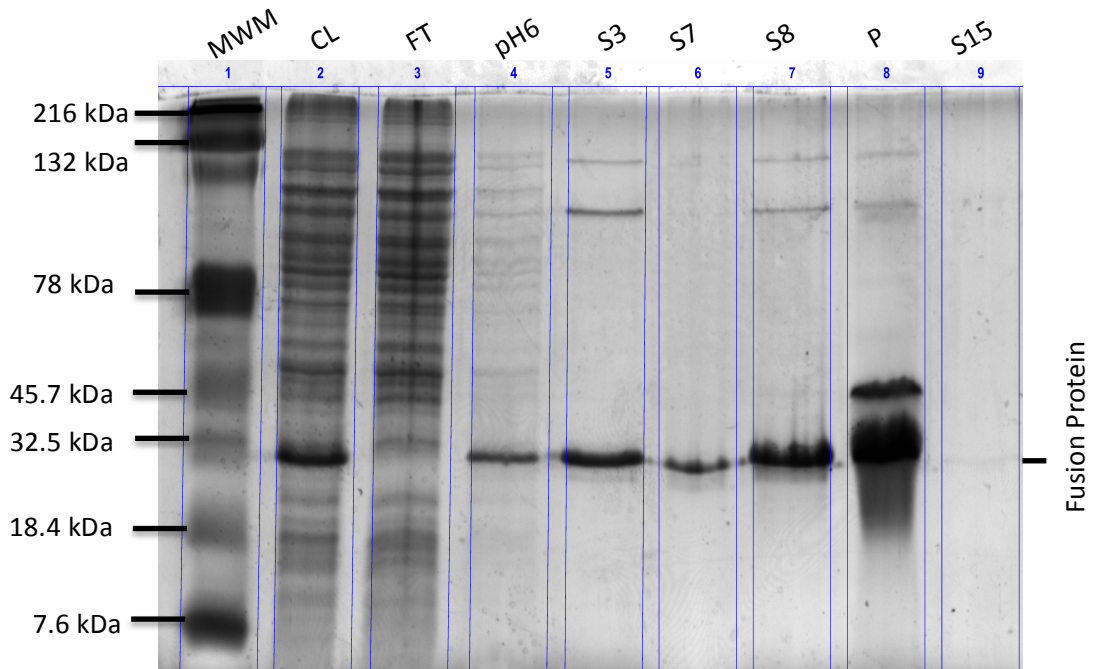
Figure 3.1.1 – Coomassie stained polyacrylamide gel following SDS-PAGE of uncleaved recombinant Aβ$_{1-42}$ at various stages of the purification process. Lanes were run as follows: Lane 1 - Molecular weight marker, Lane 2 – Cell lysate, Lane 3 – eluent from Ni-NTA column following addition of cell lysate, Lane 4 – eluent from Ni-NTA column following addition of guanidine buffer at pH6, Lanes 5, 6 and 7 and 9 – eluent from Ni-NTA column following addition of guanidine buffer at pH2 (number corresponds to the order in which 1ml samples were eluted from column i.e. S7 = 7th 1ml aliquot), Lane 8 – Pooled sample containing protein from the 3 1ml aliquots containing the highest protein concentrations).

Coomassie staining of samples from various stages of purification of the uncleaved Aβ$_{1-42}$

clearly show that passing the cell lysate through the nickel-nitriloacetic acid (Ni-NTA) column

significantly increases the purity of samples collected after passage through the column. The

initial cell lysate (lane 2) contains a large number of distinct bands representing a variety of

proteins of numerous different molecular weights and the majority of these proteins do not

bind to the column and are thus eluted (Lane 3). Following addition of guanidine buffer at

pH6 (lane 4), the proteins eluted from the column are much less numerous than those contained within the cell lysate flow-through. Following the addition of guanidine buffer at pH2 to release the proteins bound to the column with the highest affinity (i.e. containing a significant number of histidine residues) there were fewer protein bands than were detected following addition of pH6 buffer. This is illustrated by the appearance of only 3 bands in the 1ml aliquots collected at this stage (lanes 5, 6, 7 and 9). Following this purification step, the 3 aliquots with the greatest protein concentration (aliquots 6,7,8) were combined in order to pool a significant amount of the $A\beta_{1-42}$ peptide thought to be present within these samples. This sample is shown in lane 8.

The most intense band observed following Coomassie staining of these protein samples has a molecular weight of approximately 30 kDa. The cell lysate sample (lane 2) shows a significant quantity of this protein, which is not present in the flow through following the addition of the cell lysate to the Ni-NTA column (lane 3). This indicates that this protein has a strong affinity for the purification column. The elution of protein at this molecular weight following addition of pH2 buffer shows that the protein was indeed attached to the Ni-NTA column and therefore is likely to contain a substantial number of histidine residues. Although the $A\beta_{1-42}$ protein was expressed as a fusion protein with a hexa-histidine tag for purification by this method, there is no band present at the reported molecular weight of the fusion protein – 14 kDa.

Further analysis of the identity of the proteins observed following Coomassie staining was performed using western blotting as illustrated in Figure 3.1.2.
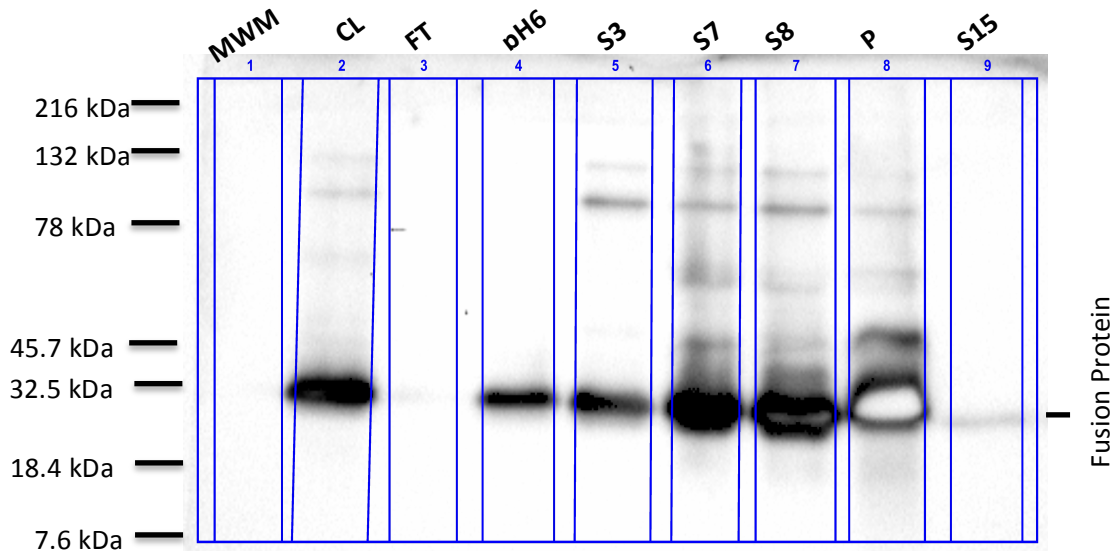
Figure 3.1.2. – Western blot of samples taken at different stages of the Aβ$_{1-42}$ purification process. Western blotting of this sample used a mouse raised anti-Aβ monoclonal antibody (6E10) as the primary antibody, and an Anti-mouse immunoglobulin antibody conjugated with HRP as the secondary antibody. Lanes were run as follows: Lane 1 - Molecular weight marker, Lane 2 – Cell lysate, Lane 3 – eluent from Ni-NTA column following addition of cell lysate, Lane 4 – eluent from Ni-NTA column following addition of guanidine buffer at pH6, Lanes 5,6,7 and 9 – eluent from Ni-NTA column following addition of guanidine buffer at pH2 (number corresponds to the order in which 1ml samples were eluted from column i.e. S7 = 7th 1ml aliquot), Lane 8 – Pooled sample containing protein from the 3 1ml aliquots containing the highest protein concentrations).

In order to determine whether the protein samples generated following the purification process contained the Aβ$_{1-42}$ peptide of interest, western blotting was performed using 6E10 as the primary antibody and therefore a positive result would confirm the presence of the Aβ$_{1-42}$ peptide. As shown in figure 3.1.2, positive labelling was detected corresponding to the molecular weight of the intense bands observed following coomassie staining (~30 kDa). Although the most intense labelling was observed of a protein of ~30 kDa, there were also other bands present at a reduced intensity. These bands of various molecular weights indicate that there were Aβ$_{1-42}$ peptides (or regions of Aβ$_{1-42}$ peptides) that had migrated through the polyacrylamide gel at different rates than the majority of the recombinantly expressed Aβ$_{1-42}$ peptide. The intensity of the labelling observed was as expected, with lanes with increased A280 readings (lanes 6 and 7) showing greater labelling than those with lower

A280 readings (lanes 5 and 9). The pooled sample contained the contents of the 3 most concentrated 1 ml aliquots following passage through the Ni-NTA column and therefore exhibited the most intense labelling (lane 8). This intense labelling appears as a white (rather than black) region on the blot. This is due to bleaching of the nitrocellulose membrane during analysis due to the intense labelling of the membrane in this region. Strong labelling can also be observed in the cell lysate before purification of the sample was performed (lane 2), indicating the presence of the uncleaved $A\beta_{1-42}$ fusion protein within the large number of different proteins contained within this sample.
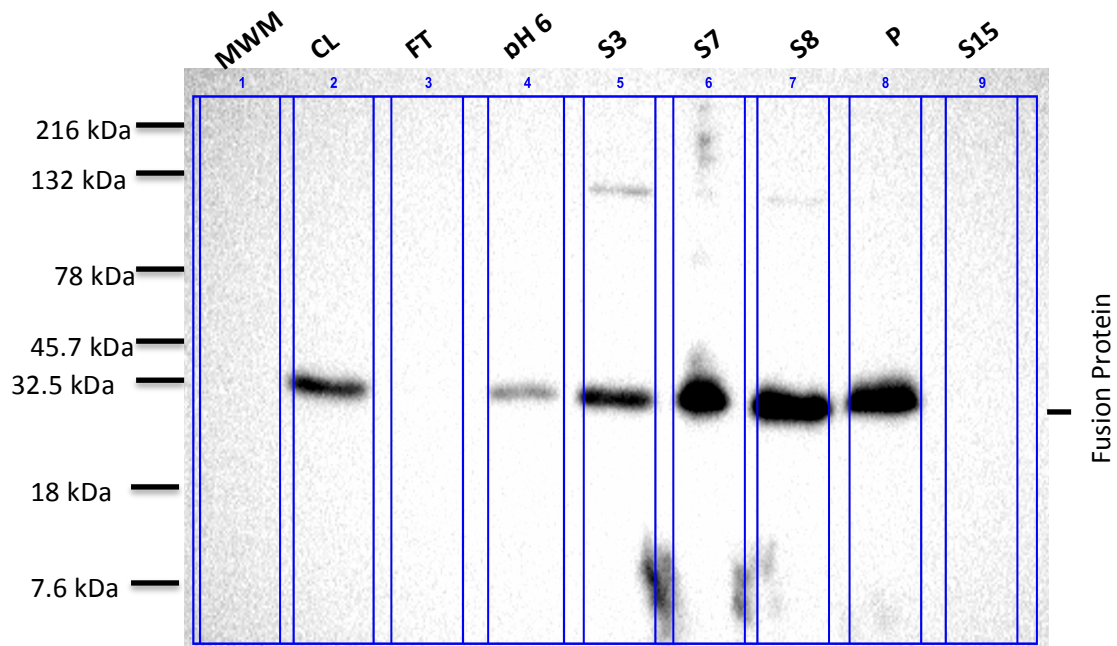
Figure 3.1.3 – Western blot of uncleaved Aβ$_{1-42}$ samples at various stages throughout the purification process. This western blot used a mouse raised primary antibody that recognised a hexa-histidine (6xHis) sequence as such a sequence is located at the N-terminus of the Aβ$_{1-42}$ fusion protein, and an Anti-mouse immunoglobulin antibody conjugated with HRP as the secondary antibody. Lanes were run as follows: Lane 1 - Molecular weight marker, Lane 2 – Cell lysate, Lane 3 – eluent from Ni-NTA column following addition of cell lysate, Lane 4 – eluent from Ni-NTA column following addition of guanidine buffer at pH6, Lanes 5,6 and 7 and 9 – eluent from Ni-NTA column following addition of guanidine buffer at pH2 (number corresponds to the order in which 1ml samples were eluted from column i.e. S7 = 7th 1ml aliquot), Lane 8 – Pooled sample containing protein from the 3 1ml aliquots containing the highest protein concentrations).

Further western blotting analysis was conducted using an antibody that recognises a hexa-histidine sequence as its epitope as shown in figure 3.1.3. Labelling using this antibody was performed as the Aβ$_{1-42}$ fusion protein contains a hexa-histidine sequence and therefore the presence of this sequence would strongly indicate the presence of the fusion protein. Again, positive labelling occurred for a protein with a molecular weight of ~30 kDa indicating that the most intense band observed following Coomassie staining represents the recombinant Aβ$_{1-42}$ fusion protein of interest, albeit at a different molecular weight than was expected (i.e. ~30 kDa rather than 14 kDa). Lanes 5 and 7 show bands of a greater molecular weight

than the positively labelled fusion protein. Interestingly, these bands appear to be of the same molecular weight as those that also showed positive labelling during western blotting with the 6E10 antibody (to detect Aβ$_{1-42}$). As was the case when undertaking western blotting with the 6E10 antibody, labelling by the hexa-histidine recognising antibody shows that labelling intensity corresponds to what was expected due to the differing A280 for the different samples, with the samples that exhibited the greatest A280 showing increased labelling compared with those with lower A280.

In order to separate the Aβ$_{1-42}$ peptide from the fusion protein, the Aβ$_{1-42}$ region must be cleaved. This is performed using the TEV protease, which recognises a specific cleavage sequence that has been inserted at the N-terminus of the Aβ$_{1-42}$ region of the fusion protein.
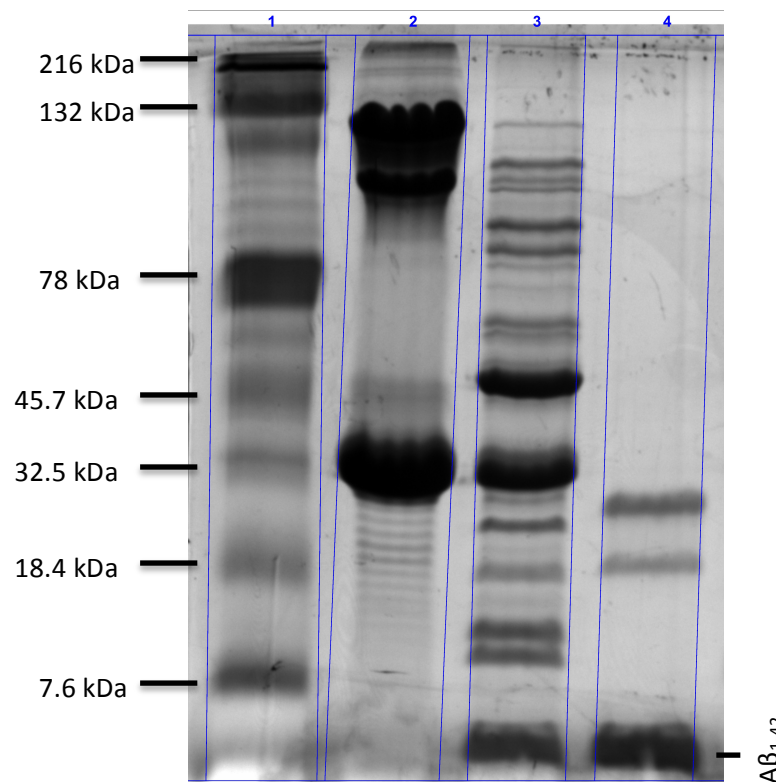

Figure 3.1.4 – Coomassie stained SDS-PAGE gel showing electrophoretic profiles of various Aβ$_{1-42}$ samples. Lanes are as follows: Lane 1 – molecular weight marker, Lane 2 – Uncleaved Aβ$_{1-42}$ taken from the 'Pooled' Aβ$_{1-42}$ sample, Lane 3 - Aβ$_{1-42}$ sample following cleavage with TEV protease, Lane 4 – Commercial Aβ$_{1-42}$ purchased from rPeptide.

Coomassie staining of the 3 different $A\beta_{1-42}$ samples (cleaved, uncleaved, commercial) revealed similarities as well as differences between the samples. The uncleaved sample showed an intense band around the ~30 kDa region as well as ~130 kDa. The presence of a band ~30 kDa was expected as this was observed when this sample was coomassie stained previously (3.1.1), however the band at ~130 kDa was not previously observed. There are multiple clear differences in the banding patterns of the uncleaved and cleaved $A\beta_{1-42}$ samples (lanes 2 and 3 respectively). The cleaved sample lacked a large intense band ~130 kDa and possessed a greater number of distinct bands of a variety of different molecular weights. The purpose of the cleavage step was to produce $A\beta_{1-42}$ which is known to have a molecular weight of ~4.5 kDa. One important difference between the uncleaved and cleaved $A\beta_{1-42}$ samples is the presence of an intense band below the lowest molecular weight marker band of 7.6 kDa in the cleaved lane, but not in the uncleaved lane. As the molecular weight is under 7.6 kDa, this intense band in the cleaved sample was considered to be the $A\beta_{1-42}$ peptide. This view was supported by the finding of an identical band at the same position in the lane containing commercially produced $A\beta_{1-42}$ (lane 4).

In order to investigate more accurately whether the band observed further down the gel than the 7.6 kDa marker indicated the presence of the $A\beta_{1-42}$ peptide, western blotting was performed.
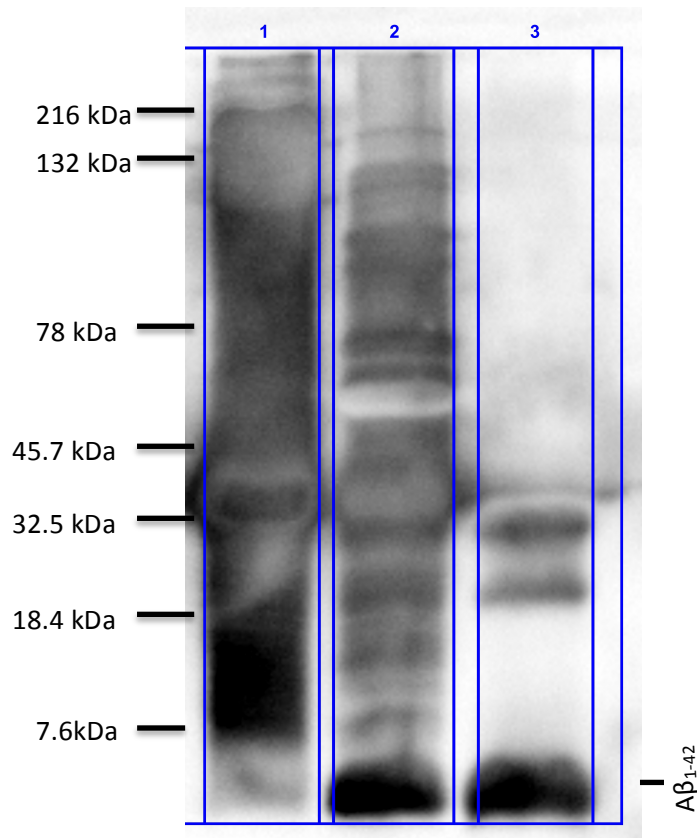
Figure 3.1.5 – Western blot analysis of cleaved and uncleaved Aβ$_{1-42}$ samples. A mouse raised anti-Aβ monoclonal antibody (6E10) was used as the primary antibody, and an Anti-mouse immunoglobulin antibody conjugated with HRP as the secondary antibody. Lanes were run as follows: Lane 1 – Uncleaved Aβ$_{1-42}$, Lane 2 - Cleaved Aβ$_{1-42}$, Lane 3 - Commercially produced Aβ$_{1-42}$ (rPeptide).

Western blotting using the 6E10 antibody to recognise Aβ$_{1-42}$ showed positive labelling in all 3 lanes as expected. The lane containing cleaved Aβ$_{1-42}$ (lane 2) shows intense labelling below the 7.6 kDa molecular weight marker band that corresponds to the bands observed following coomassie staining that were thought to be the Aβ$_{1-42}$ peptide. The positive labelling of these bands when using the 6E10 antibody confirms the presence of Aβ$_{1-42}$ in this band. The likelihood of this band is further supported by the intense labelling of a highly similar band in the lane containing commercially produced Aβ$_{1-42}$ (lane 3) and also by the lack of this band in the lane containing the uncleaved Aβ$_{1-42}$ fusion protein (lane 1).

Further western blotting was performed using an anti-Hexa-his antibody to demonstrate the cleavage of the $A\beta_{1-42}$ by the lack of a hexa-histide tag attached to the peptide.
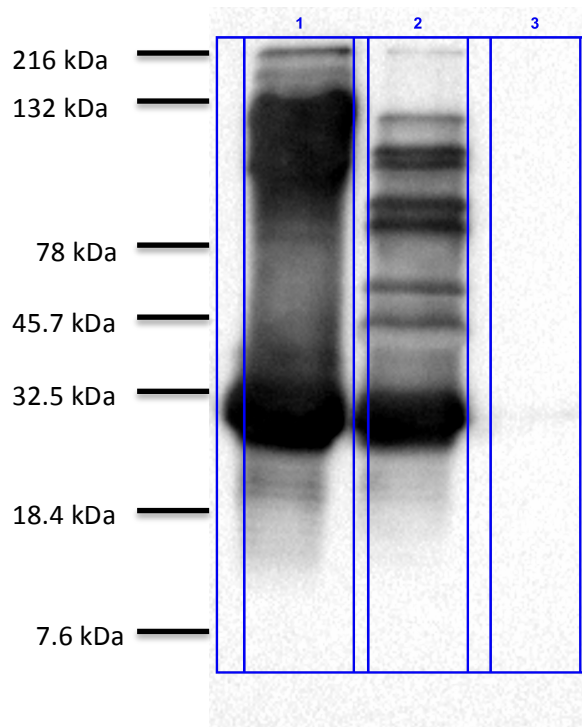
Figure 3.1.6 – Western blot analysis of various $A\beta_{1-42}$ samples following the cleavage process. This western blot used used a mouse raised anti-Hexa-his monoclonal antibody as the primary antibody, and an Anti-mouse immunoglobulin antibody conjugated with HRP as the secondary antibody. Lanes were run as follows: Lane 1 – Uncleaved $A\beta_{1-42}$, Lane 2 - Cleaved $A\beta_{1-42}$, Lane 3 - Commercially produced $A\beta_{1-42}$ (rPeptide).

The results from the western blot using antibodies targeting the hexa-histidine sequence does not show any positive labelling below the 7.6 kDa molecular weight marker band. This (combined with the reduced molecular weight) indicates that the cleavage process has effectively cleaved the $A\beta_{1-42}$ peptide from the cleavage protein possessing the hexa-histidine affinity tag. The observation of an intense band is still observed in the uncleaved sample at a molecular weight of ~30 kDa.

3.2 - Expression of Tobacco Etch Virus (TEV) protease

In order to cleave the Aβ fusion protein, the TEV protease (also known as the Nuclear Inclusion a Protease) is expressed and then used to cleave the fusion protein, producing the

Aβ$_{1-42}$ peptide. As one of the aims of this project was to develop an in-house production method for Aβ, expression of TEV was also performed in-house.

Figure 3.2.1 shows Coomassie staining of a polyacrylamide gel loaded with a number of samples collected throughout different stages of the purification process. As the sample is passed through the Nickel column, flow through (i.e. solution exiting the column) from different stages of purification can be seen to contain different proteins, which appear as bands of differing positions and intensities. The vertical position and intensity of each band reflects the levels of protein of a particular molecular weight. The nickel column is used to purify proteins by utilising the high binding affinity that histidine possesses towards the nickel in the column.
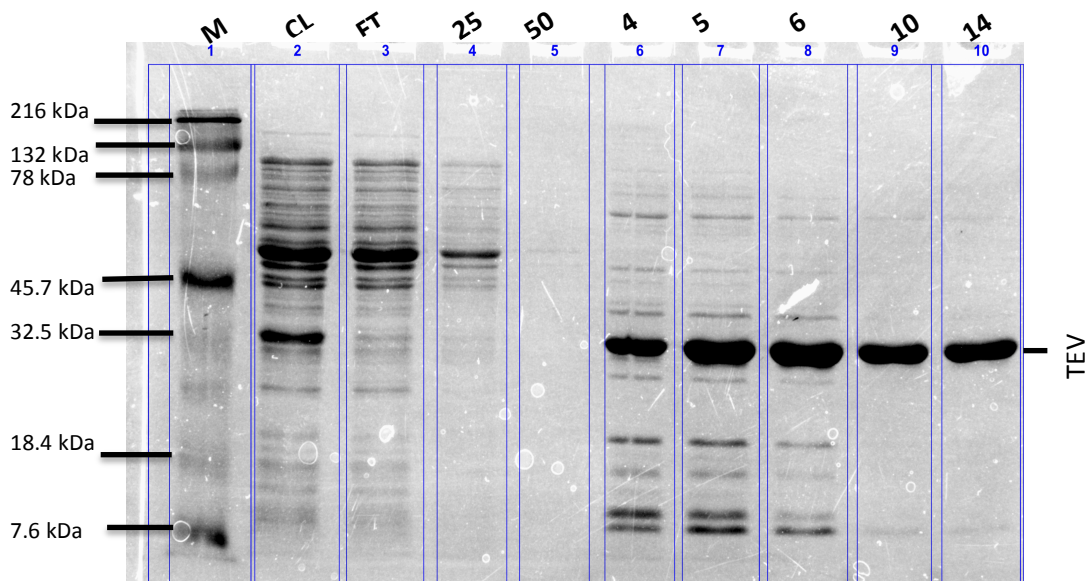
Figure 3.2.1 – Coomassie staining of a polyacrylamide gel containing samples from various stages of the TEV purification process. Lane order is as follows: Lane 1 - MW Marker (MW), Lane 2 – cell lysate (CL), Lane 3 – Cell Lysate flow-through (FT), Lane 4 – 25 mM Imidazole flow-through (25), Lane 5 – 50 mM Imidazole flow-through (50), Lanes 6-10 represent 1 ml aliquots of flow-through following addition of 500 mM Imidazole to the column (6 – 4th ml, 7 – 5th ml, 8 – 6th ml, 9 – 10th ml, 10 – 14th ml).

The cell lysate sample can be seen to form multiple distinct bands indicating the presence of numerous different proteins with different molecular weights. The lane containing the cell lysate (Lane 2) and the lanes containing the 1ml samples collected after the addition of 500 mM Imidazole (Lanes 6-10) show significant quantities of a protein with a molecular weight of approximately 29 kDa. The samples that were collected between the addition of filtered cell lysate and addition of 500 mM imidazole (lanes 3-5) to the column show a marked reduction in levels of protein of this MW. Lanes 6-10 also contain bands relating to proteins that have different molecular weights than 29 kDa. The mean total protein concentrations measured in the 1ml aliquots were as follows: 4 – 2.17 mg/ml, 5 – 3.04 mg/ml, 6 – 2.78 mg/ml, 10 – 1.81 mg/ml, 14 – 1.61 mg/ml. The levels of the proteins with weights which do not correspond to ~29 kDa appear to decrease in samples collected at later stages of the 500 mM Imidazole phase of elution compared with those collected at earlier stages. This indicates that the purity of the sample increases as more 500 mM imidazole is added and eluted from the column, leaving the majority of the remaining protein corresponding to the band observed at ~29 kDa. Although the samples are initially identical, the level of TEV in the FT sample is much reduced compared with that of the CL sample and is due to the binding of TEV to the nickel column and remaining associated with the column rather than passing through the column and exiting with the flow-through. This is in contrast to the CL, which is not passed through the column and therefore contains significant amounts of TEV upon analysis. The molecular weight of the recombinant TEV protein used in this study is 28.6 kDa.

TEV Protein Elution Profile
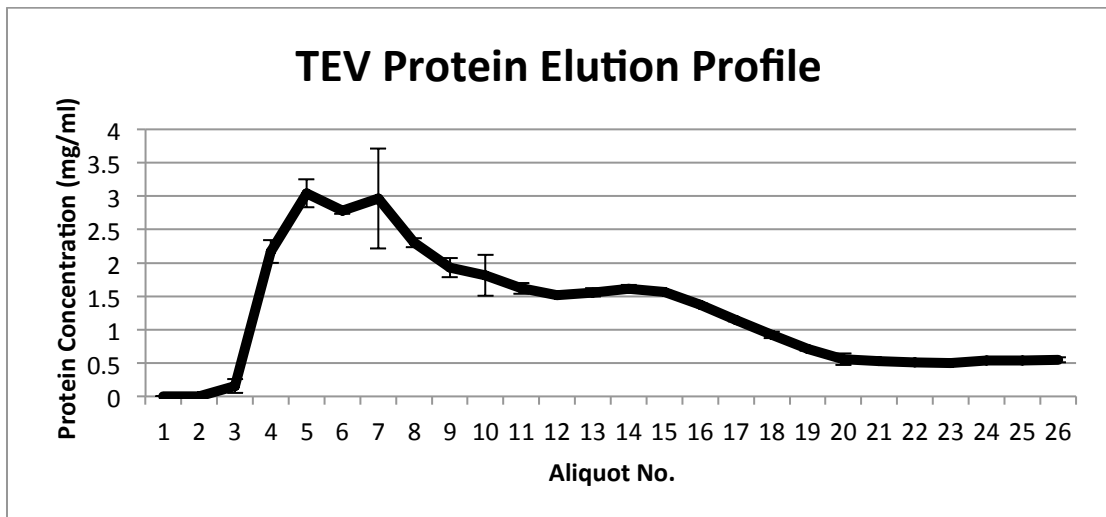
Figure 3.2.2 – TEV protein elution profile. Graphical representation of the different concentrations of TEV protein detected in 1ml samples collected from a Nickel column following addition of 500 mM Imidazole. Points represent the mean of 3 replicates ± SD.

Figure 3.2.2 shows how the measured concentration of protein in 1ml samples from the 500 mM Imidazole flow-through varied depending on the timing of collection of each sample. Initially, the first 2 samples were found to contain no protein, which was followed by a sharp increase in concentration and then a trend of decline in concentration towards the end of the 500 mM imidazole flow-through.

Figure 3.2.3 shows a western blot from different samples taken at various steps throughout the purification process. The monoclonal primary antibody (Clontech, 631212) used in this process recognised the epitope of a hexa-histidine tag, which was expressed as part of the recombinant TEV fusion protein and was raised in mouse. The polyclonal secondary antibody was an anti-mouse antibody conjugated with horseradish peroxidase (Dako, P0447).
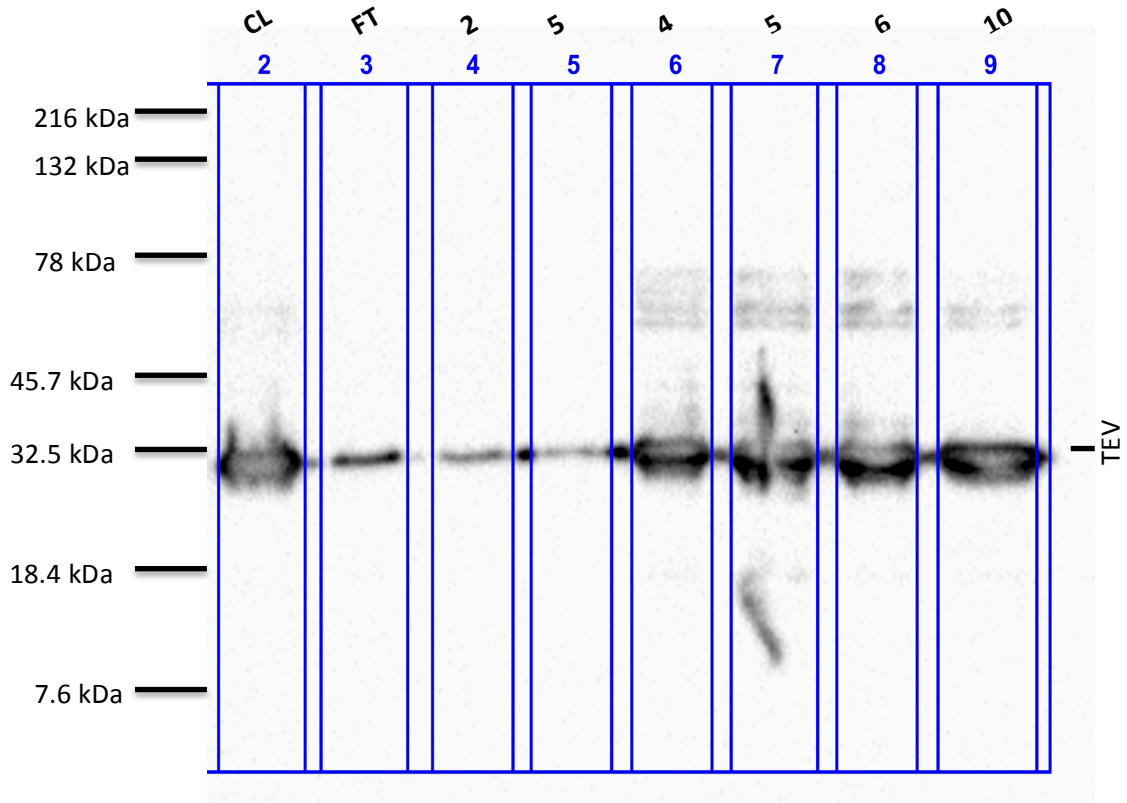
Figure 3.2.3 – Western blot using samples from various steps throughout the TEV expression process. Lane order is as follows: 2 – cell lysate, 3 – Cell Lysate flow-through, 4 – 25 mM Imidazole, 5 – 50 mM Imidazole, 6-9 represent 1ml aliquots taken following addition of 500 mM Imidazole to the column (6 – 4th ml, 7 – 5th ml, 8 – 6th ml, 9 – 10ml).

Figure 3.2.3 shows the presence of a relatively large amount of a protein associated with histidine in lanes corresponding to flow-through from cell lysate (lane 2) and 500 mM imidazole (lanes 6-9), with a significantly lower amount of protein detected in lanes corresponding to flow-thorough following addition of FT, 25 mM imidazole, 50 mM imidazole (lanes 3-5 respectively). The protein detected most strongly by this western blot appears to be present at various amounts in positions which correspond to the ~29 kDa protein observed by Coomassie staining (Figure 3.2.1). Due to the MW of TEV corresponding to the bands representing significant concentrations of protein in Figure 3.2.1 as well as the detection of a significant concentration of histidine containing protein by the western blot,

these results strongly suggest that the protein detected in significant quantities is the TEV protein.

3.3 – TEM analysis of rA$\beta_{1\text{-}42}$ aggregation

Following expression the A$\beta_{1\text{-}42}$ was purified (by IMAC and centrifugation) and analysed by electron microscopy. The purpose of analysis by TEM at 0h was to determine the level of aggregation of the recombinant A$\beta_{1\text{-}42}$ at 0h (i.e. following purification). This information is essential for future studies involving this recombinantly produced Aβ. Additionally, analysis of recombinant A$\beta_{1\text{-}42}$ following 14 days incubation at 37$^{\text{o}}$C was performed by TEM. The purpose of this analysis was to visualise the aggregation characteristics of the recombinant A$\beta_{1\text{-}42}$ following a significant period of incubation.

3.3.1 - Recombinant A$\beta_{1\text{-}42}$ at 0h

At 0h incubation, the recombinantly expressed A$\beta_{1\text{-}42}$ peptide sample was found to contain various amyloid structures of different sizes and morphologies. Figures 3.3.1.1 and 3.3.1.2 show very small amyloid structures as well as larger structures. The smaller spheroid structures (O) resemble A$\beta_{1\text{-}42}$ oligomers whilst the larger structures (P) resemble protofibrils. At 0h no mature fibrils were detected in the samples. Figures 3.3.1.1 and 3.3.1.2 appear to show that following 0h incubation, protofibrils were more common species of Aβ aggregation than small oligomers. From 0h samples: average oligomer diameter = 7.6 ± 1.1 nm, average fibril length = 80.4 ± 51.2 nm, average fibril width = 7.3 ± 1.1 nm.
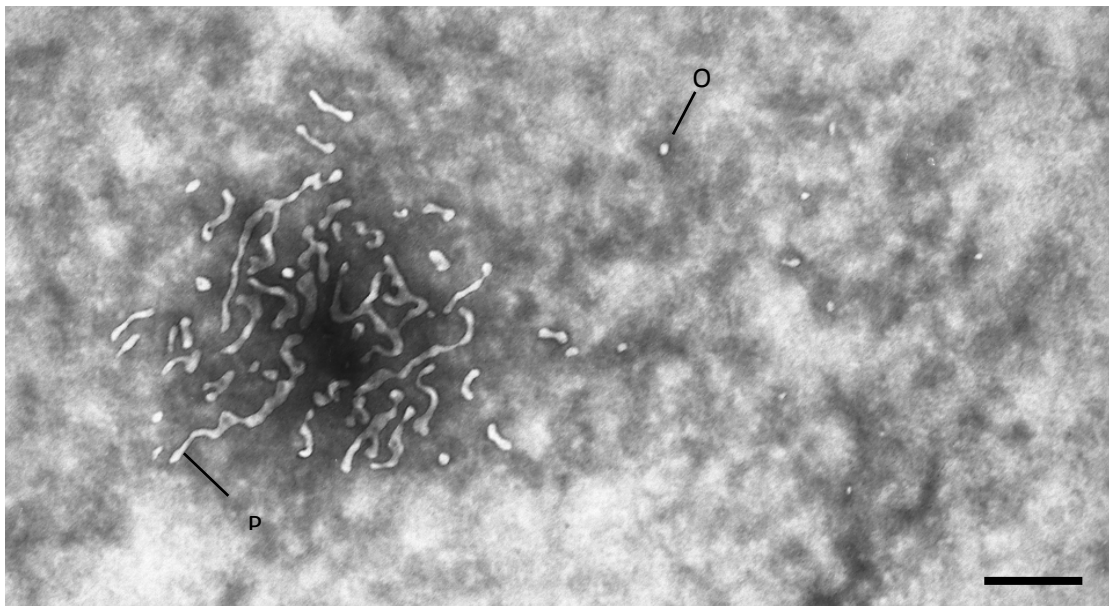
Figure 3.3.1.1 - Recombinant Aβ$_{1-42}$ at 0h. The sample has been negatively stained using 2% PTA at a pH of 7.4. Various different sized amyloid structures (O) and (P) are visible. Scale bar = 100 nm.
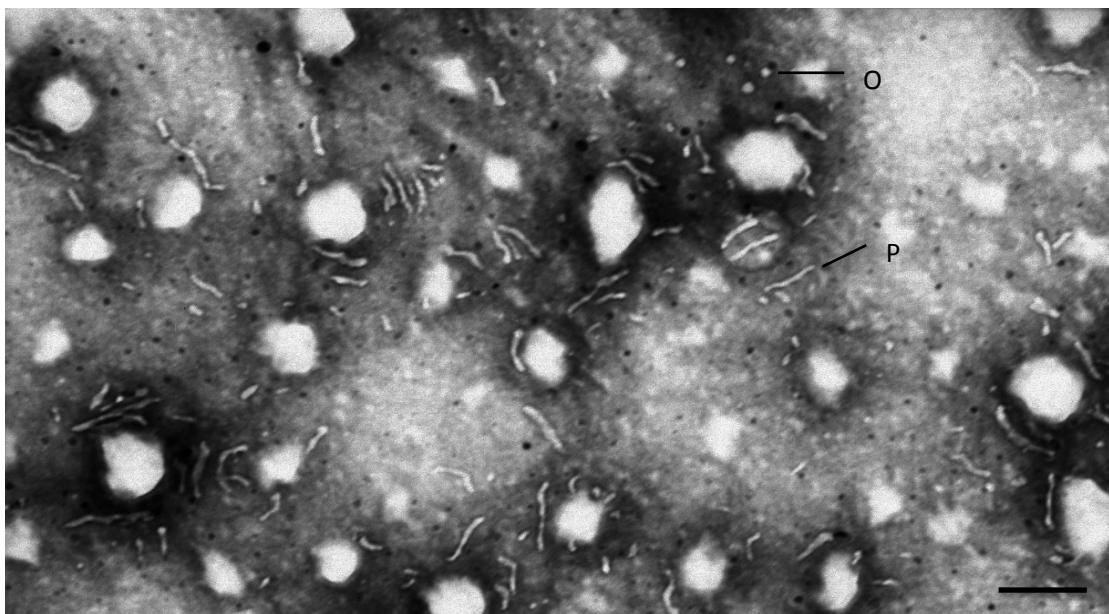
Figure 3.3.1.2 – Recombinant Aβ$_{1-42}$ at 0h. The sample has been negatively stained using 2% PTA at a pH of 7.4. Various different sized amyloid structures (O) and (P) are visible. Scale bar = 100 nm.

3.3.2 – Recombinant Aβ$_{1-42}$ after 14 day incubation at 37°C.

Following 14 days incubation in PBS at 37°C, the appearance of the amyloid structures had changed significantly from what was observed at 0h. Following 14 days incubation the Aβ$_{1-42}$ peptide had aggregated forming bundles of amyloid fibrils (figure 3.3.2.2, 3.3.2.3, 3.3.2.6-3.3.2.12) as well as individual fibrils in less concentrated regions of Aβ$_{1-42}$ (3.3.2.4). The incubated samples were also found to contain areas of dense Aβ$_{1-42}$ aggregation (figure 3.3.2.1, 3.3.2.10, 3.3.2.11). One characteristic feature of the incubated sample was that the incubation period and conditions resulted in the aggregation of the Aβ$_{1-42}$ into long fibrils. Another characteristic feature was that these fibrils were shown in multiple cases to associate with other fibrils in a parallel fashion. Figures 3.3.2.8 and 3.3.2.9 illustrate these parallel associations in greater detail, revealing them to contain as many as 10 or as few as 2 individual fibrils. The average number of fibrils per bundle was 5.2 ± 2.6. In addition to Aβ$_{1-42}$ structures in the samples, dense areas of amorphous material were also present (3.3.2.3-3.3.2.5). For the incubated sample, average fibril width was 7.3 ± 1.1 nm. Due to the density and length of fibrils exceeding the micrograph (or of insufficient clarity), fibril length was undeterminable.
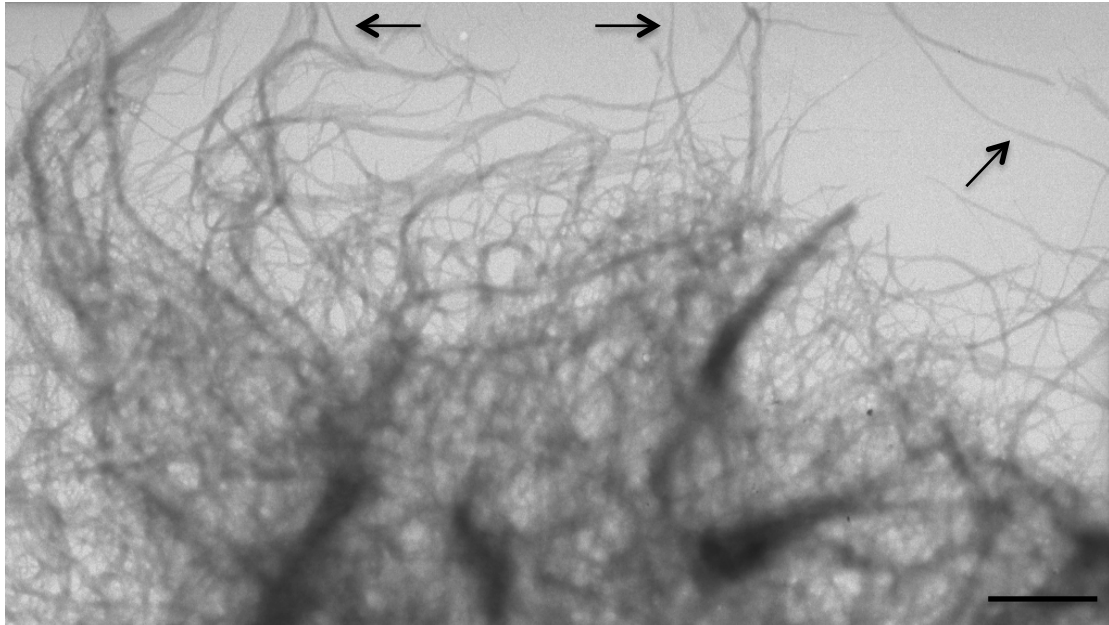
Figure 3.3.2.1 – Recombinant Aβ$_{1-42}$ (25µM) incubated for 14 days at 37°C. Dense regions of Aβ$_{1-42}$ aggregation can be seen as Aβ$_{1-42}$ monomers have aggregated into fibrils (see arrows), indicated by positive staining in this sample. Scale bar = 1 µm.
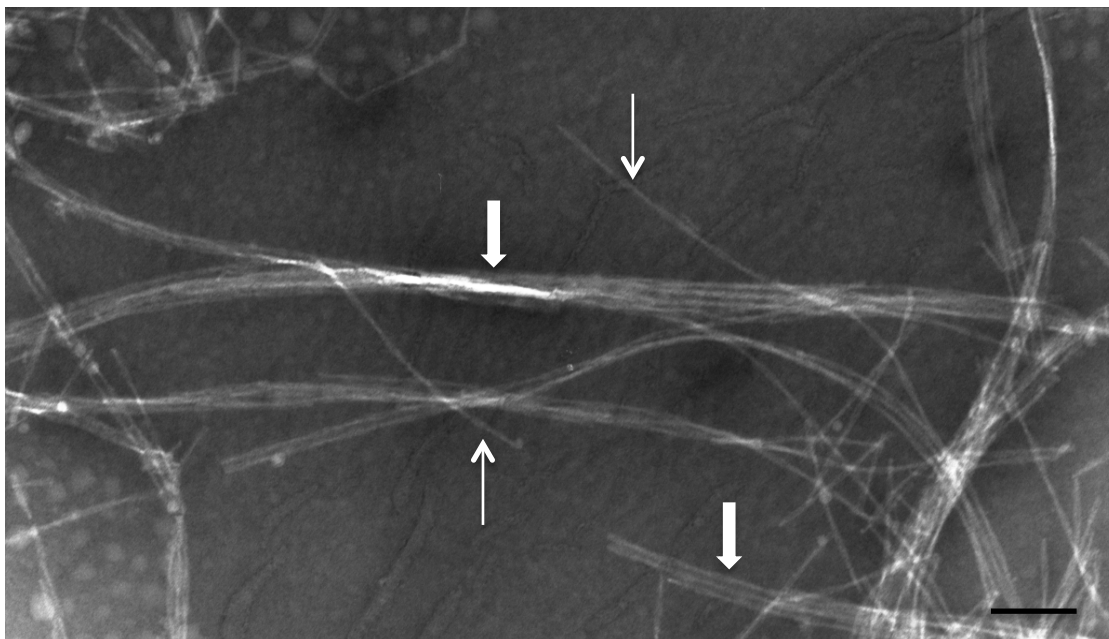

Figure 3.3.2.2 - Recombinant Aβ$_{1-42}$ (25µM) incubated for 14 days at 37°C. Bundles of fibrils are visible, consisting of multiple parallel fibrils (thick arrows). In addition to the bundles of fibrils, single fibrils can also be seen which have no such parallel association with other fibrils (thin arrows). Scale bar = 100 nm.
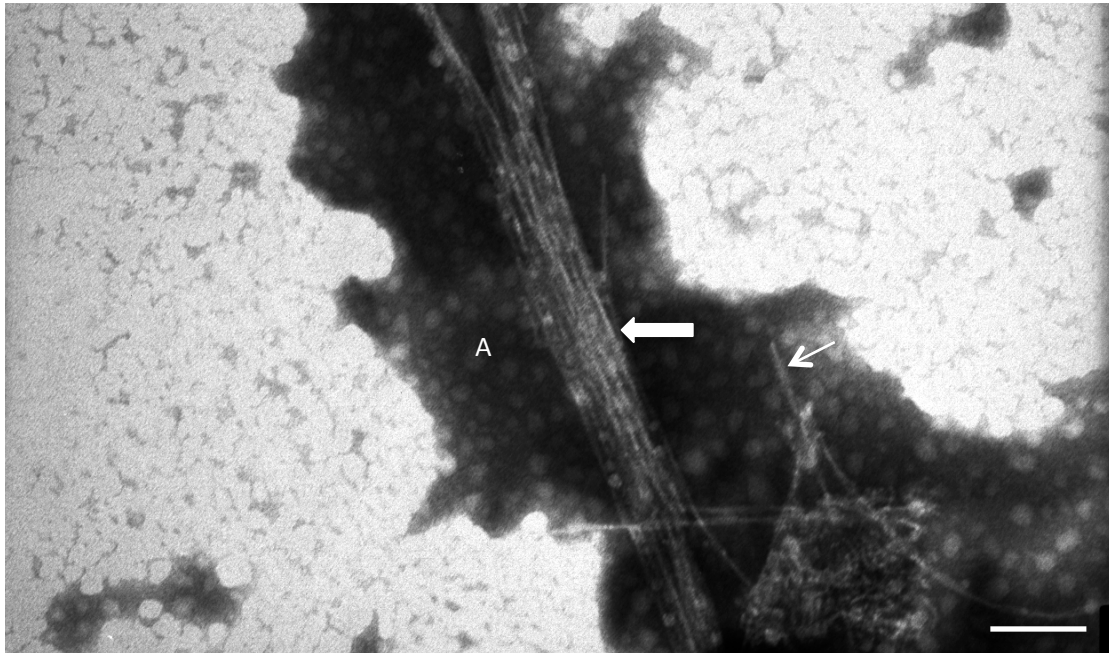
Figure 3.3.2.3 - Recombinant Aβ$_{1-42}$ (25µM) incubated for 14 days at 37°C. The sample in the image can be seen to contain numerous parallel fibrils (thick arrow), single fibrils (thin arrow) and amorphous material (A). Scale bar = 100 nm.
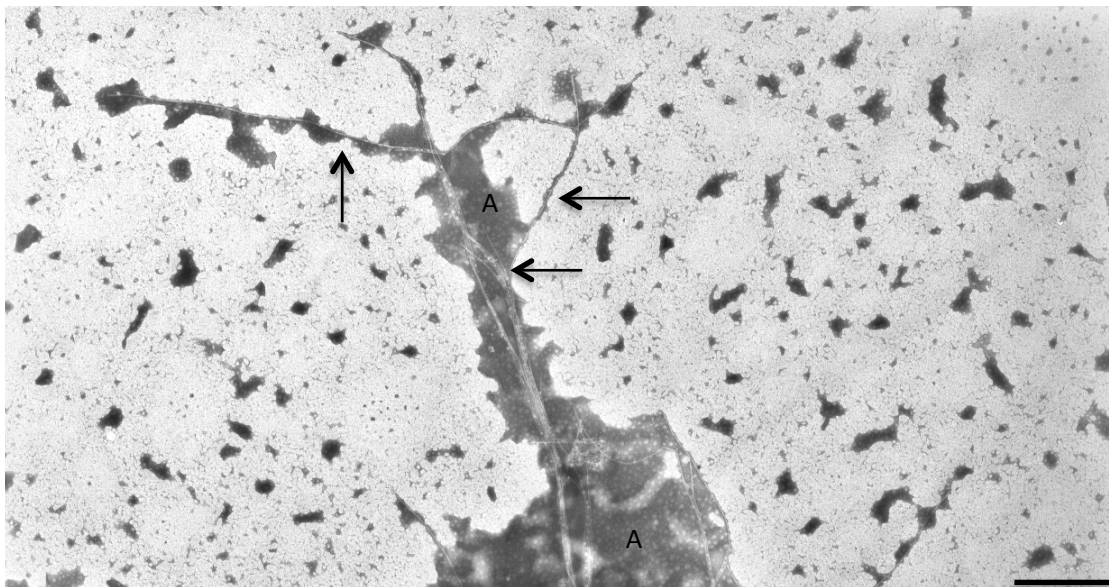
Figure 3.3.2.4 - Recombinant Aβ$_{1-42}$ (25µM) incubated for 14 days at 37°C. A small number of fibrils are present (black arrows), surrounded by amorphous material (A). Scale bar = 500 nm.

Figure 3.3.2.5 - Recombinant Aβ$_{1-42}$ (25μM) incubated for 14 days at 37°C. There are no clearly defined fibrils and large amounts of amorphous material are visible. Scale bar = 500 nm.
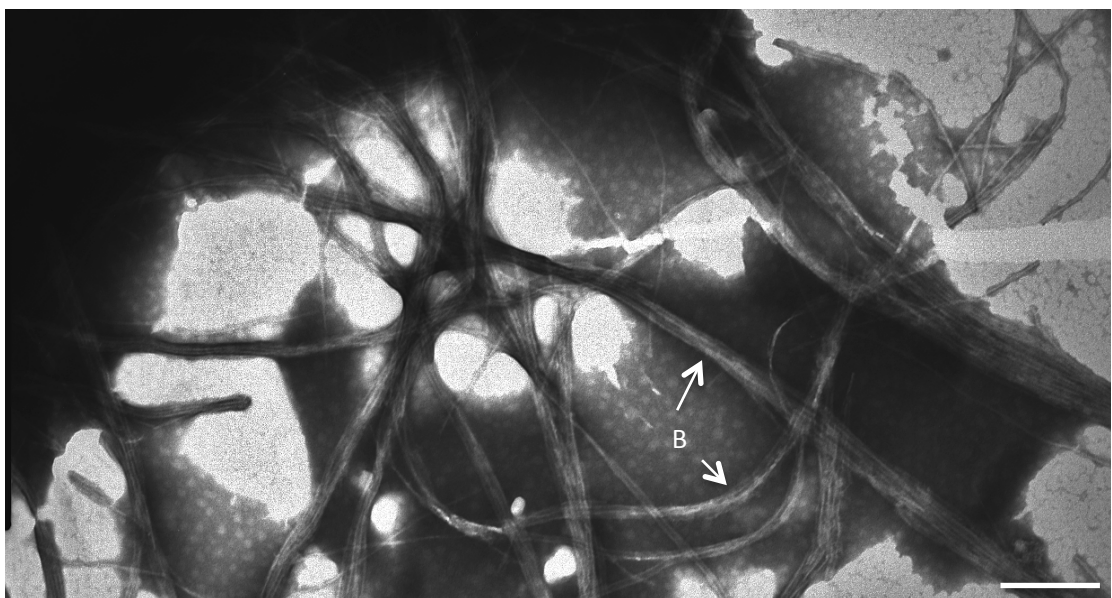
Figure 3.3.2.6 - Recombinant Aβ$_{1-42}$ (25μM) incubated for 14 days at 37°C. Multiple bundles of parallel amyloid beta fibrils are visible (B). Scale bar = 200 nm.
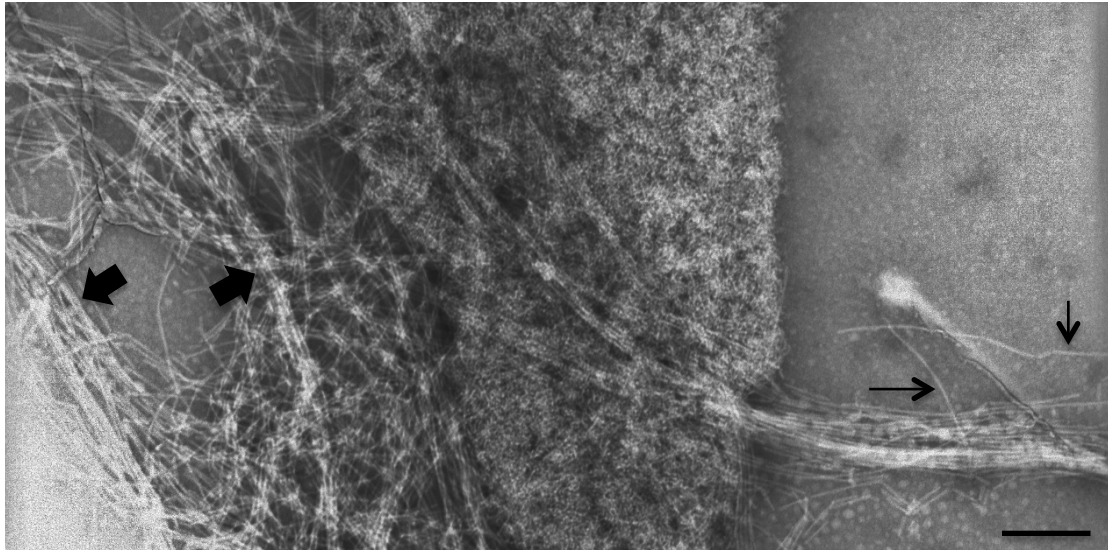
Figure 3.3.2.7 - Recombinant Aβ$_{1-42}$ (25µM) incubated for 14 days at 37°C. Many bundles (thick arrows) of Aβ$_{1-42}$ fibrils (thin arrows) are present along with many individual fibrils within the same areas, which do not appear to be associated with other Aβ$_{1-42}$ fibrils. Scale bar = 200 nm.
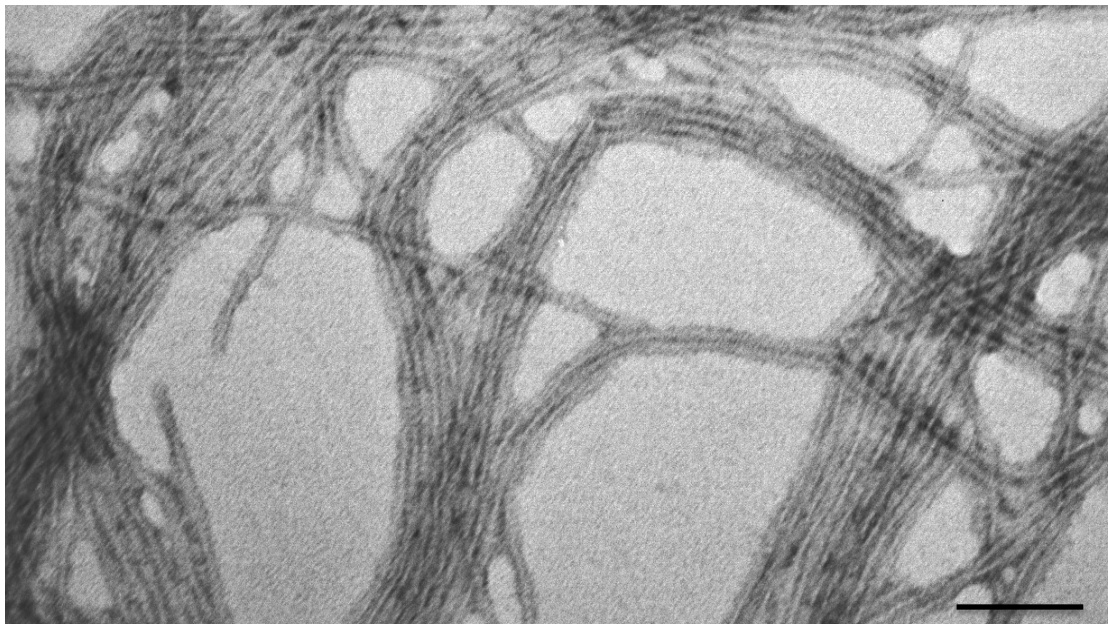
Figure 3.3.2.8 - Recombinant Aβ$_{1-42}$ (25µM) incubated for 14 days at 37°C. Multiple bundles of parallel amyloid fibrils ({) are clearly visible and there are much fewer individual fibrils. The amyloid fibrils appear straight and do not show much tendency to bend. Scale bar = 100 nm.
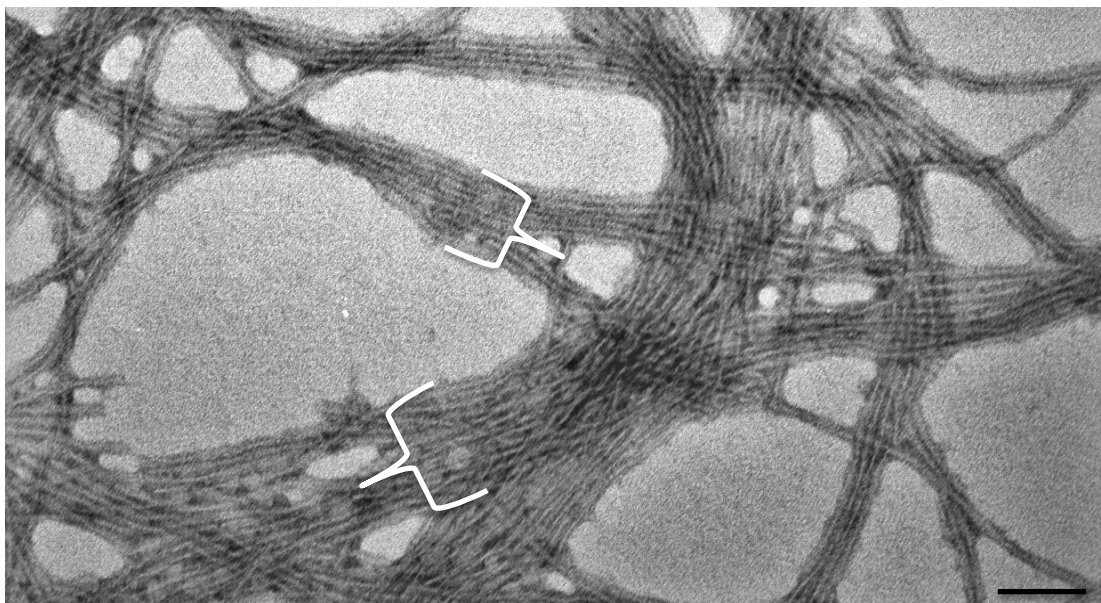
Figure 3.3.2.9 - Recombinant Aβ$_{1-42}$ (25μM) incubated for 14 days at 37°C. Many Aβ$_{1-42}$ fibrils can be seen running parallel to one another but show a greater degree of flexibility than in earlier images. Scale bar = 100 nm.
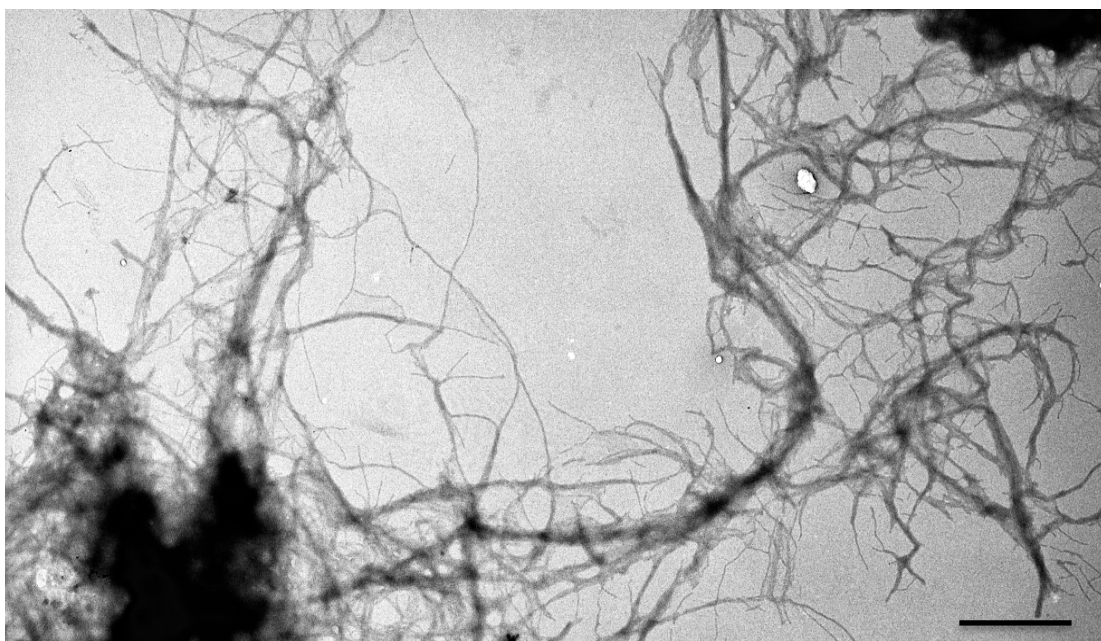
Figure 3.3.2.10 - Recombinant Aβ$_{1-42}$ (25μM) incubated for 14 days at 37°C. Individual and parallel Aβ fibrils can be seen. Dark patches represent areas with a high density of Aβ$_{1-42}$ due to positive staining of the sample. Scale bar = 1 μm.
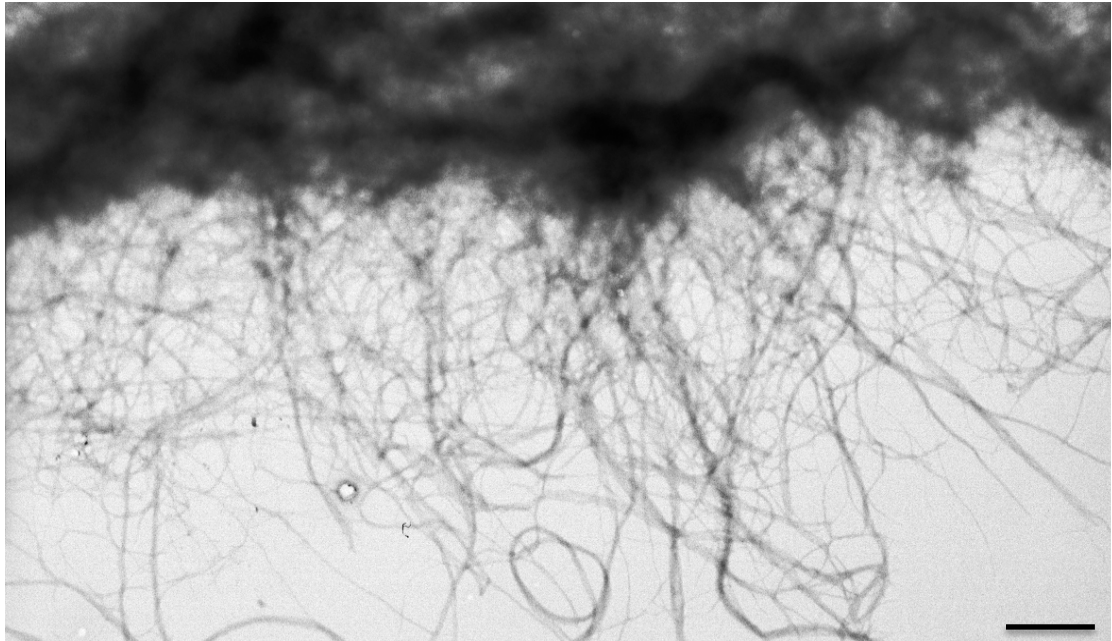
Figure 3.3.2.11 - Recombinant Aβ$_{1-42}$ (25µM) incubated for 14 days at 37°C. Dense areas of Aβ$_{1-42}$ can be seen at the top of the image whilst both individual and bundles of Aβ$_{1-42}$ fibrils are visible throughout the centre and lower thirds of the image. Aggregations show positive staining in this sample. Scale bar = 1 µm.
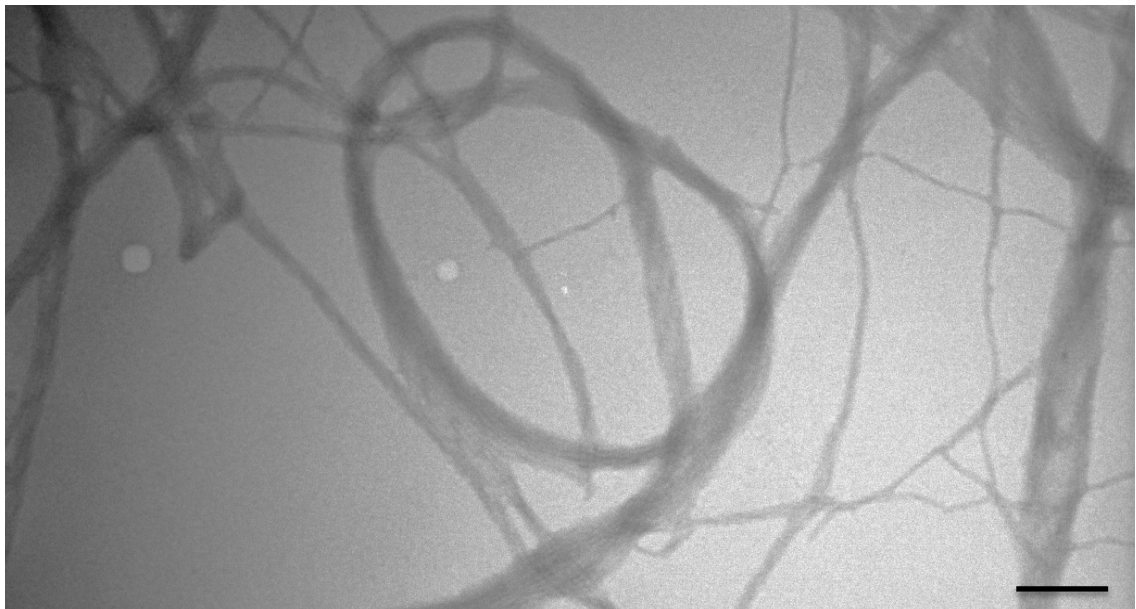
Figure 3.3.2.12 Recombinant Aβ$_{1-42}$ (25µM) incubated for 14 days at 37°C. This image shows a bundle of parallel Aβ$_{1-42}$ fibrils looping thus highlighting the flexibility of the fibrils. Aggregations show positive labeling in this sample. Scale bar = 200 nm.

3.4 – Results I - Summary and Discussion

Successful production of recombinant $A\beta_{1-42}$ was achieved in this study and is evidenced by the protein concentrations measured (by spectrophotometry) as well as the coomassie staining of SDS-PAGE gels and positive western blots when probing the nitrocellulose membranes with anti-Hexa-His ($A\beta_{1-42}$ fusion protein) and 6E10 antibodies ($A\beta_{1-42}$ peptide).

When producing the $A\beta_{1-42}$ peptide, analysis of the contents of different samples throughout the purification process of the peptide was performed. Following expression, $A\beta_{1-42}$ exists as part of a fusion protein with a reported molecular weight of ~14 kDa. However, upon analysis of protein content in *E.coli* cell lysate (fusion protein is released following cell lysis) by coomassie staining and western blotting, results lacked direct evidence of a protein at this molecular weight. Interestingly, positive labelling was observed at ~30 kDa in western blots using 6E10 as well as those using anti-Hexa-His antibodies in addition to intense banding on the coomassie stained gel. This indicated that the relatively large amount of protein (indicated by the intense band) contained the epitope for both primary antibodies used, and therefore was highly representative of a result that would be expected to indicate the presence of the fusion protein. This was initially surprising as it was expected that the most intense banding would correspond to a region representing a similar molecular weight to the $A\beta_{1-42}$ fusion protein. It is possible that due to the protocol used in this study (where cleavage of the fusion protein was perfrmed in solution rather than when the protein was immobilized on a purification column) that the fusion protein was able to aggregate, resulting in a large concentration of protein at ~30 kDa. Although samples were sonicated (to disrupt any aggregates) and subjected to denaturing conditions prior to addition to SDS-PAGE gels for analysis (by exposure to SDS and heating to 98°C) the affinity of the fusion proteins for one another appears to be great enough to resist the efforts employed in this study to obtain a denatured protein sample. The molecular weight ~30 kDa is very close to that which a dimer of ~14 kDa proteins would be expected to possess and it is therefore a

strong possibility that the ~30 kDa band observed in coomassie stained SDS-PAGE gels and western blots is due to dimerization of the fusion protein. The presence of a relatively large amount of protein at ~30 kDa that was positively labeled by antibodies recognizing Hexa-His sequeces as well as a region of the $A\beta_{1-42}$ peptide strongly indicates that this band is due to the presence of the fusion protein. Similarly in later comparisons using uncleaved fusion protein (stored at -80°C for 2 weeks) a large amount of protein which was positively labeled by anti-Hexa-His and 6E10 antibodies was observed with a molecular weight of ~130 kDa. The presence of this band of a higher molecular weight following a period of storage that was not present immediately after purification supports the hypothesis that the fusion protein is able to aggregate into larger aggregates and the $NANP_{19}$ region is not sufficient to prevent aggregation of the fusion protein when employing the expression and purification method used in this study.

Upon comparison of the uncleaved fusion protein, $A\beta_{1-42}$ cleaved from the fusion protein and commercially produced $A\beta_{1-42}$ there were clear differences observed between the samples. The uncleaved fusion protein sample did not show any bands or positive labelling that resembled $A\beta_{1-42}$ following coomassie staining and western blot analysis. However, following the cleavage process whereby the fusion protein had been incubated with the TEV protease, an intense band was present at <7.6 kDa that was not present in the uncleaved sample. This strongly indicated that the band was present as a result of the cleavage step and due to the low molecular weight represented by the band, that it represented the $A\beta_{1-42}$ peptide. This conclusion was further supported by comparison of the bands present in the cleaved $A\beta_{1-42}$ sample to those present in the sample of commercially produced $A\beta_{1-42}$. Importantly, the new band that was present in the cleaved sample (that was not present in the sample of uncleaved fusion protein) was also present as an intense band in the commercially produced $A\beta_{1-42}$ sample, providing strong evidence that $A\beta_{1-42}$ had been successfully produced in this study. Positive labeling of this intense band <7.6 kDa in the cleaved sample and commercially

produced sample by the 6E10 antibody confirmed that this protein contained residues 5-8 of the $A\beta_{1-42}$ peptide. The appearance of the new band following the cleavage event, combined with the relatively low molecular weight of the band (similar to that reported for the $A\beta_{1-42}$ peptide – ~4.5 kDa), positive labeling by 6E10 antibodies and absence of labeling by anti-Hexa-His antibodies provide strong evidence of the successful production of the $A\beta_{1-42}$ peptide. The ~30 kDa band was also detected in the sample containing cleaved $A\beta_{1-42}$ and showed positive labeling during western blotting using the anti-Hexa-His antibody and to a lesser extent with the 6E10 antibody. This indicates that in the cleaved sample there is still a relatively large amount of fusion protein forming aggregates (e.g. dimers) and containing $A\beta_{1-42}$ that has not undergone cleavage. It is possible that aggregation of the $A\beta_{1-42}$ fusion protein impairs the ability of the TEV protease to successfully cleave the fusion protein and therefore may reduce the cleavage efficiency resulting in lesser amounts of cleaved $A\beta_{1-42}$ being obtained than would occur in the absence of fusion protein aggregates.

Another important observation made during analysis of the sample containing cleaved $A\beta_{1-42}$ was the presence of a number of bands that did not correspond to the $A\beta_{1-42}$ peptide. These bands indicate the presence of proteins that are not $A\beta_{1-42}$ and therefore represent impurities within the sample. Based on these observations it is recommended that future expression of the $A\beta_{1-42}$ peptide using this protocol should be adapted to include a further purification technique following confirmation of the presence of the $A\beta_{1-42}$ peptide, such as HPLC. This would enable the collection of samples of $A\beta_{1-42}$ with increased purity that will enable more accurate analysis of the recombinant $A\beta_{1-42}$ protein when used for future research purposes.

The ability to produce $A\beta_{1-42}$ in-house enables substantial savings to be made with regard to research costs. This enables researchers to spend their research funds on other products, which increases the amount and quality of research that can be performed when operating

under finite resources such as research grants that are awarded by various funding bodies. The procedure employed in this study to produce recombinant $A\beta_{1-42}$ requires the $A\beta_{1-42}$ peptide to be cleaved following expression as a fusion protein. This study therefore also produced the TEV protease – used for this cleavage event – in-house, showing that the entire process from culturing of bacterial cells through to production of $A\beta_{1-42}$, can be performed in the laboratory and provides a cheaper source of $A\beta_{1-42}$ than buying this peptide from commercial suppliers. The expression of $A\beta_{1-42}$ presented a challenge as the yield from each expression procedure was relative low (approximately 3mg per run), and therefore steps to increase protein concentration in individuals aliquots such as dialysis and ethanol precipitation were performed. Dialysis is an extremely useful technique for purifying and concentrating protein samples, however using this technique includes risking loss of valuable protein and therefore extreme care was required when performing this step to ensure that as much protein was recovered from the dialysis cassettes as possible.

One important point to note regarding the in-house production of recombinant $A\beta_{1-42}$ is the length of time taken to perform the protocol. From start to finish the protocol takes 4 days, meaning that it is possible to produce $A\beta_{1-42}$ in the laboratory quicker than ordering and taking delivery of commercially produced $A\beta_{1-42}$ (although a small number of companies state that they may be able to deliver within 2-5 days). The rate at which 'batches' of $A\beta_{1-42}$ can be produced, combined with the low cost of production, makes in-house $A\beta_{1-42}$ production an extremely attractive option.

Following TEV protease expression, coomassie staining of samples eluted from the Ni-NTA column showed the presence of various bands of differing intensity. By measuring the absorbance of aliquots taken following addition of imidazole to the column, the three samples with the highest absorbance (representative of greatest protein concentration) were selected for analysis by SDS-PAGE and Coomassie staining. For comparison, two

samples that exhibited lower absorbance were included in the analysis. As expected, all samples appeared to contain significant levels of TEV, indicated by a dark band corresponding to a similar molecular weight that was previously known for the TEV protease. The intensity of the TEV band in each lane appeared to be greater in samples that exhibited greater absorbance, although interestingly, the presence of other bands in samples 4, 5 and 6 (lanes 6, 7 and 8 respectively) indicated that the absorbance measured for these samples was also influenced by the presence of other proteins. The fact that lane 5 (50 mM Imidazole eluent) does not show any bands following Coomassie staining indicates that there are no (or extremely low levels of) proteins present in this sample. This is due to unbound proteins having already been washed out of the column whilst proteins that had not exited the column, remained bound to the column and were not released with this sample. Therefore the bands that are visible in lanes 6-10 (500 mM imidazole eluent) must have remained associated with the column due to an affinity between the amino acid side chains of the bound proteins and a component of the IMAC column. As mentioned, histidine has a strong affinity for Ni-NTA columns and therefore the protein bands observed which do not correspond to TEV, are likely to be due to other histidine containing proteins that have bound to the column. This view is supported by the western blot analysis using an antibody that recognises hexa-histidine and therefore confirms the presence of such amino acid sequences in these proteins, providing a basis for their elution in the 500 mM stage of purification. Interestingly, not all of the bands that can be observed from the Coomassie stained gel were detected by the anti hexa-histide antibody used for Western blotting. This indicates that some of the observed proteins remained bound to the column due to other reasons rather than their possession of a hexa-histidine tag. One possibility is that during the process leading up to the washing of the column (where the proteins would be expected to be eluted) these proteins bound to the TEV proteins and thus remained associated with the column due to their binding to TEV which in turn was strongly bound to the column. Another

possibility is that these proteins are proteins that are normally expressed in *E. coli* which contain histidine residues and have an affinity with the column that is consistent with the imidazole concentration required for their elution. The expression of these proteins by *E. coli* has been previously reported to, in some cases result in co-purification of these unwanted proteins along with the protein of interest (Bolanos-Garcia & Davies, 2006). There are numerous proteins normally expressed in *E. coli* which bind Ni-NTA and require >50 mM imidazole for elution. For example, the lower bands observed in figure 1 may correspond to *Fur* and *Cu-Zn-SODM* (Superoxide dismutase), which have MWs of 16.7 kDa and 17.6 kDa respectively. Another candidate for one of the bands observed in figure 1 is *SlyD,* which has a MW of 20.8 kDa (Bolanos-Garcia & Davies, 2006). Although the potential presence of these proteins (among numerous others) provides an explanation for the impurities observed in these samples, without isolation and characterisation of these proteins, their identity cannot be definitively concluded.

Figure 3.2.2 illustrates the concentration of protein detected in each 1ml aliquot eluted from the sample following the addition of 500 mM imidazole. The first two samples that were collected did not contain any TEV protein, despite the addition of imidazole to the Ni-NTA column. A likely explanation for this observation is that due to the time taken for a solution to pass through the Ni-NTA resin, the first two 1ml aliquots were still part of the flow through from the 50 mM imidazole wash, rather than the 500 mM imidazole wash. Although the samples with the highest protein concentration were those collected earlier in the 500 mM elution phase, analysis of the proteins within the sample show a degree of impurity, with later samples containing lower levels of impurities. As the concentration of TEV required for cleaving $A\beta_{1-42}$ is relatively low (5 µM), if a similar protocol to the one used in this study is employed, then it may be beneficial to use aliquots collected later in the 500 mM elution to prevent interference in the cleavage process by any of the impurities that are present in earlier samples.

In the future, one way to possibly avoid the contamination of the TEV sample with unwanted proteins may be to incorporate a size-exclusion chromatography step prior to IMAC in order to reduce the presence of proteins of different MW than TEV. Therefore to ensure higher purity, future protocols could pass samples of the 500 mM imidazole eluent through a size exclusion chromatography step following IMAC, which is likely to enable more effective isolation of the TEV protein.

Importantly, the process of producing TEV protease takes 3 days and therefore this process can be started at the same time as $A\beta_{1-42}$ production and still provide TEV protease in ample time for the cleavage event required during the $A\beta_{1-42}$ production protocol.

To determine the ability of the $rA\beta_{1-42}$ to form aggregates resembling those seen in many investigations into $A\beta_{1-42}$ in the literature, electron microscopic examination of $A\beta_{1-42}$ aggregates immediately following $A\beta_{1-42}$ production, and following incubation at $37^{o}C$ for a period of 14 days. Samples were taken immediately following production of the recombinant $A\beta_{1-42}$ (0h hours post incubation). The samples taken at the beginning of the incubation period (0 hours) were found to contain oligomers and protofibrils but lacked fully formed $A\beta_{1-42}$ fibrils. It was anticipated that no protofibrils or fibrils would be present in these samples, and that oligomers may be present, but only at low levels. This is due to the fact that immediately following production, $A\beta_{1-42}$ would be expected to exist solely as monomers due to the very short period of time elapsed in which aggregation could have begun. As the process of preparing the samples and adding the samples to the EM grids for analysis was performed at room temperature, small $A\beta_{1-42}$ aggregates may have formed, as at this temperature $A\beta_{1-42}$ is known to rapidly aggregate. Interestingly, Finder et al., also observed fibrillar structures immediately following production of recombinant $A\beta_{1-42}$ suggesting that the observation of fibrillar structures at 0h in this study, is not likely caused by any additional delay during preparation of the sample for EM analysis in this study and rather is attributable

to the process used to produce rAβ$_{1-42}$ (Finder et al., 2010). Furthermore, the negative staining of the 0h sample was taken immediately after Aβ$_{1-42}$ production, with the staining process performed in less than 5 minutes meaning that there was very little time from production to sample preparation in which aggregation may have occurred to produce the protofibrils observed. The levels of oligomers and protofibrils were greater than expected in the 0 hour sample but may be explained by incomplete deseeding of the peptide prior to the start of the investigation. This incomplete deseeding of aggregates formed during the rAβ$_{1-42}$ production process would have provided a surface for secondary nucleation to occur, resulting in the observation of a greater number of higher order aggregations than expected. No mature fibrils were expected in this sample as the Aβ$_{1-42}$ peptides were expected to have been deseeded into monomers and thus following 0h incubation would have still been in the lag phase (rather than the 'growth' and 'plateau' phases) of aggregation and would not have had sufficient time to form these relatively large aggregates (Arosio et al., 2013). Previous studies have found the lag phase to last approximately 5 hours, suggesting that despite significant efforts, deseeding had not fully occurred in the samples prior to the start of the investigation (Arosio et al., 2013). The presence of multimeric aggregates in the results presented in this study, combined with the observation of fibrillar aggregates immediately following production by Finder et al. suggests it is highly likely that Aβ$_{1-42}$ begins to aggregate during the production process (i.e. during the cleavage steps) and is incompletely deseeded by addition of – and storage in – HFIP. For future production of Aβ$_{1-42}$, it may be recommendable to also include a sonication step in addition to the use of HFIP, to ensure that Aβ$_{1-42}$ does not exist as multimeric aggregates, especially as recombinant Aβ$_{1-42}$ has been found to aggregate more quickly than commercially available Aβ$_{1-42}$ (Finder et al., 2010). Typically the aggregation of Aβ over time produces a sigmoidal curve as illustrated in Figure 1.3. In order to increase the ability of the rAβ$_{1-42}$ to be used in future studies, it must be determined whether alteration of the production protocol is needed to prevent aggregation

or whether post-production treatment of the $A\beta_{1-42}$ (e.g. increasing the number of rounds of sonication/HFIP treatment that the peptide is exposed to) is sufficient to obtain a monomeric sample of $A\beta_{1-42}$. Only when $rA\beta_{1-42}$ exists as monomers can the true potential of this recombinant peptide be utilized by researchers, as investigations into inhibitors of $A\beta$ aggregation will require monomeric $A\beta$ as a starting point from which to assess the aggregation inhibiting ability of a particular agent.

Following 14 days incubation at $37^{o}C$ the appearance of the $A\beta_{1-42}$ was markedly different to that observed at 0h incubation. The 14-day sample contained many areas of dense $A\beta_{1-42}$ aggregation, evidenced by dark masses of fibrils upon electron microscopic investigation. These aggregations were expected as small $A\beta_{1-42}$ structures were observed in 0h samples indicating that aggregation was underway at the beginning of the experiment and therefore that sufficient aggregation would have occurred following 14 days incubation. The results from the aggregation investigations show that following 14 days of incubation, the $A\beta_{1-42}$ fibrils had associated into bundles where the fibrils run parallel to one another. Again, this is consistent with some previous studies that have also shown such parallel associations (Chiti et al., 1999). The results obtained from this investigation showed that the number of fibrils per bundle varied from 2-10 with an average of 5.2 ± 2.6 fibrils per bundle. The finding that the recombinant $A\beta_{1-42}$ produced at Lancaster University is able to self-aggregate forming oligomers, protofibrils and mature fibrils indicates that recombinant production of $A\beta_{1-42}$ for future research needs is a realistic and viable option.

In order to further investigate the changes that occur during $A\beta_{1-42}$ aggregation and to compare the fibrils formed from recombinant $A\beta_{1-42}$ with commercially available $A\beta_{1-42}$, the widths of the protofibrils seen following 0h incubation were measured and compared with those present following 14-day incubation. For 0h and 14 day incubates samples, the average fibril width was found to be 7.3 ± 1.1 nm which falls in line with fibril dimensions

reported in the literature using commercially available $A\beta_{1-42}$, where the width of amyloid fibrils lie between 7-10 nm (Soto, 2003).

The observations from this initial series of experiments into the aggregation of $A\beta_{1-42}$ produced at Lancaster University strongly indicate that this peptide is a useful source of recombinant $A\beta_{1-42}$ as fibril width, aggregation ability and bundling of $A\beta_{1-42}$ fibrils are consistent with the literature where commercially produced $A\beta_{1-42}$ has been used. However, for future recombinant $A\beta_{1-42}$ production, the current method of purification and deseeding should be refined to increase the purity of the sample, ensuring that the $A\beta_{1-42}$ peptides in a given sample exist as monomers and are not associated with other $A\beta_{1-42}$ peptides.

Chapter 4 - Results II: Investigating the effect of PINPs upon Aβ$_{1-42}$ aggregation

Since Dr Alec Bangham's discovery of liposomes in 1963, investigating their therapeutic uses has been an intense and constant focus for many researchers. Their use as drug delivery agents began in 1995 when the FDA approved Doxil® for use in the treatment of AIDS related Kaposi's sarcoma and in 2012 there were 12 liposomal formulations licenced for treatment of human disease (Chang & Yeh, 2012). Liposomes are capable of carrying therapeutic agents in a number of ways. Hydrophilic substances can be transported inside the aqueous core of the liposome whilst lipophilic substances can be transported in the liposomal bilayer. Another way in which liposomes can transport therapeutic agents is by attachment to their surface. In the case of PINPs, RI-OR2-TAT is attached to the surface of the liposomes (Cholesterol: Sphingomyelin 1:1) via 'click-chemistry' between a cysteine residue on the peptide and a maleimide group attached to PEG incorporated into the liposomal bilayer (Figure 1.6).

Chapter 4.1 - Appearance of PINPS

In order to characterize the appearance of the PINPs before their effect upon Aβ was investigated, electron microscopic analysis was performed on PINPs suspended in PBS and distilled water. PBS was chosen as a suspension medium as the PINPs are produced in PBS and it is therefore present within the aqueous core of the liposomes. A disadvantage of imaging structures suspended in PBS by electron microscopy is that PBS can produce artifacts upon examination, which could hinder the ability to accurately analyze the contents of the samples. For this reason, samples suspended in distilled water were also examined in order to provide an alternative to PBS where fewer artifacts would be expected to be present.

As the formation of Aβ aggregates is widely believed to play a significant role in the effects of AD, treatments to reduce levels of the peptide or peptide aggregations have been a logical avenue for research. Treatment approaches investigated so far include immunotherapy, as well as targeting β- and γ-secretases in an attempt to reduce APP cleavage activity by these enzymes (Schenk, 2002; Wolfe, 2008; Klaver et al., 2010). Unfortunately however, many of these drugs have provided poor results in clinical trials meaning that alternative therapeutic candidates must continue to be investigated. This study focused on evaluating the ability of PINPs to reduce levels of $A\beta_{1-42}$ aggregation.

To ensure a detailed investigation into the effects of PINPs upon $A\beta_{1-42}$ aggregation, a number of techniques were performed. Investigations began with the use of TEM to visualize any PINP-$A\beta_{1-42}$ interactions, followed by fluorescence-based assays such as the Thioflavin T assay and a sandwich ELISA. By using two different fluorescence-based assays, the effect of PINPs upon oligomers (ELISA) and fibrils (ThT Assay) could be investigated. The techniques used in this investigation therefore provided both qualitative and quantitative results to enable evaluation of the ability of PINPs to reduce $A\beta_{1-42}$ aggregation.

4.1.1 – PINPS + dH2O

Upon electron microscopic analysis, PINPs exhibited varied appearances (Figures 4.1.1.1 and 4.1.1.2). However, the general shape of the PINPs consistently appeared to be circular or slightly elliptical. Some of the PINPs from the samples diluted in dH_2O were surrounded by a slightly darker region, indicating the presence of a substance that appeared to be associated with the PINPs. Another observation made from EM investigation of PINPs was that PINPs appeared to interact with other PINPs, as well as the presence of smaller spheroid structures within the PINPs themselves.
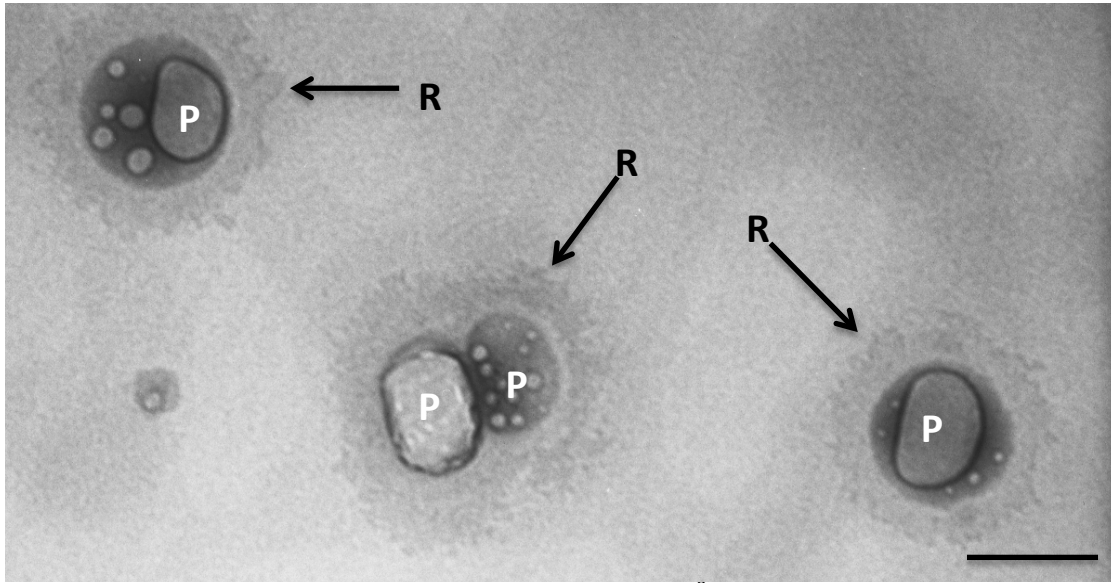
Figure 4.1.1.1 – PINPs in dH$_2$O. PINPs were incubated at 4°C. Also visible in this micrograph are dark regions (R) surrounding the PINPs (P). Scale bar = 100 nm.
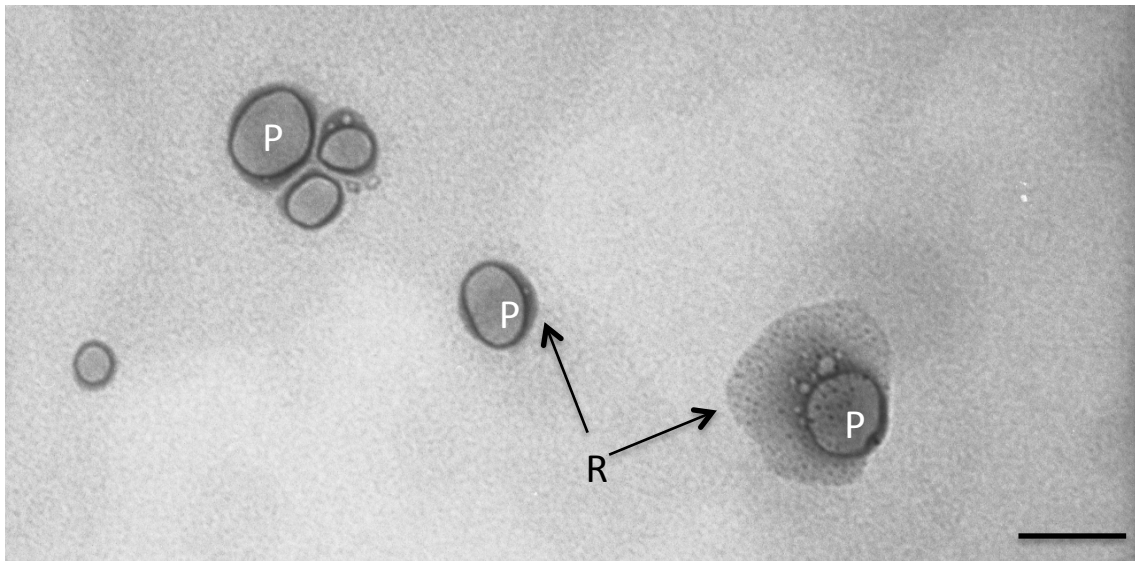
Figure 4.1.1.2 – PINPs in dH$_2$O. PINPs were incubated at 4°C. Dark regions (R) can be observed surrounding PINPs (P). Scale bar = 100 nm.

Analysis of the PINPs in PBS again showed that the liposomes were spheroid in shape and interactions between multiple liposomes were observed (Figures 4.1.2.1 and 4.1.2.2). The darker regions surrounding the PINPs in dH$_2$O were also present in these samples.
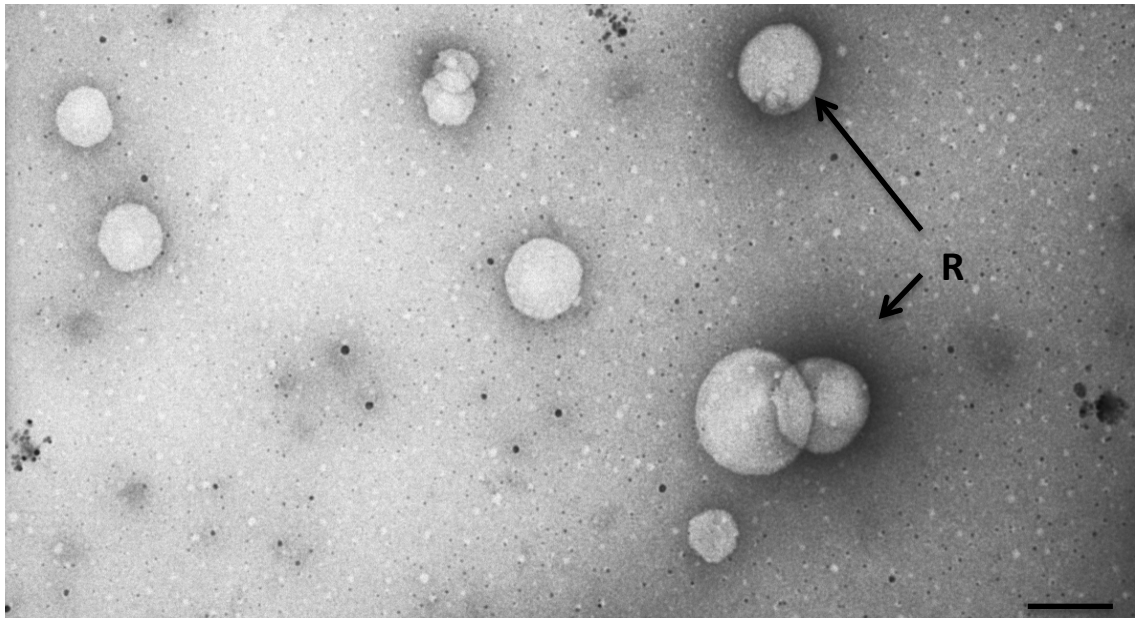
Figure 4.1.2.1 - PINPs in PBS. Dark regions (R) are visible surrounding the PINPs. PINPs were incubated at 4°C. Scale bar = 100 nm.
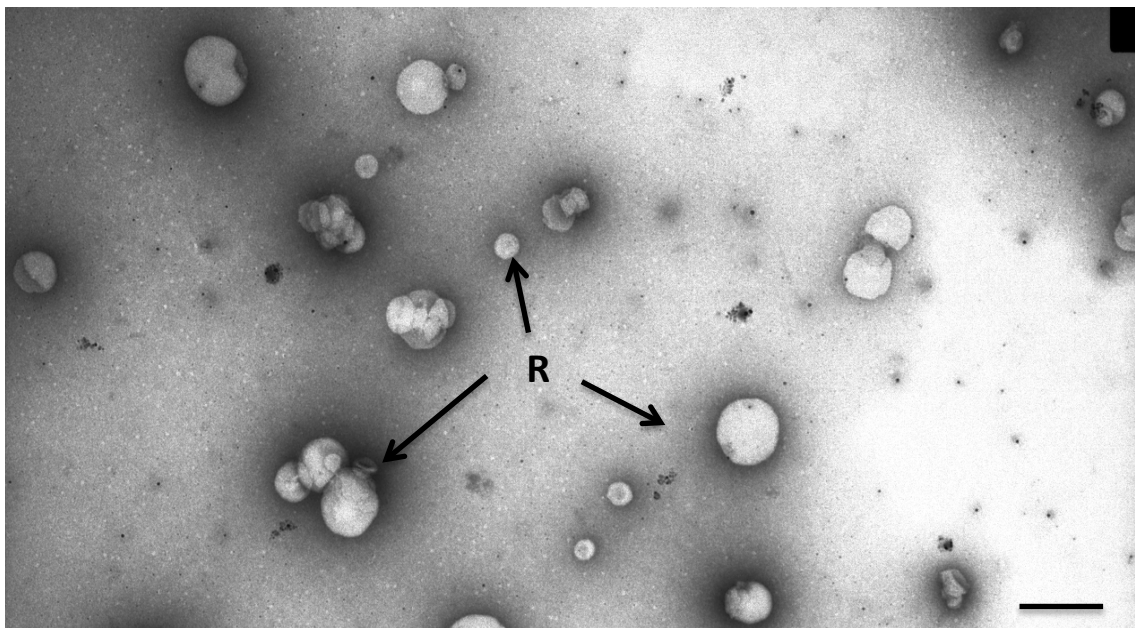
Figure 4.1.2.2 - PINPs in PBS. Dark regions (R) are visible surrounding the PINPs. PINPs were incubated at 4°C. Scale bar = 200 nm.

Chapter 4.2 - Effect of PINPs on $A\beta_{1-42}$ Aggregation

In order to determine the effect of the PINPs upon aggregation of $A\beta_{1-42}$, samples containing $A\beta_{1-42}$ with and without PINPs were incubated at 21°C for 48 hours. The control samples did not contain PINPs whereas the test samples did contain PINPs. In this investigation the purpose of the control sample was to determine the appearance of $A\beta_{1-42}$ when no inhibitor was present and compare the appearance with that of the test samples containing both $A\beta_{1-42}$ and PINPs to observe whether the PINPs had a visual effect upon $A\beta_{1-42}$ aggregation.

4.2.1 – $A\beta_{1-42}$ + PB2S + PBS

The control sample containing $A\beta_{1-42}$ + PB2S + PBS was found to contain mature fibrils as well as smaller amyloid structures (Figure 4.2.1.1) following 48 hours incubation at 21°C. There were also multiple dense aggregations of $A\beta_{1-42}$ (Figure 4.2.1.2). These results represent the aggregation properties of $A\beta_{1-42}$ at physiological pH (7.4) and in the absence of any aggregation inhibitors.
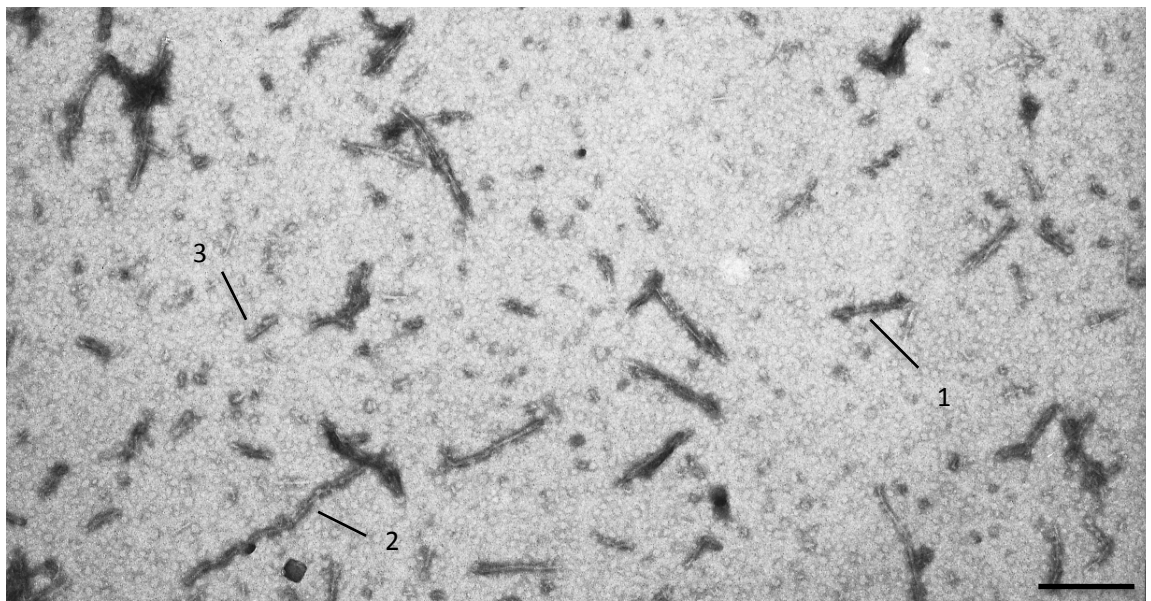
Figure 4.2.1.1 – $A\beta_{1-42}$ incubated in the absence of PINPs at 21°C for 48 hours. Amyloid structures of different sizes are visible (1, 2, 3). Scale bar = 200 nm.

Figure 4.2.1.2 – Aβ$_{1-42}$ incubated in the absence of PINPs at 21°C for 48 hours. Fibrillar structures can be seen (arrows) in addition to dense areas of Aβ$_{1-42}$ (D). Scale bar = 500 nm.

4.2.2 - Aβ + PB2S + PINPs

The test sample containing Aβ$_{1-42}$ + PB2S + PINPS also contained mature fibrils and dense Aβ$_{1-42}$ aggregations. The fibrils in the test samples can be seen bound to PINPs along parts of the length of the fibril as well as at fibril termini (Figure 4.2.2.1-4.2.2.4). The binding of the PINPs is also visible in the dense aggregations (figure 4.2.2.5), indicating that they are not able to completely inhibit this activity of Aβ$_{1-42}$ peptides. The size of the PINPs varies both within and between figures. At the start of the test (fully hydrated) they had diameters of ~130 nm, however the process of drying the sample on the carbon/formvar coated grids may have decreased the hydration of the PINPs resulting in a decreased size.
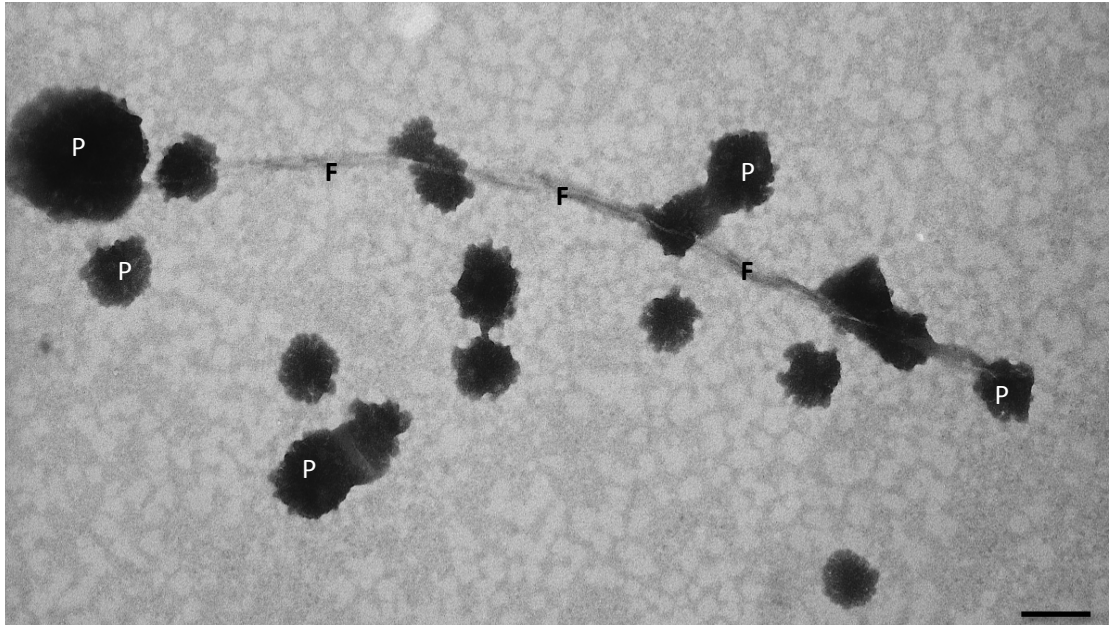
Figure 4.2.2.1 – Aβ$_{1-42}$ incubated in the presence of PINPs for 48 hours at 21°C. PINPs (P) can be seen bound along the length of the fibril (F) and to its termini. Scale bar = 100 nm.
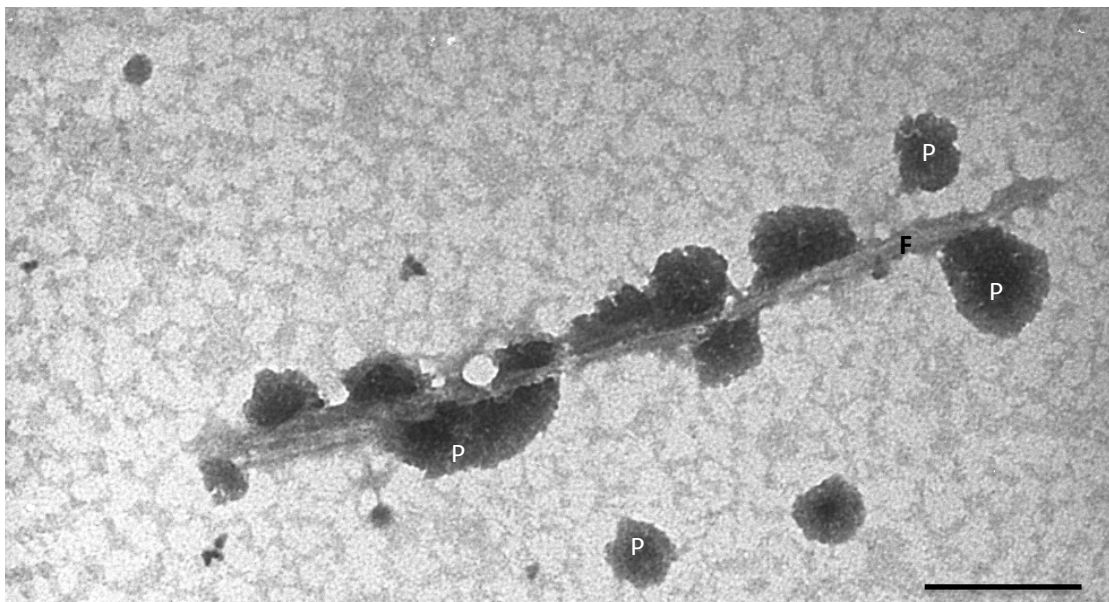
Figure 4.2.2.2 – Aβ incubated in the presence of PINPs for 48 hours at 21°C. PINPs (P) are visible bound along the length of the fibril (F). Scale bar = 100 nm.
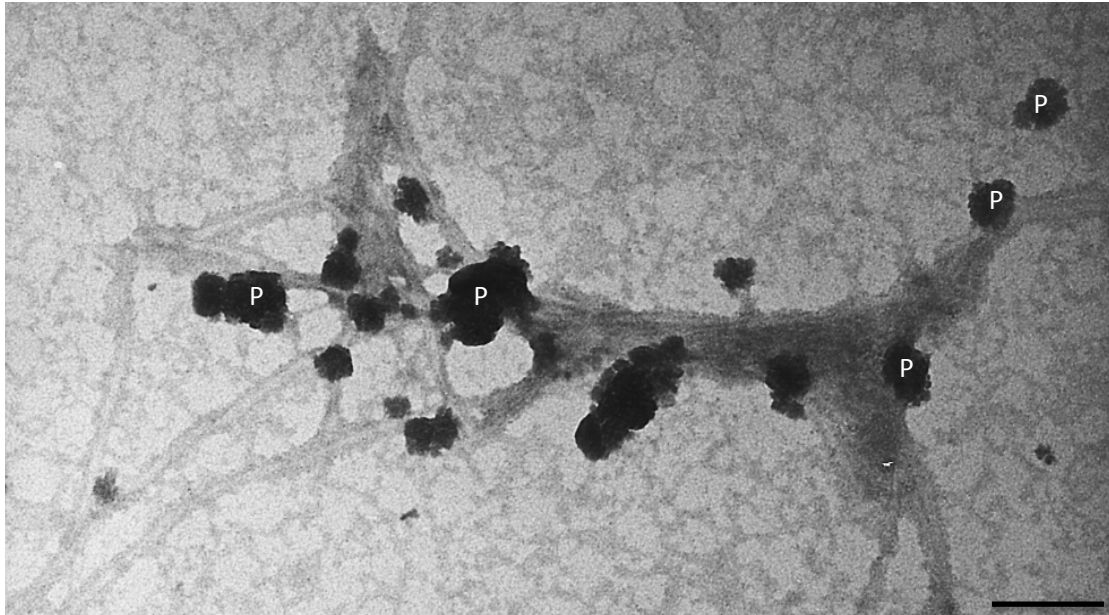
Figure 4.2.2.3 – Aβ incubated in the presence of PINPs for 48 hours at 21°C. PINPs (P) are visible bound to bundles of parallel Aβ$_{1-42}$ fibrils. Scale bar = 100 nm.
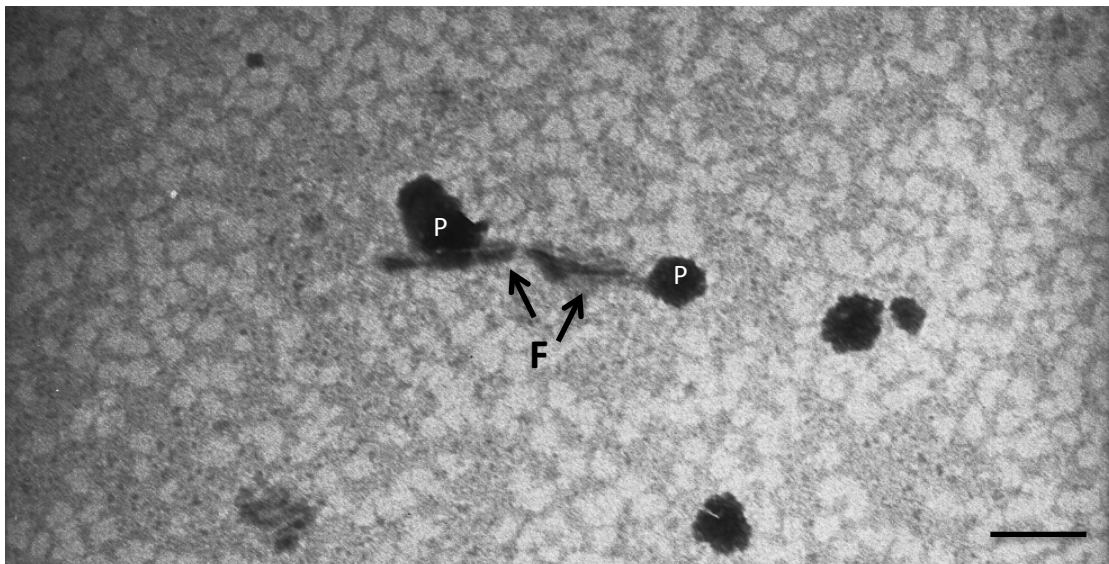
Figure 4.2.2.4 - Aβ incubated in the presence of PINPs for 48 hours at 21°C. PINPS (P) can be seen bound to Aβ$_{1-42}$ fibrils (F). Scale bar = 100 nm.
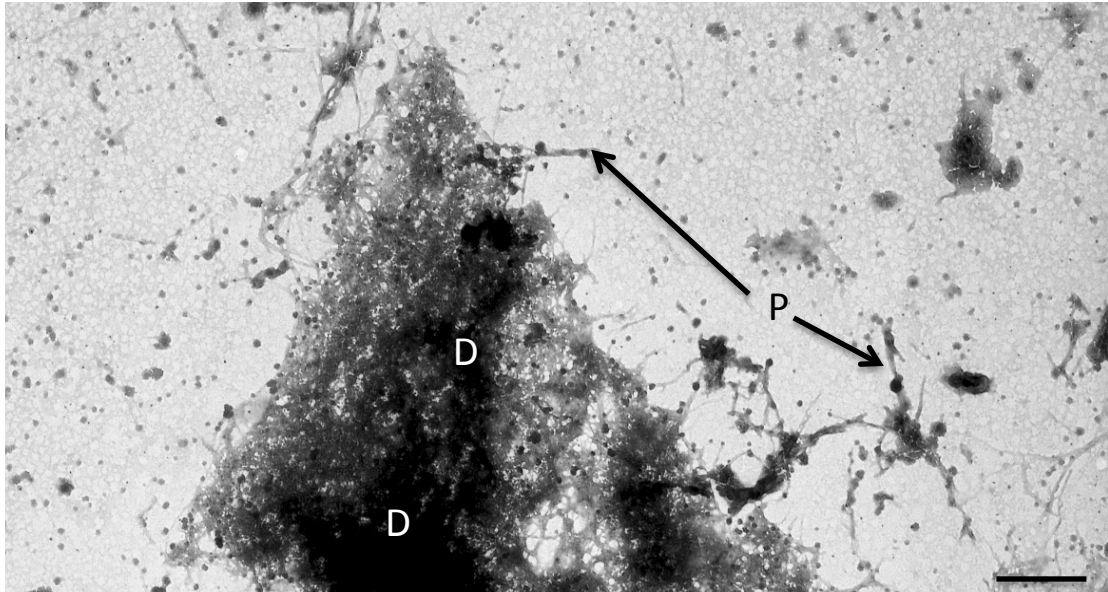
Figure 4.2.2.5 - Aβ incubated in the presence of PINPs for 48 hours at 21°C. Dense regions of Aβ$_{1-42}$ aggregation can be seen (D). PINPs (P) are also visible with many bound to Aβ$_{1-42}$ structures. Scale bar = 500 nm.

4.3– Immunogold labeling to detect Aβ$_{1-42}$ oligomers

As the amyloid hypothesis has continued to evolve in light of on-going research into the mechanisms of Aβ toxicity, emphasis has shifted substantially from insoluble fibrillar aggregates as the main culprit for toxicity (Haas & Selkoe, 2007). The smaller Aβ aggregates known as oligomers, which consist of a small number of aggregated Aβ monomers are now widely regarded as the most neurotoxic species of Aβ aggregate. Therefore, investigations into novel disease-modifying therapies must determine the ability of the therapeutic agent to interact with these smaller soluble aggregates as well as the insoluble fibrils. To test the hypothesis that the altered appearance of PINPs when incubated with Aβ$_{1-42}$ was due to binding of oligomers to the PINP surface, immunogold labeling was performed. The primary antibody used was a monoclonal anti-Aβ antibody raised in mouse whilst the secondary was an anti-mouse antibody with 10 nm colloidal gold conjugate.
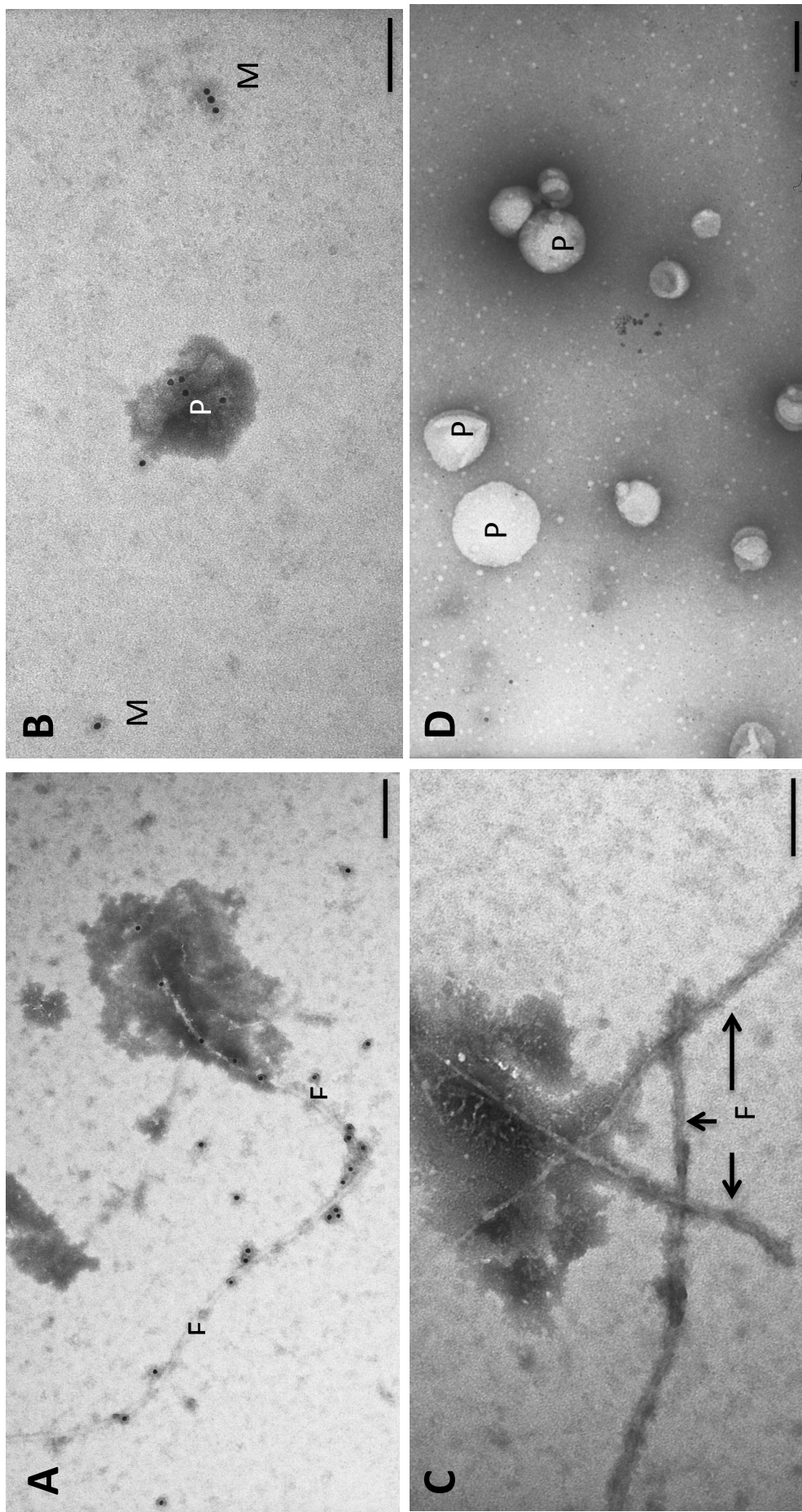
Figure 4.3.1 – Immunogold labelling to detect PINP-bound Aβ$_{1-42}$ oligomers. Test and control samples were incubated for 24 hours at 37°C prior to immunogold labelling: Positive labelling of fibrils (A) and PINPs (B) was observed in test samples. Control samples showed no labelling of fibrils or PINPs in the absence of the primary antibody (C) or Aβ$_{1-42}$peptide (D). F-Fibrils, M-Amorphous material, P-PINPs. Scale bars = 100nm.

The immunogold investigation was performed using a monoclonal anti Aβ_{1-42} primary antibody (6E10) raised in mouse, and a monoclonal anti-mouse secondary antibody conjugated to 10nm gold nanoparticles. Test samples (PINPs+ Aβ_{1-42}+Primary+Secondary) were found to display positive labeling, indiated by the presence of antibody-conjugated gold particles (small black circles). Positive labeling was observed along Aβ_{1-42} fibrils (Figure 4.4.4A) and also on PINPs (Figure 4.4.4B), indicating the presence of Aβ_{1-42}.

Control samples lacking the primary antibody and the Aβ_{1-42} peptide demonstrated that the labeling observed in the test samples was not due to non-specific binding of the primary antibody or the binding of secondary antibodies directly to PINPs. The lack of fibril labeling in the absence of primary antibody demonstrates that in the absence of 6E10, no labeling occurs and therefore that binding is specific to locations where the Aβ_{1-42} peptide is present (Figure 4.4.4C). Additionally, the lack of labeling of PINPs in the absence of Aβ_{1-42} peptide - but in the presence of primary and secondary antibodies – strongly suggests that the labeling that is observed in test samples is due to specific binding of the primary antibody to Aβ_{1-42} and subsequent binding of the secondary antibody to the primary antibody (Figure 4.4.4D). This shows that the secondary antibody only binds to the sample where its epitope is present (6E10 primary antibody).

4.4 – ELISA to detect levels of Aβ_{1-42} oligomers

This approach involved using a sandwich ELISA to detect levels of oligomeric Aβ_{1-42} present in samples containing Aβ_{1-42} alone, and in samples containing Aβ_{1-42} co-incubated with various concentrations of PINPs. This method uses standard 6E10 antibody to bind Aβ_{1-42} and a biotinylated form of 6E10 as the detection antibody. This method does not detect monomers as monomeric Aβ_{1-42} possesses only 1 6E10 epitope (bound by the non-biotinylated 6E10) and therefore the detection antibody is unable to bind. This method enables detection of small aggregates not detectable by ThT assay, whilst ensuring that monomeric Aβ_{1-42} is not unintentionally measured.
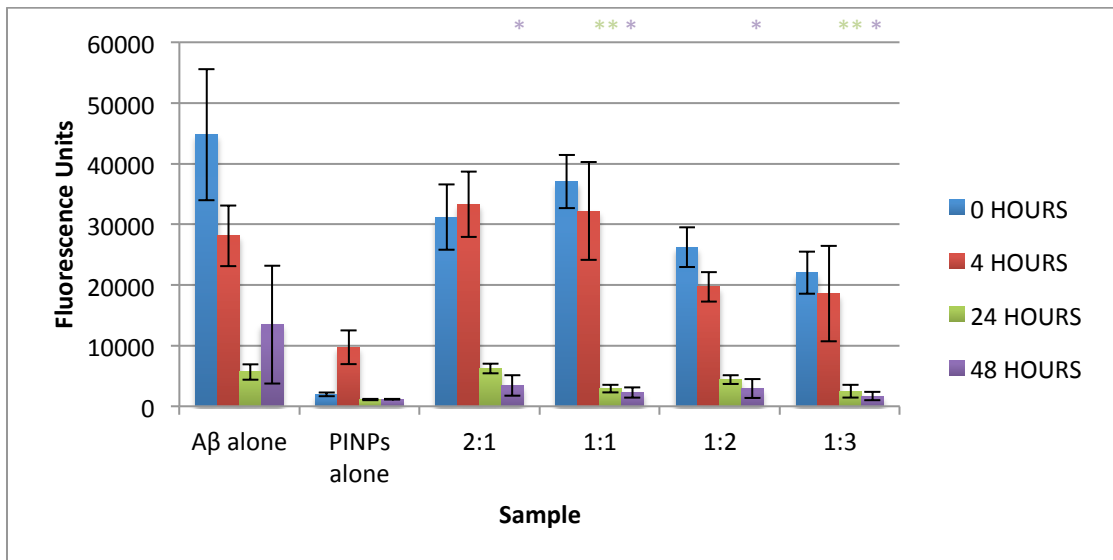
Figure 4.4.1 – ELISA to detect Aβ$_{1-42}$ oligomers. This figure illustrates the mean fluorescence for each sample from measurements taken at 4 different time points (0h, 4h, 24h, 48h) during a 48-hour 37°C incubation of Aβ$_{1-42}$-PINPs at numerous different relative concentrations (In addition to Aβ$_{1-42}$ alone and PINPs alone). Aβ$_{1-42}$ was present at 12.5 μM in each sample (with the exception of 'PINPs alone' where no Aβ$_{1-42}$ was present) with the relative Aβ$_{1-42}$:PINPs ratio of 2:1, 1:1, 1:2, 1:3 (6.25 μM, 12.5 μM, 25 μM, 37.5 μM PINPs respectively) investigated in this assay. Bars represent the mean fluorescence of each sample ± SD. Aβ$_{1-42}$ + PINPs coincubations were compared to the sample containing Aβ$_{1-42}$ alone: * represents $p < 0.05$ and ** represents $p <= 0.001$.

The sandwich ELISA to detect Aβ$_{1-42}$ oligomers found that PINPs are able to reduce the levels of oligomeric Aβ$_{1-42}$ species, indicated by reduced fluorescence in samples containing Aβ$_{1-42}$ + PINPs when compared to the control sample containing solely Aβ$_{1-42}$ ('Aβ alone') (Figure 4.4.1). After 4 hours incubation of the Aβ$_{1-42}$+PINPs samples, no significant differences were observed in the levels of Aβ$_{1-42}$ oligomers between the control sample and Aβ$_{1-42}$+PINPs coincubations. However, following 24h incubation, the samples with Aβ$_{1-42}$:PINPs ratios of 1:1 and 1:3 were found to containing significantly less Aβ$_{1-42}$ oligomers than were present in the control sample. Following 48h incubation all Aβ$_{1-42}$+PINPs coincubations were found to contain significantly lower levels of oligomeric Aβ$_{1-42}$ compared to the control sample.

4.5 – Thioflavin T Assay to detect levels of Aβ$_{1-42}$ fibrils

The ThT assay enables quantification of fibrillar aggregates formed during incubation of Aβ$_{1-42}$ and was employed to examine the effects of coincubation of Aβ$_{1-42}$ with MAL-PEG liposomes, PINPs and the RI-OR2-TAT peptide.

Figure 4.5.1 illustrates the mean fluorescence measurements (indicating levels of fibrillar Aβ$_{1-42}$ aggregates) recorded from control samples (Aβ alone, ThT alone) and test samples where Aβ$_{1-42}$ was coincubated with PINPs at numerous relative molar ratios.
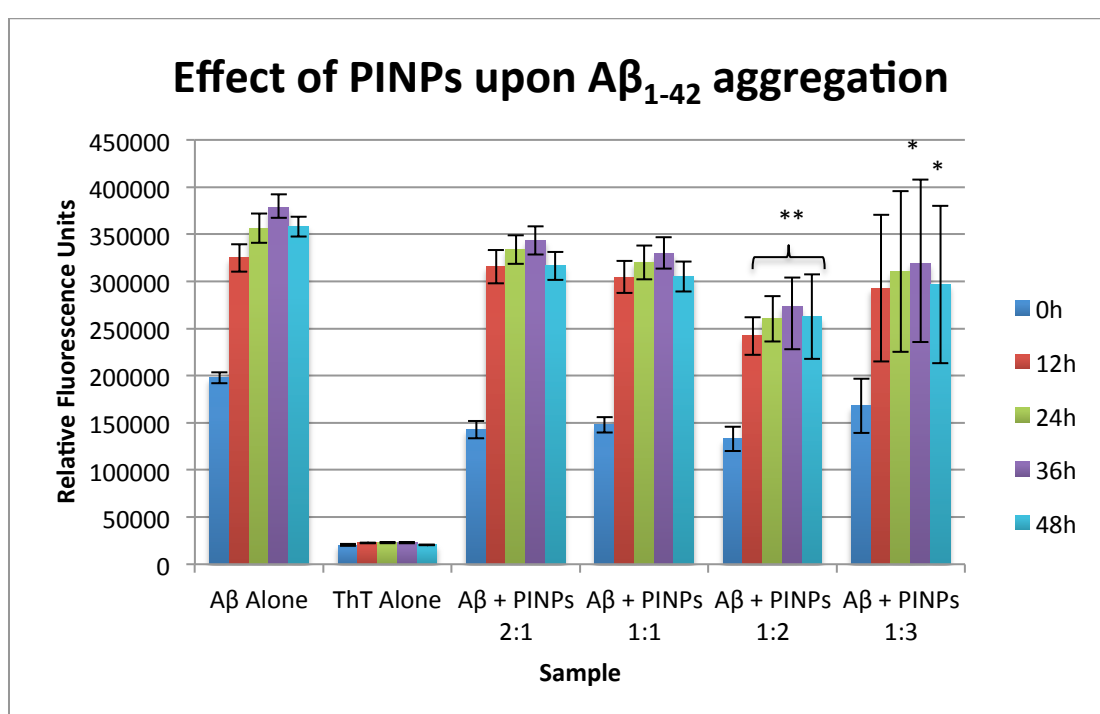
Figure 4.5.1 – Effect of PINPs upon Aβ$_{1-42}$ aggregation. Samples were plated in triplicate and incubated at 37°C for 48h in a black 384 well plate with a clear bottom. Each bar represents the mean value for each sample at a particular time point (0h, 12h, 24h, 36h, 48h). Samples containing Aβ$_{1-42}$ did so at a concentration of 25 μM with Aβ$_{1-42}$:PINPs coincubations containing PINPs at ratios of 2:1, 1:1, 1:2 and 1:3 (12.5 μM, 25 μM, 50 μM and 100 μM PINPs respectively). Error bars represent ± SD. Aβ$_{1-42}$ + PINPs coincubations were compared to the sample containing Aβ$_{1-42}$ alone: * represents $p < 0.05$ and ** represents $p \leq 0.001$.

Following 48h incubation, the Aβ$_{1-42}$ coincubations at Aβ$_{1-42}$:PINPs relative molar ratios of 1:2 and 1:3 were found to exhibit significantly lower fluorescence than the control sample

containing Aβ$_{1-42}$ alone (Figure 4.5.1). This indicates that after 48h, there were significantly

reduced levels of fibrillar Aβ$_{1-42}$ aggregations in the two Aβ$_{1-42}$ + PINPs coincubations with the

greatest concentration of PINPs. Interestingly, these samples (1:2 and 1:3) were also shown

to exhibit significantly reduced fluorescence when compared to Aβ$_{1-42}$ alone after 36 hours.

Throughout all time periods, the Aβ$_{1-42}$ + PINPs coincubation at a ratio of 1:2 exhibited

significantly reduced fluorescence when compared to Aβ$_{1-42}$ alone.

In order to determine whether any effects of PINPs were due to the combination of the

liposome particle and the RI-OR2-TAT peptide, or whether pegylated liposomes were

sufficient for such effects, MAL-PEG liposomes were also included in the ThT assay. Results

for RI-OR2-TAT are also presented showing the efficacy of PINPs ability to reduce Aβ$_{1-42}$

aggregation compared with equimolar concentrations of MAL-PEG liposomes and RI-OR2-

TAT (Figure 4.5.2).
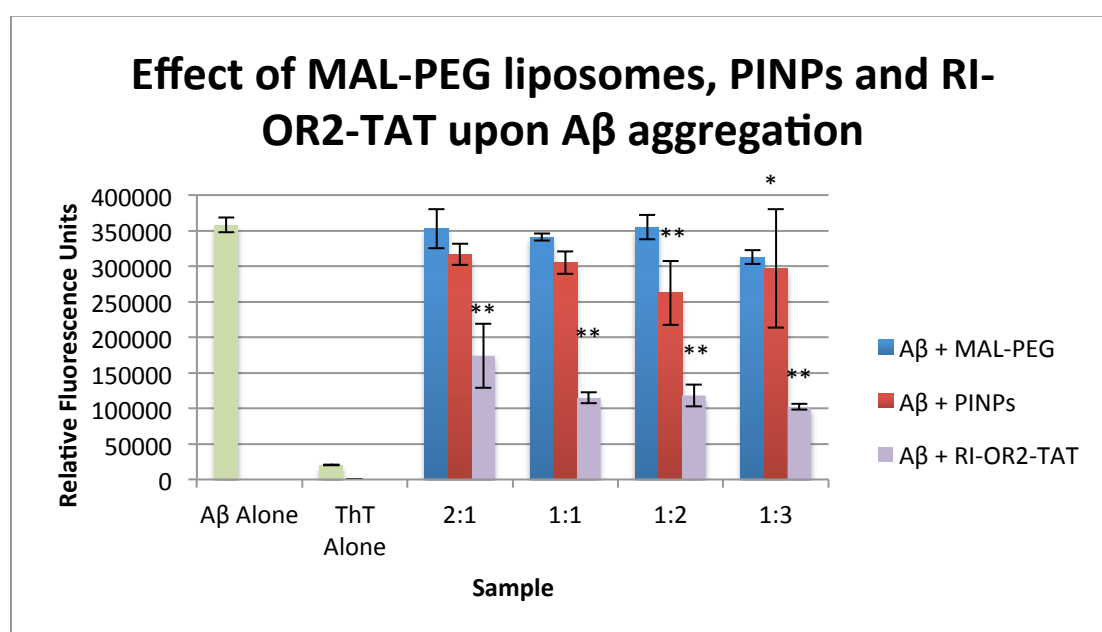
Figure 4.5.2 - Effect of MAL-PEG liposomes, PINPs and RI-OR2-TAT upon Aβ aggregation.
Data shown represents measurements recorded following 48h coincubation of 25 μM Aβ$_{1-42}$
with either MAL-PEG liposomes, PINPs or RI-OR2-TAT at relative concentrations of 2:1, 1:1,
1:2, 1:3 (i.e. 12.5 μM, 25 μM, 50 μM, 100 μM). Samples were plated in triplicate and bars
represent the mean values for each sample and error bars represent ± SD. All coincubations
were compared to the sample containing Aβ$_{1-42}$ alone: * represents $p<0.05$ and **
represents $p<=0.001$.

Analysis of ThT fluorescence from $A\beta_{1-42}$ + MAL-PEG coincubations showed that no difference in fluorescence was observed when compared to the control sample (Aβ alone) for any of the $A\beta_{1-42}$:MAL-PEG ratios investigated. This indicates that the presence of MAL-PEG liposomes has no effect upon aggregation of the $A\beta_{1-42}$ peptide. Consistent with previous investigations performed during development of RI-OR2-TAT, this peptide was found to significantly reduce the aggregation of the $A\beta_{1-42}$ peptide at all of the concentrations and time points tested. This is in contrast to results observed from the PINPs samples where only the 1:2 sample showed significant reductions in ThT fluorescence at 12h, 24h, 36h and 48h, with the 1:3 sample showing reduction at 36h and 48h time points. The reductions in fluorescence detected from $A\beta_{1-42}$:RI-OR2-TAT coincubations were significantly greater than those detected from $A\beta_{1-42}$:PINPs coincubations at all concentrations tested (Figure 4.5.3).

(A)
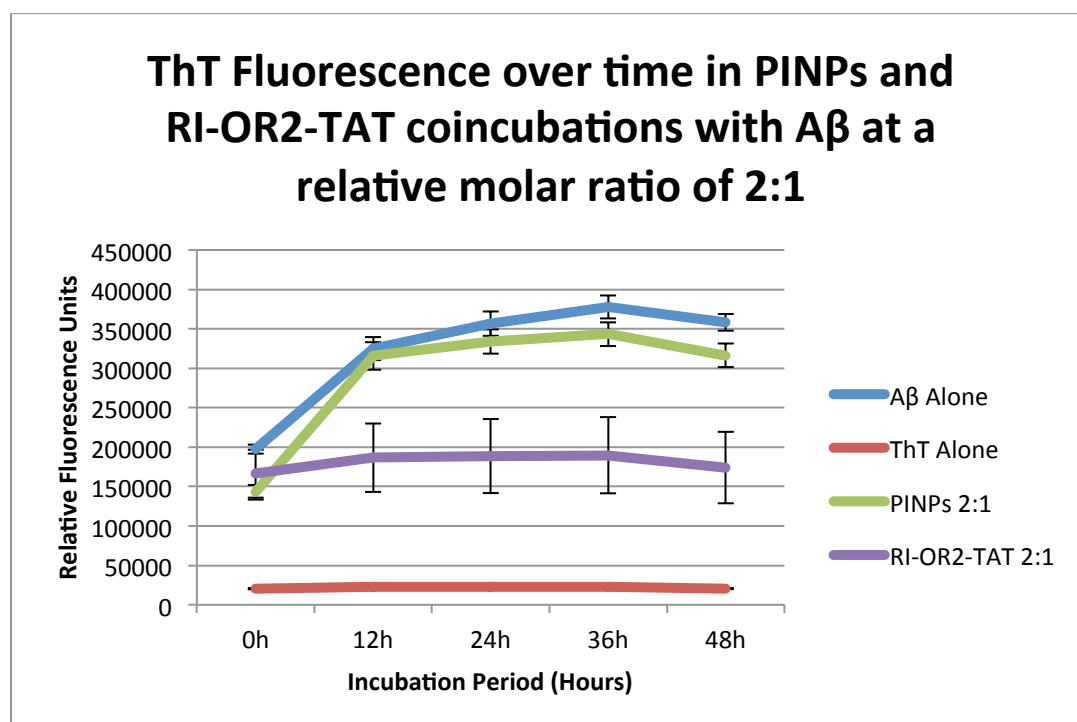
(B)
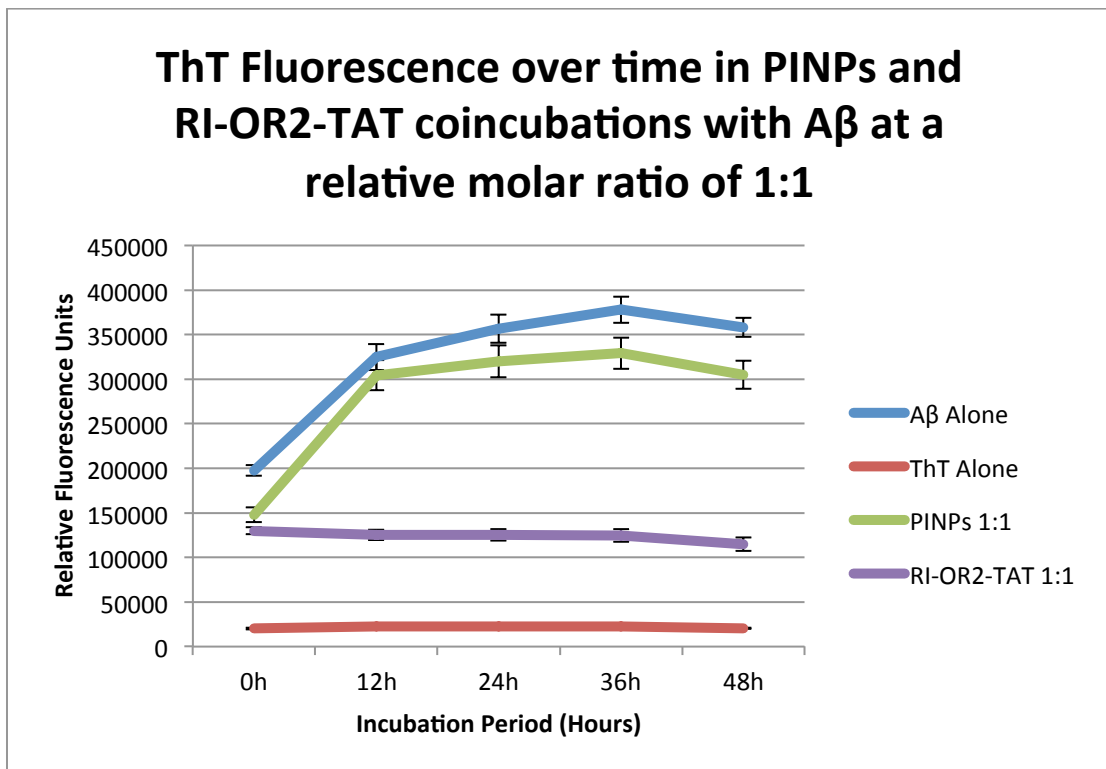
(C)
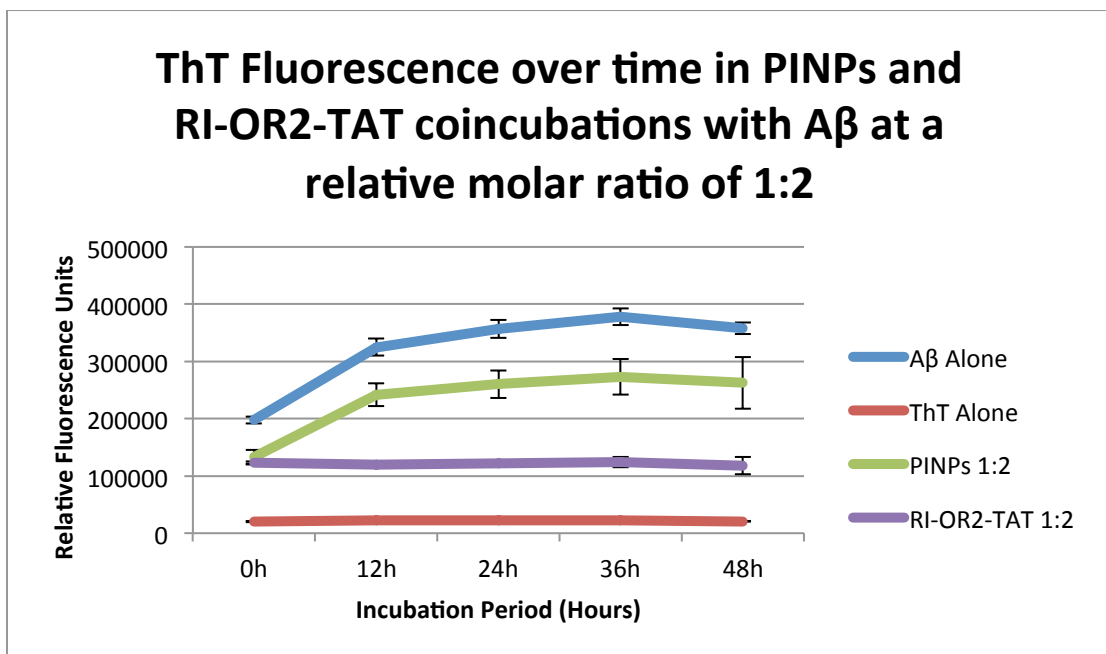
(D)
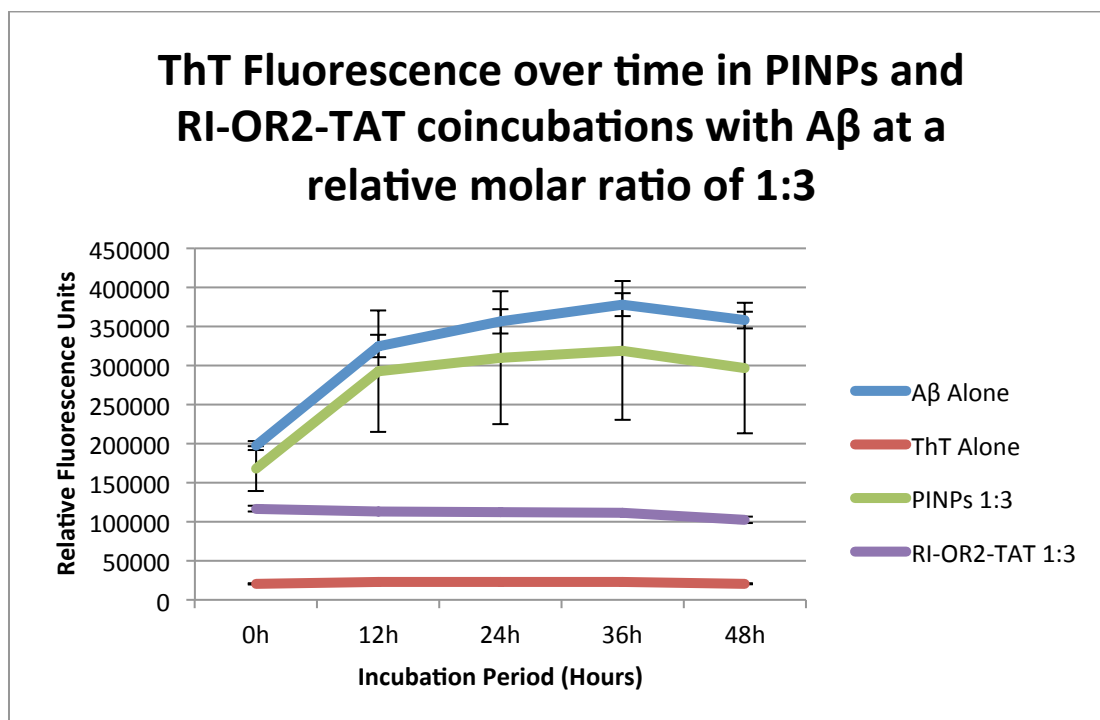
Figure 4.5.3 – ThT Fluorescence at 12h intervals at various relative concentrations (Aβ$_{1-42}$:PINPs/RI-OR2-TAT) of PINPs and RI-OR2-TAT when coincubated with Aβ$_{1-42}$. Points represent the mean of samples plated in triplicate and incubated at 37°C for 48h. Error bars show ± SD. (A) 2:1, (B) 1:1, (C) 1:2, (D) 1:3.

4.6– Results II – Summary and Discussion

4.6.1 – Liposome Morphology

The results of this investigation revealed that both PINPs appeared spheroid or ovoid in shape and formed heterogeneous liposome populations. Based on findings by other groups in the literature, the shape of the liposomes corresponded with what would be expected due to the nature of phospholipid bilayers and their stability in aqueous solution when forming an energetically favourable concentric structure (due to their amphipathic nature) (Balazs & Godbey, 2010). Although previous literature has described the appearance of liposomes, there have been no previous studies investigating PINPs. Therefore this investigation indicates that the addition to the RI-OR2-TAT peptide to liposomes – forming PINPs, does not appear to have an effect upon the basic morphology of the liposomes. Due to the difference

in composition of distilled water and PBS, the stability evidenced by the results from this test suggest that the PINPs are stable under exposure to different osmotic gradients and a pH range of 6-7.4. Stability in this pH range indicates that the PINPs are likely to be stable when traveling through the human circulatory system where the pH of blood is tightly regulated between pH 7.35-7.45. This is important for a potential therapy that directly targets the pathological features of AD in the brain (i.e. plaques) as the drug must first cross the BBB to reach its targets. Therefore investigating the appearance of the PINPs demonstrates that they appear to be stable in solutions of different concentrations despite the attachment of the RI-OR2-TAT peptide and do not appear to be affected under physiological pH.

When analyzing the appearance of PINPs, dark regions were commonly observed surrounding the liposomes. The dark regions appeared more pronounced in samples where the PINPs were diluted ten-fold in distilled water than in samples where liposomes had been in PBS solution. One possible explanation for this observation is that the dark patches may be due to leakage of PBS from liposomes. As PINPs are suspended in PBS during production, the aqueous core of the liposome retains PBS solution. Upon dehydration and exposure to the PTA stain during the negative staining process, PINPs may rupture thus releasing the contents of their aqueous core – PBS – into the surrounding area. This hypothesis would appear to be supported by the less pronounced dark regions surrounding the PINPs suspended in PBS. In this case it is possible that the uniform spread of PBS across the EM grid results in a darker background to the sample thus reducing the contrast between the PBS released from liposomes and rest of the sample.

Another feature observed in this investigation was the tendency of liposomes to associate with one another. PINPs appeared to aggregate with other liposomes and in some instances appeared to overlap with other PINPs. Previous studies have implicated PEG in the aggregation of liposomes, stating that increased levels of PEG result in increased fusion

between ULVs (Boni et al., 1981). As PINPs have PEG as a constituent, it is highly likely that the association observed is to some degree mediated by the presence of PEG. It is also important to note that although the induction of aggregation by PEG is well documented, the use of PTA stain has also been reported to increase association of lipid structures (Zhang et al., 2010). Therefore the association observed between the PINPs is likely to be a due to the presence of PEG in combination with the association induced by the PTA stain.

Throughout the investigations into liposomal morphology, the size of liposomes observed from TEM micrographs have been consistently lower than was reported upon production of the liposomes. Following liposomal production, mean diameter was calculated using dynamic light scattering that analyses the liposomes in their fully hydrated state. TEM analysis of liposomes involves the dehydration of samples during transfer to a solid support, as well as exposure to PTA and the high vacuum environment of a TEM. Dehydration of the liposomes is highly likely to result in a reduction in their size and therefore is expected to be responsible for the discrepancies observed when comparing size of the liposomes using the different techniques.

4.6.2 – TEM analysis of $A\beta_{1-42}$ – PINP interactions

Following characterisation of $A\beta_{1-42}$ aggregation and liposome structure and morphology, the next step was to use TEM to investigate the effect of PINPs upon $A\beta_{1-42}$ aggregation. This experiment therefore investigated whether attachment of RI-OR2-TAT to nanoliposomes prevented the ability of the peptide to inhibit $A\beta_{1-42}$ aggregation or whether this ability had been retained. The ability of RI-OR2-TAT to reduce $A\beta_{1-42}$ aggregation had been previously documented in the literature (Taylor et al., 2010), thus an inability to reduce $A\beta_{1-42}$ aggregation in this test could be directly attributable to the attachment of the peptide to liposomes. Therefore this experiment provided new information regarding the ability of PINPs to be carried forward as a novel therapeutic option for the treatment of AD.

Additionally, these results represent the first time electron microscopy has been employed to investigate RI-OR2-TAT and PINPs.

Samples of $A\beta_{1-42}$ that were incubated in the absence of liposomes formed $A\beta$ aggregates, with many areas covered with dense regions of these structures. Fibrils of varying sizes could be seen dispersed throughout the samples. Some dense regions of $A\beta_{1-42}$ aggregation were also observed in the samples containing PINPs, however these regions were less abundant than in samples lacking PINPs. When investigating the samples containing PINPs + $A\beta_{1-42}$ at high magnification, it was found that PINPs could be observed bound to $A\beta_{1-42}$ fibrils, both along the length of fibrils and to their termini. An interesting observation from this investigation was that PINPs appeared able to prevent further fibril elongation. Additionally, the presence of PINPs along the length of fibrils indicates that binding of the PINPs does not result in disaggregation of fibrils. Furthermore, based on earlier investigations into the shape and morphology of PINPs which revealed smooth spheroid structures, PINPs imaged following incubation with $A\beta_{1-42}$ appeared to lose their smooth appearance and instead appeared much more coarse. As a result of these observations, a hypothesis was formulated which attributed the change in appearance to the binding of small $A\beta_{1-42}$ oligomers to the surface of PINPs.

4.6.3 – Immunogold labelling to detect PINP-bound $A\beta_{1-42}$ oligomers

Results from control sample A showed the presence of $A\beta_{1-42}$ fibrils, with no positive labeling by the gold conjugated secondary antibody. The presence of some fibrils in this sample was expected as earlier investigations had shown that although PINPs are able to bind fibrils and possibly prevent their elongation by binding to their termini, $A\beta_{1-42}$ fibrils were still present. It is logical to presume that by increasing the ratio of PINPs to $A\beta_{1-42}$ that the number of fibrils seen in these samples would be reduced. However, the most significant finding from analysis of control sample A is the lack of labeling when the primary (anti-$A\beta$) antibody was not present. This lack of labeling showed that in the absence of the primary antibody, the

secondary antibody did not bind to the samples. This removes the possibility that binding of the secondary antibody was unspecific and therefore strongly suggests that the labeling observed indicates the precise presence of Aβ aggregates. Another important control sample included in this study was Control sample B. This purpose of this control sample was to determine whether the primary and/or secondary antibody bound to PINPs in the absence of $Aβ_{1-42}$. Analysis of this sample showed that no labeling of the PINPs occurred meaning that any labeling of PINPs observed during analysis of Test samples (i.e. containing PINPS + $Aβ_{1-42}$) could be attributed to the presence of $Aβ_{1-42}$ and not due to non-specific labeling of PINPs.

The test samples (i.e. PINPs and $Aβ_{1-42}$ incubated together) were found to contain PINPs that showed positive labeling. As the control samples appeared very clean, with very little background labeling, the labeling observed from the test samples can be directly attributed the presence of $Aβ_{1-42}$ at the PINP surface. Although the incubation period of 24 hours was sufficient for the formation of amyloid fibrils, many regions show labeling of the PINPs in the absence of fibrils. This therefore strongly suggests that the labeling observed in this investigation can be attributed to smaller $Aβ_{1-42}$ aggregations such as the highly toxic Aβ oligomers. The inability to directly observe the oligomers on the surface of the fibrils is likely attributable to the dark appearance of the PINP as well as the small size of oligomers, which have been reported to exist with heights as low as 1 nm and widths as low as 5 nm (Sakono & Zako, 2010). Binding of the oligomers with such close proximity to the PINP (due to the small size of the RI-OR2-TAT peptide) makes distinguishing oligomers on the surface of PINPs by TEM highly unlikely and therefore other features such as the positive labeling and altered PINP morphology can be used to indicate the presence of oligomers on the PINP surface. If this is indeed the case, as is predicted, these results suggest that the protective effects of RI-OR2-TAT that have been documented in previous studies are retained following attachment to liposomes (forming PINPs). This therefore shows that PINPs are a viable drug delivery system for the RI-OR2-TAT peptide.

4.6.4 – Investigating the effect of PINPs upon $A\beta_{1-42}$ oligomer formation

Following on from the positive immunogold labelling observed during EM analysis of $A\beta_{1-42}$+PINPs coincubations, quantitative analysis was performed to determine whether the interactions between PINPs and $A\beta_{1-42}$ had a significant effect upon $A\beta_{1-42}$ aggregation. Using a fluorescence-based sandwich ELISA, levels of oligomeric $A\beta_{1-42}$ species were analysed over a 48h period in the absence and presence of PINPs at a range of concentrations.

Analysis after 4h incubation showed no significant difference in $A\beta_{1-42}$ aggregation between $A\beta_{1-42}$ alone and when coincubated with PINPs. However analysis after 24h showed that two samples (1:1 and 1:3) possessed significantly lower levels of oligomeric $A\beta_{1-42}$ than the control sample ($A\beta_{1-42}$ alone). Surprisingly the results obtained after 24h incubation showed significantly reduced oligomer concentrations at $A\beta_{1-42}$:PINPs ratios of 1:1 and 1:3, but not at 2:1 or 1:2. It is likely that following 24h incubation at 2:1, the levels of PINPs present are not sufficient to significantly effect the formation of oligomers compared with the control sample. As 1:1 was found to reduce levels of oligomers after 24h, it would be expected that 1:2 (therefore twice the concentration of PINPs as in the 1:1 sample) would also significantly reduce $A\beta_{1-42}$ oligomer levels however this was not observed. It is possible that this is attributable to human error during sample preparation whereby insufficient mixing of the sample lead to less interaction between PINPs and $A\beta_{1-42}$ and therefore PINPs were not able to bind $A\beta_{1-42}$ and inhibit further aggregation. Analysis of the coincubations after 48h incubation revealed that all coincubations possessed significantly reduced levels of oligomeric $A\beta_{1-42}$ compared with the control sample. This indicates that the reduced oligomer levels are attributable to the presence of the PINPs in the samples. These results combined with the results from the immunogold labeling TEM analysis (Chapter 6) suggest that the inhibition of oligomer formation in the presence of PINPs is due to sequestration of $A\beta_{1-42}$ by PINPs.

These results strongly indicate that PINPs are able to reduce the formation of oligomers by monomeric Aβ$_{1-42}$, and thus represent a strong candidate for a novel therapetutic option for the treatment of AD. As Aβ$_{1-42}$ oligomers are widely regarded as the most toxic species of Aβ$_{1-42}$ aggregate, the ability of PINPs to prevent oligomer formation could have significant disese modifying outcomes for sufferers if this effect could be replicated *in vivo*.

4.6.5 – Investigating the effect of PINPs upon Aβ$_{1-42}$ fibril formation

Further quantitative analysis of the effect of PINPs upon aggregation of Aβ$_{1-42}$ was performed using the ThT assay. Unlike the sandwich ELISA mentioned in the previous paragraphs which is used to investigate the presence of oligomeric (early) species of Aβ$_{1-42}$ aggregates, the ThT assay is used to investigate levels of later stage (fibrillar) aggregates. This is due to the fact that ThT binds Aβ$_{1-42}$ fibrils in the channels between ladders in the fibril side chains (Biancalana & Koide, 2010), and as a result of this binding, the excitation and emission wavelengths of ThT are increased and can be measured. This enables quantitative analysis of the ability of potential inhibitors of Aβ$_{1-42}$ aggregation to be accurately analysed and for comparisons to be made.

The quantitative investigation of Aβ$_{1-42}$ aggregation in the presence of different inhibitors/potential inhibitors (MAL-PEG liposomes, PINPs and RI-OR2-TAT) by ThT assay in this study confirmed the previously reported ability of RI-OR2-TAT to reduce Aβ$_{1-42}$ aggregation, whilst also revealing the ability of PINPs to reduce Aβ$_{1-42}$ aggregation (Parthsarathy et al., 2013). At relative molar ratios (Aβ$_{1-42}$:PINPs) of 1:2 and 1:3, PINPs were found to reduce aggregation of Aβ$_{1-42}$ and therefore demonstrating their anti-Aβ$_{1-42}$ aggregation effects, providing encouraging results for PINPs to be taken forward for further investigation as a potential novel therapeutic option for the treatment of AD.

At all ratios investigated, the coincubations of Aβ$_{1-42}$ with RI-OR2-TAT showed increased ability to reduce Aβ$_{1-42}$ aggregation than PINPs. However it is important to note that as RI-

OR2-TAT only accounts for ~5% of the surface area of PINPs, the concentration of RI-OR2-TAT in PINPs samples was greatly reduced (20-fold reduction) compared to RI-OR2-TAT samples and therefore this reduced ability to prevent $A\beta_{1-42}$ aggregation by PINPs when compared to RI-OR2-TAT is not surprising. Therefore the concentration of RI-OR2-TAT peptide in PINPs samples enables PINPs to significantly reduce aggregation with $A\beta_{1-42}$:RI-OR2-TAT ratios as high as 10:1. This is consistent with previous investigations into the ability of RI-OR2-TAT to reduce $A\beta_{1-42}$ aggregation (Parthsarathy et al., 2013).

The finding in this assay that MAL-PEG liposomes did not have any significant effect upon $A\beta_{1-42}$ aggregation illustrate that the liposome carrier particles do not possess any intrinsic ability to reduce $A\beta_{1-42}$ aggregation.

This data shows that attaching RI-OR2-TAT to liposome carrier particles (forming PINPs) preserves the aggregation inhibiting ability of this peptide, whilst providing a delivery system that is likely to increase the efficacy of the peptide. This is due to the increased circulation times afforded to RI-OR2-TAT by attachment to stealth liposomes, which have been shown in many studies to exhibit low immunogenicity, reducing the risk of further illness to an individual following administration than might be the case when using RI-OR2-TAT alone.

Although $A\beta_{1-42}$ oligomers are now widely regarded as being the most toxic forms of $A\beta_{1-42}$ aggregates, there is evidence to suggest that fibrillar species are also able to contribute to disease pathology, for example by being involved in the production of ROS (Mayes et al., 2014). Therefore the ability of PINPs to reduce formation of fibrillar $A\beta_{1-42}$ species is an important quality and the value of this ability should not be underestimated.

Taken together, the ability of PINPs to reduce the levels of formation of both early and late stage $A\beta_{1-42}$ aggregates represents an exciting step towards development of an effective DMT for the treatment of AD.

Chapter 5 – Study Conclusions

Due to advances in medicine and healthcare, individuals in many countries worldwide are living longer and contributing to ageing populations. As there are increased numbers of elderly individuals, diseases of old age such as AD (although some genetic variants can produce early onset AD) are becoming increasingly common and as a result their impact upon sufferers and the wider society continues to increase. In order to tackle this growing issue, new treatments need to be developed which are more effective than the currently available therapeutic options, which are only capable of temporarily alleviating the symptoms of the disease without addressing the underlying cause of the clinical symptoms. Therefore in order to effectively tackle AD, extensive research into disease modifying therapies -which effectively halt (and possibly even reverse) disease progression – is being undertaken.

In order to ensure that research groups are able to use their funds to the greatest effect, there is a constant requirement to reduce unneccesary costs. This study aimed to address this issue by producing the $A\beta_{1-42}$ peptide 'in-house' using a recombinant expression system. In-house production of $A\beta_{1-42}$ by this method provides a much cheaper way of obtaining the peptide, and is able to produce a peptide more similar to that produced naturally, which is not the case with many commercially procured batches of $A\beta_{1-42}$ that are produced using peptide synthesisers. Therefore by producing recombinant $A\beta_{1-42}$ in-house, there is the potential for significant cost savings whilst improving the similarity between $A\beta_{1-42}$ used for research purposes to that which is involved in the pathogenesis of AD.

With regard to research into potential treatments for AD, one candidate for a novel disease modifying therapy is the peptide inhibitor RI-OR2-TAT, which significantly reduces the self-aggregation of Aβ peptides as well as microglial activation and damage by ROS. Additionally, RI-OR2-TAT has also been found to stimulate neurogenesis, providing an exciting therapeutic

option to continue to investigate further. Advances in knowledge regarding liposomes and their therapeutic applications have enabled production of second generation liposomes which have much greater circulation times due to their ability to avoid detection by the MPS. By covalently attaching RI-OR2-TAT to second-generation liposomes (forming PINPs), it is hypothesized that the PINPs will constitute multivalent $A\beta_{1-42}$ inhibitors that are able to improve the effects observed using RI-OR2-TAT alone and will ultimately provide a novel disease modifying therapy for the treatment of AD. Using a number of different methods, the ability of PINPs to reduce self-aggregation of $A\beta_{1-42}$ was investigated.

5.1 – Summary of findings

In this study, $A\beta_{1-42}$ peptides were produced recombinantly using an adapted version of the production protocol published by Finder et al. (Finder et al., 2010), The ability to produce $A\beta_{1-42}$ at a much lower cost than purchasing this peptide commercially represents a significant step towards ensuring that the funding provided to researchers investigating highly prevalent and serious diseases such as AD is used to greatest effect. By reducing expenditure on $A\beta_{1-42}$ – of which a significant amount is used when undertaking research into methods of preventing $A\beta_{1-42}$ aggregation – research funds can be spent on other products which may enable researchers to carry out investigations that would not have been fiscally possible due to expenditure on $A\beta_{1-42}$. This in turn may help to build a greater basis of knowledge surrounding AD and in turn may assist researchers in developing novel therapies for this disease.

In addition to the financial benefits of in-house production of $A\beta_{1-42}$, the procedure for production of the peptide can be completed within 4 days. This includes production of a protease required for cleavage of $A\beta_{1-42}$ from its expressed fusion protein form, meaning that researchers may be able to produce their own $A\beta_{1-42}$ in a shorter period of time than they would have to wait for delivery of the peptide from a commercial supplier.

Following production of Aβ$_{1-42}$ at Lancaster University by the in-house method detailed earlier in this study, significant analysis of the Aβ$_{1-42}$ peptide was undertaken to determine its characteristics and suitability as an alternative to commercially purchased Aβ$_{1-42}$. This investigation involved negatively staining samples with PTA and then examining the characteristics of the peptide by transmission electron microscopy. Results from this analysis indicated that the peptide appeared to display similar characteristics to commercially produced Aβ$_{1-42}$ regarding the ability of the peptide to self-aggregate and form larger structures such as oligomers and fibrils, as well as being similar in size to aggregates reported in the literature. During these investigations the fibrillar aggregates were found to associate with other fibrils in an ordered, parallel manner and this is another characteristic that has been reported to have been observed following analysis of commercially purchased Aβ$_{1-42}$. Taken together, the aggregations observed from self-association of the Aβ$_{1-42}$ peptides and the size of such aggregates, strongly suggests that Aβ$_{1-42}$ produced recombinantly and in-house, has the potential to replace commercially produced Aβ$_{1-42}$.

Despite the confirmation that Aβ$_{1-42}$ was produced and purified in this study, the current protocol requires further refinement before Aβ$_{1-42}$ produced in-house can be used for research purposes. One issue with the current protocol is that the fusion proteins appear to aggregate in solution and that following cleavage with the TEV protease, many of the fusion proteins still contain the Aβ$_{1-42}$ peptide region. It is likely that the self-association of the fusion proteins restricts the ability of the TEV protease to access/cleave the TEV protease cleavage site on the fusion protein, reducing the levels of cleavage Aβ$_{1-42}$ obtained through this process. A possible step to reduce aggregation of the fusion protein is to perform the cleavage whilst the fusion protein is immobilized on the Ni-NTA column rather than in solution. This would result in less interaction between Aβ$_{1-42}$ peptide regions of the fusion protein and may therefore reduce levels of fusion protein aggregation. Another issue with the current process is that despite efforts to reduce aggregation of monomers and to deseed

any aggregations that do exist prior to experiemental use, aggregates are still detectable immediately following production and purification. It is important for research purposes that the Aβ_{1-42} peptide initially exists in the monomeric form and therefore in future, extra steps (e.g. further rounds of sonication) should be performed to reduce levels of aggregates following production and purification.

By producing this protein recombinantly rather than synthetically, it is hoped that the peptide will provide a source of Aβ_{1-42} that is representative of naturally produced Aβ_{1-42} and will not display the variability between different batches and manufacturers that exists for the synthetic Aβ_{1-42} sold commercially. This reduction in variability would allow more accurate comparison between results from different studies when using rAβ_{1-42} compared with synthetic Aβ_{1-42}.

The combination of the production method (recombinant rather than using a peptide synthesizer) reduced cost, relatively short production time, and aggregation characteristics of Aβ_{1-42} produced in-house means that self-production of Aβ_{1-42} is a realistic and cost effective alternative to commercial procurement, available to researchers. By incorporating the steps recommended in this study to improve the amounts of Aβ_{1-42} peptide recovered after this process and to ensure that the peptide exists in a monomeric state, future efforts are likely to see greater peptide yields per batch, and that levels of Aβ_{1-42} peptide aggregates are reduced following purification. This would increase the benefits of adopting an in-house production approach to sourcing of Aβ_{1-42} for research use.

Initial investigations into the potential use of PINPs to reduce aggregation of Aβ_{1-42} peptides, analysed the morphology of PINP suspensions in both PBS and distilled water suspensions. Such analysis revealed that PINPs appear stable at physiological pH, supporting the feasibility of PINPs to be used as a therapeutic option in humans.

The ability of the RI-OR2-TAT peptide to retain its anti-Aβ_{1-42} aggregation effect when bound to the liposome nanoparticles – against early (oligomeric) and late (fibrillar) stage Aβ_{1-42} aggregates - represents a significant step in development of PINPs as a potential therapeutic agent. Results in this study demonstrated that PINPs were able to reduce aggregation of Aβ_{1-42} into oligomers and fibrils. This is particularly important for a potential disease modifying treatment for AD whereby the brains of sufferers contain significantly elevated levels of both oligomeric and fibrillar Aβ_{1-42} aggregates, as a reduction in aggregation would mean a reduction in the neurotoxicity caused by Aβ_{1-42} aggregates. Attachment of peptides to liposomes has been shown to improve peptide stability in circulation by reducing opsonisation as well as improving absorbance of the therapeutic from the small intestine (Bruno et al., 2013). These advantages provide two extremely important characteristics of this potential therapy: 1) PINPs are likely to improve circulation times of RI-OR2-TAT (compared with direct injection of the RI-OR2-TAT peptide), enabling a greater period of anti-aggregation activity of RI-OR2-TAT and 2) Providing the possibility of delivery via an oral administration route rather than intravenously, which has been shown previously to improve patient compliance with treatments (Maher & Brayden, 2012). This is in addition to the anti-Aβ_{1-42} effect of RI-OR2-TAT that has been demonstrated previously.

5.2 – Future Directions

By refining the method for producing rAβ_{1-42} at Lancaster University, it is hoped that in-house production of the peptide will prove a realistic source of the Aβ_{1-42} peptide for future research use. In addition to reduced cost, another key benefit of producing Aβ_{1-42} recombinantly is the avoidance of racemization of amino acids in the peptide, reducing batch-to-batch variability and increasing the accuracy and reproducibility of results. In order to ensure that the rAβ_{1-42} offers this reduced variability, future studies should aim to sequence the rAβ_{1-42} (e.g. via Edman degradation) to ensure that the rAβ_{1-42} provides a high quality and relevant source of Aβ_{1-42}.

The findings from this study can be used to build upon previous investigations into the efficacy of RI-OR2-TAT as a potential novel therapeutic option for the treatment of AD, to be used as a disease modifying therapy (DMT) (Parthsarathy et al., 2013). By analysing the results from this study in the context of previous investigations, it can be concluded with a significant degree of confidence that PINPs represent an exciting potential DMT and that PINPs should be carried forward into further investigations to determine their on- and off-target effects in human subjects. The attachment of RI-OR2-TAT to liposomes represents a potential improvement upon RI-OR2-TAT alone due to the increased stability and potential for oral administration that arises following conjugation to nanoliposomes (Bruno et al., 2013). For this reason, future work should aim to further assess the suitability of this potential treatment for use in humans to halt or reverse the progress of AD in individuals suffering from this devastating disease.

As PINPs have been designed to cross the BBB in order to reduce aggregation of $A\beta_{1-42}$ within the brain, future studies should use animal models of AD to evaluate the effect of PINPs upon behavior, memory and cognition. These aspects of brain function can be investigated and measured using tasks such as the Morris Water Maze and Radial Arm Maze. These tasks will provide information relating to the condition of the reference and working memory of the mice being tested and therefore would be reliable indicators of any improved performance observed between AD model groups and control groups when treated with PINPs (Webster et al., 2014). By performing these investigations in mouse models of the disease it will be possible to gain a clearer idea regarding the potential of PINPs to have the desired disease modifying effects in humans (e.g. improvements in memory and cognition). This will then enable specific elements of cognition to be measured in human trials based upon what may be expected following trials in mouse models.

In addition to evaluating potential beneficial effects of PINPs upon behaviour and cognition, investigations should be undertaken through human clinical trials to investigate the pharmacokinetics of this potential novel treatment in order to effectively analyse the safety of using PINPs in humans. First-in-man human trials of PINPs would be a realistic next step in the development of this potential therapy and due to the formulation of the delivery mechanism (PEGylated stealth liposomes) which is already used in drugs that have been approved for use in humans such as liposomal doxorubicin (e.g. Doxil), it is likely that PINPs will not raise any severe health issues in the individuals taking part in this trial (Immordino et al., 2006). PINPs however differ from other liposomal formulations in the sense that they have RI-OR2-TAT attached to the liposome exterior and therefore the safety of this arrangement must be determined. Pharmacokinetic studies could be performed in order to determine important parameters that constitute essential knowledge before a drug can be effectively used as a viable therapy (assuming clinical trials progress successfully) such as C_{max}, half-life and mean residence time (Li & Huang, 2008). Measuring these vital parameters will enable the accurate production of safe and effective dosing regimens for clinical usage (Li & Huang, 2008).

As mentioned in the introduction to this study, for a potential therapy to be effective against AD, it is likely that administration of the drug will need to begin when an individual is in the preclinical phase or a very early stage of AD – recently exemplified by the results for Solenezumab (where the drug exhibited beneficial effects upon individuals with mild AD but not those with moderate AD) (Liu-Seifert et al., 2015). This highlights the importance of continuing to develop methods of detecting and measuring changes in amyloid deposition in the brain that could be used to aid early diagnosis of AD. Due to the ability of RI-OR2-TAT to bind $A\beta_{1-42}$, this suggests that PINPs may also be used as a method of measuring $A\beta_{1-42}$ deposition. By incorporating detectable 'tags' (e.g. a radiolabel) into RI-OR2-TAT, imaging approaches such as PET could be employed to detect regions of $A\beta_{1-42}$

aggregation/deposition. This may represent an improvement upon current methods such as

the use of PiB and therefore enable earlier detection of $A\beta_{1-42}$ aggregation which may

improve the prognosis for patients if/when effective DMTs become available.

References

Albert, M. S., DeKosky, S. T., Dickson, D., Dubois, B., Feldman, H. H., Fox, N. C., Gamst, A., Holtzman, D. M., Jagust, W. J., Petersen, R. C., Snyder, P. J., Carrillo, M. C., Thies, B., & Phelps, C. H. (2011). The diagnosis of mild cognitive impairment due to Alzheimer's disease: Recommendations from the National Institute on Aging-Alzheimer's Association workgroups on diagnostic guidelines for Alzheimer's disease. *Alzheimers Dement*, 7, 270-279.

Al-Hilaly, Y. K., Williams, T. L., Stewart-Parker, M., Ford, L., Skaria, E., Cole, M., Bucher, W. G., Morris, K. L., Sada, A. A., Thorpe, J. R., & Serpell, L. C. (2013). A central role for dityrosine crosslinking of Amyloid-β in Alzheimer's disease. *Acta Neuropathol Commun*, 1, 1-17.

Allinson, T. M., Parkin, E. T., Turner, A. J., & Hooper, N. M. (2003). ADAMs family members as amyloid precursor protein α-secretases. *J Neurosci Res*, 74, 342-352.

Allsop, D., & Mayes, J. (2014). Amyloid β-peptide and Alzheimer's disease. *Essays Biochem*, 56, 99-110

Almkvist, O., Darreh-Shori, T., Stefanova, E., Spiegel, R., & Nordberg, A. (2004). Preserved cognitive function after 12 months of treatment with rivastigmine in mild Alzheimer's disease in comparison with untreated AD and MCI patients. *Eur J Neurol*, 11, 253-261.

Alzheimer, A. (1907). Uber eine eigenartige Erkrankung der Hirnrinde. *Allgemeine Zeitschrife Psychiatrie*, 64, 146-148.

Alzheimer's Association. (2006). Early onset dementia: a national challenge, a future crisis. Alzheimer's Association, Washington, DC, 68.

American Psychiatric Association. (2000). *Diagnostic and statistical manual of mental disorders* (4th ed.). Washington, DC: American Psychiatric Association.

Anand, R., Gill, K. D., & Mahdi, A. A. (2014). Therapeutics of Alzheimer's disease: Past, present and future. *Neuropharmacology*, 76, 27-50.

Andreasen, N., Hesse, C., Davidsson, P., Minthon, L., Wallin, A., Winblad, B., Vanderstichele, H., Vanmechelen, E., & Blennow, K. (1999). Cerebrospinal fluid β-amyloid (1-42) in Alzheimer disease: differences between early-and late-onset Alzheimer disease and stability during the course of disease. *Arch Neurol*, 56, 673-680.

Apostolova, L. G., Green, A. E., Babakchanian, S., Hwang, K. S., Chou, Y. Y., Toga, A. W., & Thompson, P. M. (2012). Hippocampal atrophy and ventricular enlargement in normal aging, mild cognitive impairment and Alzheimer's disease. *Alz Dis Assoc Dis*, 26, 17-27.

Arosio, P., Cukalevski, R., Frohm, B., Knowles, T. P., & Linse, S. (2013). Quantification of the concentration of Aβ1-42 propagons during the lag phase by an amyloid chain reaction assay. *J Am Chem Soc*, 136, 219-225.

Atri, A., Shaughnessy, L. W., Locascio, J. J., & Growdon, J. H. (2008). Long-term course and effectiveness of combination therapy in Alzheimer's disease. *Alz Dis Assoc Dis*, 22, 209-221.

Atwood, C. S., Scarpa, R. C., Huang, X., Moir, R. D., Jones, W. D., Fairlie, D. P., Tanzi, R. E., & Bush, A. I. (2000a). Characterization of copper interactions with Alzheimer amyloid β peptides. *J Neurochem*, 75, 1219-1233.

Austen, B. M., Paleologou, K. E., Ali, S. A., Qureshi, M. M., Allsop, D., & El-Agnaf, O. M. (2008). Designing peptide inhibitors for oligomerization and toxicity of Alzheimer's β-amyloid peptide. *Biochemistry*, 47, 1984-1992.

Baines, S., Saxby, P., & Ehlert, K. (1987). Reality orientation and reminiscence therapy. A controlled cross-over study of elderly confused people. *Br J Psychiatry*, 151, 222-231.

Balazs, D. A., & Godbey, W. T. (2010). Liposomes for use in gene delivery. *J Drug Deliv, 2011,* 326497.

Ballard, C., & Howard, R. (2006). Neuroleptic drugs in dementia: benefits and harm. *Nat Rev Neurosci, 7,* 492-500.

Ballard, C. G., Waite, J., & Birks, J. (2006). Atypical antipsychotics for aggression and psychosis in Alzheimer's disease (review). *Cochrane Database Syst Rev*.

Bangham, A. D., & Horne, R. W. (1964). Negative staining of phospholipids and their structural modification by surface-active agents as observed in the electron microscope. *J Mol Biol*, 8, 660.

Barnham, K. J., McKinstry, W. J., Multhaup, G., Galatis, D., Morton, C. J., Curtain, C. C., Williamson, N. A., White, A. R., Hinds, M. G., Norton, R. S., Beyreuther, K., Masters, C. L., Parker, M. W., & Cappai, R. (2003). Structure of the Alzheimer's disease amyloid precursor protein copper binding domain A regulator of neuronal copper homeostasis. *J Biol Chem*, 278, 17401-17407.

Bartolini, M., Bertucci, C., Bolognesi, M. L., Cavalli, A., Melchiorre, C., & Andrisano, V. (2007). Insight Into the Kinetic of Amyloid β (1–42) Peptide Self-Aggregation: Elucidation of Inhibitors' Mechanism of Action. *ChemBioChem*, 8, 2152-2161.

Beister, A., Kraus, P., Kuhn, W., Dose, M., Weindl, A., & Gerlach, M. (2004). The N-methyl-D-aspartate antagonist memantine retards progression of Huntington's disease. *J Neural Transm Suppl*, 117-122.

Bennett, D. A., Schneider, J. A., Wilson, R. S., Bienias, J. L., & Arnold, S. E. (2004). Neurofibrillary tangles mediate the association of amyloid load with clinical Alzheimer disease and level of cognitive function. *Arch Neurol*, 61, 378-384.

Berkman, L. F. (1986). The association between educational attainment and mental status examinations: of etiologic significance for senile dementias or not?. *J Chronic Dis*, 39, 171-174.

Bertoni-Freddari, C., Fattoretti, P., Casoli, T., Meier-Ruge, W., & Ulrich, J. (1990). Morphological adaptive response of the synaptic junctional zones in the human dentate gyrus during aging and Alzheimer's disease. *Brain Res*, 517, 69-75.

Biancalana, M., & Koide, S. (2010). Molecular mechanism of Thioflavin-T binding to amyloid fibrils. *Biochim Biophys Acta*, 1804, 1405-1412.

Said Hassane, F., Frisch, B., & Schuber, F. (2006). Targeted liposomes: convenient coupling of ligands to preformed vesicles using "click chemistry". *Bioconjugate Chem*, *17*, 849-854.

Bird, M., Alexopoulos, P., & Adamowicz, J. (1995). Success and failure in five case studies: used of cued recall to ameliorate behaviour problems in senile dementia. *Int J Geriatr Psychiatry*, 10, 305-311.

Birks J. (2006). Cholinesterase inhibitors for Alzheimer's disease. *Cochrane Database Syst Rev*.

Blanquet, V., Goldgaber, D., Turleau, C., Creau-Goldberg, N., Delabar, J., Sinet, P. M., Roudier, M., de Grouchy, J (1987). In situ hybridization of the beta amyloid protein (APP) cDNA to the vicinity of the interface of 21q21 and q22 in normal and Alzheimer's disease individuals. *Cytogenet Cell Genet*, 46, 582.

Blennow, K., & Hampel, H. (2003). CSF markers for incipient Alzheimer's disease. *Lancet Neurol*, 2, 605-613.

Blennow, K., de Leon, M. J., & Zetterburg, H. (2006) Alzheimer's disease. *Lancet,* 368, 387-403.

Bolanos-Garcia, V. M., & Davies, O. R. (2006). Structural analysis and classification of native proteins from E. coli commonly co-purified by immobilised metal affinity chromatography. *Biochim Biophys Acta*, 1760, 1304-1313.

Boni, L. T., Stewart, T. P., Alderfer, J. L., & Hui, S. W. (1981). Lipid-polyethylene glycol interactions: I. Induction of fusion between liposomes. *J Membr Biol*, 62, 65-70.

Bordji, K., Becerril-Ortega, J., Nicole, O., & Buisson, A. (2010). Activation of extrasynaptic, but not synaptic, NMDA receptors modifies amyloid precursor protein expression pattern and increases amyloid-β production. *J Neurosci*, 30, 15927-15942.

Boyles, J. K., Zoellner, C. D., Anderson, L. J., Kosik, L. M., Pitas, R. E., Weisgraber, K., Hui, D. Y., Mahley, R. W., Gebicke-Haerter, P. J., & Ignatius, M. J. (1989). A role for apolipoprotein E, apolipoprotein AI, and low density lipoprotein receptors in cholesterol transport during regeneration and remyelination of the rat sciatic nerve. *J Clin Invest*, 83, 1015-1031.

Bozzuto, G., & Molinari, A. (2015). Liposomes as nanomedical devices. *Int J Nanomedicine*, 10, 975-999.

Brodaty, H., Ames, D., Snowdon, J., Woodward, M., Kirwan, J., Clarnette, R., Lee, E., Lyons, B., & Grossman, F. (2003). A randomized placebo-controlled trial of risperidone for the treatment of aggression, agitation, and psychosis of dementia. *J Clin Psychiatry*, 64, 134-143.

Bruno, B. J., Miller, G. D., & Lim, C. S. (2013). Basics and recent advances in peptide and protein drug delivery. *Ther Deliv*, 4, 1443-1467.

Buerger, K., Teipel, S. J., Zinkowski, R., Blennow, K., Arai, H., Engel, R., Hofmann-Kiefer, K., McCulloch, C., Ptok, U., Heun, R., Andreasen, N., DeBarnardis, J., Kerkman, D., Moeller, H, J., Davies, P., & Hampel, H. (2002). CSF tau protein phosphorylated at threonine 231 correlates with cognitive decline in MCI subjects. *Neurology*, 59, 627-629.

Campos-Peña, V., & Meraz-Ríos, M. A. (2014). Alzheimer Disease: The Role of Aβ in the Glutamatergic System, Neurochemistry, Dr. Thomas Heinbockel (Ed.), ISBN: 978-953-51-1237-2, InTech, DOI: 10.5772/57367. Available from: http://www.intechopen.com/books/neurochemistry/alzheimer-disease-the-role-of-a-in-the-glutamatergic-system

Chang, H. I., & Yeh, M. K. (2012). Clinical development of liposome-based drugs: formulation, characterization, and therapeutic efficacy. *Int J Nanomedicine*, 7, 49-60.

Chiti, F., Webster, P., Taddei, N., Clark, A., Stefani, M., Ramponi, G., & Dobson, C. M. (1999). Designing conditions for in vitro formation of amyloid protofilaments and fibrils. *Proc Natl Acad Sci USA*, 96, 3590-3594.

Cirrito, J. R., Yamada, K. A., Finn, M. B., Sloviter, R. S., Bales, K. R., May, P. C., Schoepp, D. D., Paul, S. M., Mennerick, S., & Holtzman, D. M. (2005). Synaptic activity regulates interstitial fluid amyloid-β levels in vivo. *Neuron*, 48, 913-922.

Courtney, C., Farrell, D., Gray, R. A. C. G., Hills, R., Lynch, L., Sellwood, E., Edwards, S., Hardyman, W., Raftery, J., Crome, P., Lendon, C., Shaw, H., & Bentham, P. (2004). Long-term donepezil treatment in 565 patients with Alzheimer's disease (AD2000): randomised double-blind trial. *Lancet*, 363, 2105-2115.

Deane, R., Wu, Z., Sagare, A., Davis, J., Du Yan, S., Hamm, K., Xu, F., Parisi, M., LaRue, B., Hu, H. W., Spijkers, P., Guo, H., Song, X., Lenting, P. J., Van Nostrand, W. E., & Zlokovic, B. V. (2004). LRP/amyloid β-peptide interaction mediates differential brain efflux of Aβ isoforms. *Neuron*, 43, 333-344.

Deane, R., Du Yan, S., Submamaryan, R. K., LaRue, B., Jovanovic, S., Hogg, E., Welch, D., Manness, L., Lin, C., Yu, J., Zhu, H., Ghiso, J., Frangione, B., Stern, A., Schmidt, A. M., Armstrong, D. L., Arnold, B., Liliensiek, B., Nawroth, P., Hofman, F., Kindy, M., Stern, D., & Zlokovic, B. (2003). RAGE mediates amyloid-β peptide transport across the blood-brain barrier and accumulation in brain. *Nat Med*, 9, 907-913.

De Strooper, B., Annaert, W., Cupers, P., Saftig, P., Craessaerts, K., Mumm, J. S., Schroeter, E. H., Chrijvers, V., Wolfe, M. S., Ray, W. J., Goate, A. & Kopan, R. (1999). A presenilin-1-dependent γ-secretase-like protease mediates release of Notch intracellular domain. *Nature*, 398, 518-522.

Döbeli, H., Draeger, N., Huber, G., Jakob, P., Schmidt, D., Seilheimer, B., Stüber, D., Wipf, B., & Zulauf, M. (1995). A biotechnological method provides access to aggregation competent monomeric Alzheimer's 1–42 residue amyloid peptide. *Nat Biotechnol*, 13, 988-993.

Drubin, D*., Kirschner, M.,* (*1986*). Tau protein function in living cells*. J Cell Biol,* 103, 2739–2746*.

Du Yan, S., Chen, X., Fu, J., Chen, M., Zhu, H., Roher, A., Slattery, T., Zhao, L., Nagashima, M., Morser, J., Migheli, A., Nawroth, P., Stern, D., & Schmidt, A. M. (1996). RAGE and amyloid-β peptide neurotoxicity in Alzheimer's disease. *Nature*, 382, 685-691.

Eckerström, C., Olsson, E., Bjerke, M., Malmgren, H., Edman, Å., Wallin, A., & Nordlund, A. (2013). A combination of neuropsychological, neuroimaging, and cerebrospinal fluid markers predicts conversion from mild cognitive impairment to dementia. *J Alzheimers Dis*, 36, 421-431.

Farlow, M., Anand, R., Messina Jr, J., Hartman, R., & Veach, J. (2000). A 52-week study of the efficacy of rivastigmine in patients with mild to moderately severe Alzheimer's disease. *Eur Neurol*, 44, 236-241.

Finder, V. H., Vodopivec, I., Nitsch, R. M., & Glockshuber, R. (2010). The recombinant amyloid-β peptide Aβ1–42 aggregates faster and is more neurotoxic than synthetic Aβ1–42. *J Mol Biol*, 396, 9-18.

Frankel, A. D., & Pabo, C. O. (1988). Cellular uptake of the tat protein from human immunodeficiency virus. *Cell*, 55, 1189-1193.

Frankiewicz, T., & Parsons, C. G. (1999). Memantine restores long term potentiation impaired by tonic N-methyl-d-aspartate (NMDA) receptor activation following reduction of Mg2+ In hippocampal slices. *Neuropharmacology*, 38, 1253-1259.

Fukumoto, H., Cheung, B. S., Hyman, B. T., & Irizarry, M. C. (2002). β-Secretase protein and activity are increased in the neocortex in Alzheimer disease. *Arch Neurol*, 59, 1381-1389.

Gauthier, S., Loft, H., & Cummings, J. (2008). Improvement in behavioural symptoms in patients with moderate to severe Alzheimer's disease by memantine: a pooled data analysis. *Int J Geriatr Psychiatry*, 23, 537-545.

Ghiso, J., & Frangione, B. (2002). Amyloidosis and Alzheimer's disease. *Adv Drug Deliv Rev*, 54, 1539-1551.

Giacobini, E. (2000). Cholinesterase inhibitors stabilize Alzheimer's disease. *Ann N Y Acad Sci*, 920, 321-327.

Glenner, G. G., & Wong, C. W. (1984). Alzheimer's disease: initial report of the purification and characterization of a novel cerebrovascular amyloid protein. *Biochem Biophys Res Commun*, 120, 885-890.

Goldgaber, D., Lerman, M. I., McBride, O. W., Saffiotti, U., & Gajdusek, D. C. (1987). Characterization and chromosomal localization of a cDNA encoding brain amyloid of Alzheimer's disease. *Science*, 235, 877-880.

Goldwasser, A. N., Auerbach, S. M., & Harkins, S. W. (1987). Cognitive, affective, and behavioral effects of reminiscence group therapy on demented elderly. *Int J Aging Hum Dev*, 25, 209-222.

Gunawardena, S., & Goldstein, L. S. (2001). Disruption of Axonal Transport and Neuronal Viability by Amyloid Precursor Protein Mutations in Drosophila. *Neuron*, 32, 389-401.

Haass, C., & Selkoe, D. J. (2007). Soluble protein oligomers in neurodegeneration: lessons from the Alzheimer's amyloid β-peptide. *Nat Rev Mol Cell Biol*, 8, 101-112.

Hane, F., & Leonenko, Z. (2014). Effect of Metals on Kinetic Pathways of Amyloid-β Aggregation. *Biomolecules*, 4, 101-116.

Hardingham, G. E., Fukunaga, Y., & Bading, H. (2002). Extrasynaptic NMDARs oppose synaptic NMDARs by triggering CREB shut-off and cell death pathways. *Nat Neurosci*, 5, 405-414.

Hardy, J., & Allsop, D. (1991). Amyloid deposition as the central event in the aetiology of Alzheimer's disease. *Trends Pharmacol Sci*, 12, 383-388.

Hebert, L. E., Weuve, J., Scherr, P. A., & Evans, D. A. (2013). Alzheimer disease in the United States (2010–2050) estimated using the 2010 census. *Neurology*, 80, 1778-1783.

Hemming, M. L., Elias, J. E., Gygi, S. P., & Selkoe, D. J. (2009). Identification of β-secretase (BACE1) substrates using quantitative proteomics. *PloS One*, 4, 8477.

Hoey, S. E., Williams, R. J., & Perkinton, M. S. (2009). Synaptic NMDA receptor activation stimulates α-secretase amyloid precursor protein processing and inhibits amyloid-β production. *J Neurosci*, 29, 4442-4460.

Holmes, C., Boche, D., Wilkinson, D., Yadegarfar, G., Hopkins, V., Bayer, A., Jones, R. W., Bullock, R., Love, S., Neal, J. W., Zotova, E., & Nicoll, J. A. (2008). Long-term effects of Aβ1-42 immunisation in Alzheimer's disease: follow-up of a randomised, placebo-controlled phase I trial. *Lancet*, 372, 216-223.

Huang, X., Atwood, C. S., Hartshorn, M. A., Multhaup, G., Goldstein, L. E., Scarpa, R. C., Cuajungco, M. P., Gray, D. N., Lim, J., Moir, R. D., Tanzi, R. E., & Bush, A. I. (1999). The Aβ peptide of Alzheimer's disease directly produces hydrogen peroxide through metal ion reduction. *Biochemistry*, 38, 7609-7616.

Immordino, M. L., Dosio, F., & Cattel, L. (2006). Stealth liposomes: review of the basic science, rationale, and clinical applications, existing and potential. *Int J Nanomedicine*, 1, 297-315.

Ince, P. G. (2001). Pathological correlates of late-onset dementia in a multicentre community-based population in England and Wales. *Lancet*, 357, 169–175.

Ivanov, A., Pellegrino, C., Rama, S., Dumalska, I., Salyha, Y., Ben-Ari, Y., & Medina, I. (2006). Opposing role of synaptic and extrasynaptic NMDA receptors in regulation of the extracellular signal-regulated kinases (ERK) activity in cultured rat hippocampal neurons. *J Physiol*, 572, 789-798.

Iwata, A., & Iwatsubo, T. (2013). Disease-modifying therapy for Alzheimer's disease: Challenges and hopes. *Neurol Clin Neurosci*, 1, 49-54.

Jimenez, S., Torres, M., Vizuete, M., Sanchez-Varo, R., Sanchez-Mejias, E., Trujillo-Estrada, L., Carmona-Cuenca, I., Caballero, C., Ruano, D., Gutierrez, A., & Vitorica, J. (2011). Age-dependent accumulation of soluble amyloid β (Aβ) oligomers reverses the neuroprotective effect of soluble amyloid precursor protein-α (sAPPα) by modulating phosphatidylinositol 3-kinase (PI3K)/Akt-GSK-3β pathway in Alzheimer mouse model. *J Biol Chem*, 286, 18414-18425.

Johnson, J. W., & Kotermanski, S. E. (2006). Mechanism of action of memantine. *Curr Opin Pharmacol*, 6, 61-67.

Judd, N. (2007). The Journal of Quality Research in Dementia, Issue 4.

Kamenetz, F., Tomita, T., Hsieh, H., Seabrook, G., Borchelt, D., Iwatsubo, T., Sisodia, S., & Malinow, R. (2003). APP processing and synaptic function. *Neuron*, 37, 925-937.

Kang, J., Lemaire, H. G., Unterbeck, A., Salbaum, J. M., Masters, C. L., Grzeschik, K. H., Multhaup, G., Beyreuther, K., & Müller-Hill, B. (1987). The precursor of Alzheimer's disease amyloid A4 protein resembles a cell-surface receptor. Nature, 325, 733-736.

Kasuga, K., Shimohata, T., Nishimura, A., Shiga, A., Mizuguchi, T., Tokunaga, J., Ohno, T., Miyashita, A., Kuwano, R., Matsumoto, N., Onodera, O., Nishizawa, M., & Ikeuchi, T. (2009). Identification of independent APP locus duplication in Japanese patients with early-onset Alzheimer disease. *J Neurol, Neurosurg Psychiatry*, 80, 1050-1052.

Kimberly, W. T., LaVoie, M. J., Ostaszewski, B. L., Ye, W., Wolfe, M. S., & Selkoe, D. J. (2003). γ-Secretase is a membrane protein complex comprised of presenilin, nicastrin, aph-1, and pen-2. *Proc Natl Acad Sci USA*, 100, 6382-6387.

Kitaguchi, N., Takahashi, Y., Tokushima, Y., Shiojiri, S., & Ito, H. (1988). Novel precursor of Alzheimer's disease amyloid protein shows protease inhibitory activity. *Nature*, 331, 530-532.

Kittner, S. J., White, L. R., Farmer, M. E., Wolz, M., Kaplan, E., Moes, E., Brody, J. A., & Feinleib, M. (1986). Methodological issues in screening for dementia: the problem of education adjustment. *J Chronic Dis*, 39, 163-170.

Klaver, D. W., Wilce, M. C., Cui, H., Hung, A. C., Gasperini, R., Foa, L., & Small, D. H. (2010). Is BACE1 a suitable therapeutic target for the treatment of Alzheimer's disease? Current strategies and future directions. *Biol Chem*, 391, 849-859.

Klunk, W. E., Engler, H., Nordberg, A., Wang, Y., Blomqvist, G., Holt, D. P., Bergström, M., Savicheva, I., Huang, G. F., Estrada, S., Ausen, B., Debnath, M. L., Barletta, J., Price, J. C., Sandell, J., Lopresti, B. J., Wall, A., Kovisto, P., Antoni, G., Mathis, C. A., & Långström, B. (2004). Imaging brain amyloid in Alzheimer's disease with Pittsburgh Compound-B. *Ann Neurol*, 55, 306-319.

Klyubin, I., Walsh, D. M., Lemere, C. A., Cullen, W. K., Shankar, G. M., Betts, V., Spooner, E. T., Jiang, L., Anwyl, R., Selkoe, D. J., & Rowan, M. J. (2005). Amyloid β protein immunotherapy neutralizes Aβ oligomers that disrupt synaptic plasticity in vivo. *Nat Med*, 11, 556-561.

Kondo, J., Honda, T., Mori, H., Hamada,Y., Miura, R., Ogawara, M., Ihara, Y. (1988). The carboxyl third of tau is tightly bound to paired helical filaments. *Neuron,* 1, 827–834.

Kontush, A. (2001). Amyloid-β: an antioxidant that becomes a pro-oxidant and critically contributes to Alzheimer's disease. *Free Radic Biol Med*, 31, 1120-1131.

Lamb, B. T., Sisodia, S. S., Lawler, A. M., Slunt, H. H., Kitt, C. A., Kearns, W. G., Pearson, P. L., Price, D. L., & Gearhart, J. D. (1993). Introduction and expression of the 400 kilobase precursor amyloid protein gene in transgenic mice. *Nat Genet*, 5, 22-30.

Lanctôt, K. L., Rajaram, R. D., & Herrmann, N. (2009). Review: Therapy for Alzheimer's disease: how effective are current treatments?. *Ther Adv Neurol Disord*, 2, 163-180.

Lasner, C. J., & Lee, J. M. (1998). Pharmacological drug treatment of Alzheimer disease: the cholinergic hypothesis revisited. *J Neuropathol Exp Neurol*, 57, 719-731.

Lautenschlager, N. T., Riemenschneider, M., Drzezga, A., & Kurz, A. F. (2001). Primary degenerative mild cognitive impairment: study population, clinical, brain imaging and biochemical findings. *Dement Geriatr Cogn Disord*, 12, 379-386.

Lazo, N. D., Grant, M. A., Condron, M. C., Rigby, A. C., & Teplow, D. B. (2005). On the nucleation of amyloid β-protein monomer folding. *Protein Sci*, 14, 1581-1596.

Lee, V. M. Y., Balin, B. J., Otvos, L., Trojanowski. J. Q. (1991). A68: a major subunit of paired helical filaments and derivatized forms of normal tau. *Science*, 251, 675–678

Li, L., Sengupta, A., Haque, N., Grundke-Iqbal, I., & Iqbal, K. (2004). Memantine inhibits and reverses the Alzheimer type abnormal hyperphosphorylation of tau and associated neurodegeneration. *FEBS Lett*, 566, 261-269.

Liu, Y., Walter, S., Stagi, M., Cherny, D., Letiembre, M., Schulz-Schaeffer, W., Heine, H., Penke, B., Neumann, H., & Fassbender, K. (2005). LPS receptor (CD14): a receptor for phagocytosis of Alzheimer's amyloid peptide. *Brain*, 128, 1778-1789.

Liu-Seifert, H., Siemers, E., Holdridge, K. C., Andersen, S. W., Lipkovich, I., Carlson, C., Sethuraman, G., Hoog, S., Hayduk, R., Doody, R., & Aisen, P. (2015). Delayed start analysis: mild Alzheimer's disease patients in solanezumab trials, 3.5 years. *Alzheimers Dement TRCI*.

Mackic, J. B., Stins, M., McComb, J. G., Calero, M., Ghiso, J., Kim, K. S., Yan, S. D., Stern, D., Schmidt, A. M., Frangione, B., & Zlokovic, B. V. (1998). Human blood-brain barrier receptors for Alzheimer's amyloid-beta 1-40. Asymmetrical binding, endocytosis, and transcytosis at the apical side of brain microvascular endothelial cell monolayer. *J Clin Invest*, 102, 734-743.

Maher, S., & Brayden, D. J. (2012). Overcoming poor permeability: translating permeation enhancers for oral peptide delivery. *Drug Discov Today Technol*, 9, 113-119.

Mandelkow, E., Von Bergen, M., Biernat, J., & Mandelkow, E. M. (2007). Structural principles of tau and the paired helical filaments of Alzheimer's disease. *Brain Pathol*, 17, 83-90.

Masliah, E., Mallory, M., Hansen, L., Alford, M., Albright, T., Terry, R., Shapiro, P., Sundsmo, M., & Saitoh, T. (1991). Immunoreactivity of CD45, a protein phosphotyrosine phosphatase, in Alzheimer's disease. *Acta Neuropathol*, 83, 12-20.

Masters, C. L., Simms, G., Weinman, N. A., Multhaup, G., McDonald, B. L., & Beyreuther, K. (1985). Amyloid plaque core protein in Alzheimer disease and Down syndrome. *Proc Natl Acad Sci USA,* 82, 4245-4249.

Mattson, M. P., Cheng, B., Culwell, A. R., Esch, F. S., Lieberburg, I., & Rydel, R. E. (1993). Evidence for excitoprotective and intraneuronal calcium-regulating roles for secreted forms of the β-amyloid precursor protein. *Neuron*, 10, 243-254.

Mayes, J., Tinker-Mill, C., Kolosov, O., Zhang, H., Tabner, B. J., & Allsop, D. (2014). β-Amyloid Fibrils in Alzheimer Disease Are Not Inert When Bound to Copper Ions but Can Degrade Hydrogen Peroxide and Generate Reactive Oxygen Species. *J Biol Chem*, 289, 12052-12062.

McLean, C. A., Cherny, R. A., Fraser, F. W., Fuller, S. J., Smith, M. J., Beyreuther, K. V., Bush, A. I., & Masters, C. L. (1999). Soluble pool of Aβ amyloid as a determinant of severity of neurodegeneration in Alzheimer's disease. *Ann Neurol*, 46, 860-866.

McClean, P. L., & Hölscher, C. (2014a). Lixisenatide, a drug developed to treat type 2 diabetes, shows neuroprotective effects in a mouse model of Alzheimer's disease. *Neuropharmacology*, 86, 241-258.

McClean, P. L., & Hölscher, C. (2014b). Liraglutide can reverse memory impairment, synaptic loss and reduce plaque load in aged APP/PS1 mice, a model of Alzheimer's disease. *Neuropharmacology*, 76, 57-67.

Metcalfe, M. J., & Figueiredo-Pereira, M. E. (2010). Relationship between tau pathology and neuroinflammation in Alzheimer's disease. *Mt Sinai J Med,* 77, 50-58.

Morgan, D., Diamond, D. M., Gottschall, P. E., Ugen, K. E., Dickey, C., Hardy, J., Duff, K., Jantzen, P., DiCarlo, G., Wilcock, D., Connor, K., Hatcher, J., Hope, C., Gordon, M., & Arendash, G. W. (2000). Aβ peptide vaccination prevents memory loss in an animal model of Alzheimer's disease. *Nature*, 408, 982-985.

Morris, J. C. (2004). Early-stage and preclinical Alzheimer disease. *Alzheimer Dis Assoc Disord*, 19, 163-165.

Nagele, R. G., D'andrea, M. R., Anderson, W. J., & Wang, H. Y. (2002). Intracellular accumulation of β-amyloid 1–42 in neurons is facilitated by the α7 nicotinic acetylcholine receptor in Alzheimer's disease. *Neuroscience*, 110, 199-211.

Nalivaeva, N. N., Beckett, C., Belyaev, N. D., & Turner, A. J. (2012). Are amyloid-degrading enzymes viable therapeutic targets in Alzheimer's disease?. *J Neurochem*, 120, 167-185.

Oddo, S., Caccamo, A., Shepherd, J. D., Murphy, M. P., Golde, T. E., Kayed, R., Metherate, R., Mattson, M, P., Akbari, Y., & LaFerla, F. M. (2003). Triple-transgenic model of Alzheimer's disease with plaques and tangles: intracellular Aβ and synaptic dysfunction. *Neuron*, 39, 409-421.

Palop, J. J., & Mucke, L. (2010). Amyloid-[beta]-induced neuronal dysfunction in Alzheimer's disease: from synapses toward neural networks. *Nat Neurosci*, 13, 812-818.

Parsons, C. G., Danysz, W., & Quack, G. (1999). Memantine is a clinically well tolerated N-methyl-d-aspartate (NMDA) receptor antagonist—a review of preclinical data. *Neuropharmacology*, 38, 735-767.

Parthsarathy, V., McClean, P. L., Hölscher, C., Taylor, M., Tinker, C., Jones, G., Kolosov, O., Salvati, E., Gregori, M., Masserini, M., & Allsop, D. (2013). A novel retro-inverso peptide inhibitor reduces amyloid deposition, oxidation and inflammation and stimulates neurogenesis in the APPswe/PS1ΔE9 mouse model of Alzheimer's disease. *PloS One*, 8, e54769.

Patel, S. S. (2006). Liposome: A versatile platform for targeted delivery of drugs. *Pharmainfo.net*, 4, 1-5.

Pedersen, J. T., Østergaard, J., Rozlosnik, N., Gammelgaard, B., & Heegaard, N. H. (2011). Cu (II) mediates kinetically distinct, non-amyloidogenic aggregation of amyloid-β peptides. *J Biol Chem,* 286, 26952-26963.

Petersen, R. C. (2004). Mild cognitive impairment as a diagnostic entity. *J Intern Med*, 256, 183-194.

Pimentel, C., Batista-Nascimento, L., Rodrigues-Pousada, C., & Menezes, R. A. (2012). Oxidative stress in Alzheimer's and Parkinson's diseases: insights from the yeast Saccharomyces cerevisiae. *Oxid Med Cell Longev*, 132146.

Ponte, P., DeWhitt, P. G., Schilling, J., Miller, J., Hsu, D., Greenberg, B., Davis, K., Wallace, W., Lieberburg, I., Fuller, F., & Cordell, B. (1988). A new A4 amyloid mRNA contains a domain homologous to serine proteinase inhibitors. *Nature*, 331, 525-527.

Qahwash, I., Weiland, K. L., Lu, Y., Sarver, R. W., Kletzien, R. F., & Yan, R. (2003). Identification of a mutant amyloid peptide that predominantly forms neurotoxic protofibrillar aggregates. *J Biol Chem*, 278, 23187-23195.

Riemenschneider, M., Lautenschlager, N., Wagenpfeil, S., Diehl, J., Drzezga, A., & Kurz, A. (2002). Cerebrospinal fluid tau and β-amyloid 42 proteins identify Alzheimer disease in subjects with mild cognitive impairment. *Arch Neurol*, 59, 1729-1734.

Sakono, M., & Zako, T. (2010). Amyloid oligomers: formation and toxicity of Aβ oligomers. *FEBS J,* 277, 1348-1358.

Schenk, D., Barbour, R., Dunn, W., Gordon, G., Grajeda, H., Guido, T., Hu, K., Huang, J., Johnson-Wood, K., Khan, K., Kholodenko, D., Lee, M., Liao, Z., Lieberburg, I., Motter, R., Mutter, L., Soriano, F., Shopp, G., Vasquez, N., Vandevert, C., Walker, S., Wogulis, M., Yednock, T., Games, D., & Seubert, P. (1999). Immunization with amyloid-β attenuates Alzheimer-disease-like pathology in the PDAPP mouse. *Nature*, 400, 173-177.

Schenk, D. (2002). Amyloid-β immunotherapy for Alzheimer's disease: the end of the beginning. *Nat Rev Neurosci,* 3, 824-828.

Schnabel, J. (2011). Amyloid: little proteins, big clues*. Nature,* 475, S12-S14.

Schofield, P. W., Logroscino, G., Andrews, H. F., Albert, S., & Stern, Y. (1997). An association between head circumference and Alzheimer's disease in a population-based study of aging and dementia. *Neurology*, 49, 30-37.

Selkoe, D. J., Bell, D. S., Podlisny, M. B., Price, D. L., & Cork, L. C. (1987). Conservation of brain amyloid proteins in aged mammals and humans with Alzheimer's disease. *Science*, 235, 873-877.

Selkoe, D. J. (1998). The cell biology of β-amyloid precursor protein and presenilin in Alzheimer's disease. *Trends Cell Biol*, 8, 447-453.

Selkoe, D. J. (2001). Alzheimer's disease: genes, proteins, and therapy. *Physiol Reviews,* 81, 741-766.

Seubert, P., Oltersdorf, T., Lee, M. G., Barbour, R., Blomquist, C., Davis, D. L., Bryant, K., Fritz, L. C., Galasko, D., Thal, L. J., Leiberburg, I., & Schenk, D. B. (1993). Secretion of β-amyloid precursor protein cleaved at the amino terminus of the β-amyloid peptide. *Nature*, 361, 260-263.

Shah, R. S., Lee, H. G., Xiongwei, Z., Perry, G., Smith, M. A., & Castellani, R. J. (2008). Current approaches in the treatment of Alzheimer's disease. *Biomed Pharmacother*, 62, 199-207.

Shankar, G. M., Bloodgood, B. L., Townsend, M., Walsh, D. M., Selkoe, D. J., & Sabatini, B. L. (2007). Natural oligomers of the Alzheimer amyloid-β protein induce reversible synapse loss by modulating an NMDA-type glutamate receptor-dependent signaling pathway. *J Neurosci*, 27, 2866-2875.

Shibata, M., Yamada, S., Kumar, S. R., Calero, M., Bading, J., Frangione, B., Holtzman, D. M., Miller, C. A., Strickland, D. K., Ghiso, J., & Zlokovic, B. V. (2000). Clearance of Alzheimer's amyloid-β1-40 peptide from brain by LDL receptor–related protein-1 at the blood-brain barrier. *J Clin Invest*, 106, 1489-1499.

Silverberg, G. D., Mayo, M., Saul, T., Rubenstein, E., & McGuire, D. (2003). Alzheimer's disease, normal-pressure hydrocephalus, and senescent changes in CSF circulatory physiology: a hypothesis. *Lancet Neurol*, 2, 506-511.

Sinha, S., Anderson, J. P., Barbour, R., Basi, G. S., Caccavello, R., Davis, D., Doan, M., Dovey, H. F., Frigon, N., Hong, J., Jacobson-Croak, K., Jewett, N., Keim, P., Knops, J., Lieberburg, I., Power, M., Tan, H., Tatsuno, G., Tung, J., Schenk, D., Seubert, P., Suomensaari, S. M., Wang, S., Walker, D., Zhao, J., McConlogue, L., & John, V. (1999). Purification and cloning of amyloid precursor protein β-secretase from human brain. *Nature*, 402, 537-540.

Sisodia, S. S., & Price, D. L. (1995). Role of the beta-amyloid protein in Alzheimer's disease. *FASEB J,* 9, 366-370.

Sloboda, R. D., Rudolph, S. A., Rosenbaum, J. L., Greengard, P. (1975). Cyclic AMP-dependent endogenous phosphorylation of a microtubule-associated protein.*Proc Natl Acad Sci USA,* 72, 177-181*.*

Small, D. H., Nurcombe, V., Reed, G., Clarris, H., Moir, R., Beyreuther, K., & Masters, C. L. (1994). A heparin-binding domain in the amyloid protein precursor of Alzheimer's disease is involved in the regulation of neurite outgrowth. *J Neurosci*, 14, 2117-2127.

Smolarkiewicz, M., Skrzypczak, T., & Wojtaszek, P. (2013). The very many faces of presenilins and the γ-secretase complex. *Protoplasma*, 250, 997-1011.

Snyder, E. M., Nong, Y., Almeida, C. G., Paul, S., Moran, T., Choi, E. Y., Nairn, A. C., Salter, M. W., Lombroso, P. J., Gouras, G. K., & Greengard, P. (2005). Regulation of NMDA receptor trafficking by amyloid-β. *Nat Neurosci*, 8, 1051-1058.

Soto, C., Castaño, E. M., Kumar, R. A., Beavis, R. C., & Frangione, B. (1995). Fibrillogenesis of synthetic amyloid-β peptides is dependent on their initial secondary structure. *Neurosci Lett*, 200, 105-108.

Soto, C. (2003). Unfolding the role of protein misfolding in neurodegenerative diseases. *Nat Rev Neurosci,* 4, 49-60.

Sperling, R. A., Aisen, P. S., Beckett, L. A., Bennett, D. A., Craft, S., Fagan, A. M., Iwatsubo, T., Jack, . R., Kaye, J., Montine, T. J., Park, D. C., Reiman, E. M., Rowe, C. C., Seimers, E., Stern, Y., Yaffe, K., Carrillo, M. C., Thies, B., Morrison-Bogorad, M., Wagster, M. V., & Phelps, C. H. (2011). Toward defining the preclinical stages of Alzheimer's disease: Recommendations from the National Institute on Aging-Alzheimer's Association workgroups on diagnostic guidelines for Alzheimer's disease. *Alzheimers Dement*, 7, 280-292.

Stelzmann, R. A., Norman Schnitzlein, H., & Reed Murtagh, F. (1995). An English translation of Alzheimer's 1907 paper,"Über eine eigenartige Erkankung der Hirnrinde". *Clin Anat*, 8, 429-431.

Stern, Y., Gurland, B., Tatemichi, T. K., Tang, M. X., Wilder, D., & Mayeux, R. (1994). Influence of Education and Occupation on the Incidence of Alzheimer's Disease. *JAMA*, 271, 1004-1010.

Stern, Y. (2012). Cognitive reserve in ageing and Alzheimer's disease. *Lancet Neurol*, 11, 1006-1012.

Stratman, N. C., Castle, C. K., Taylor, B. M., Epps, D. E., Melchior, G. W., & Carter, D. B. (2005). Isoform-specific interactions of human apolipoprotein E to an intermediate conformation of human Alzheimer amyloid-beta peptide. *Chem Phys Lipids*, 137, 52-61.

Tanzi, R. E., Moir, R. D., & Wagner, S. L. (2004). Clearance of Alzheimer's Aβ peptide: the many roads to perdition. *Neuron*, 43, 605-608.

Tanzi, R. E., & Bertram, L. (2005). Twenty years of the Alzheimer's disease amyloid hypothesis: a genetic perspective. *Cell*, 120, 545-555.

Tayeb, H. O., Yang, H. D., Price, B. H., & Tarazi, F. I. (2012). Pharmacotherapies for Alzheimer's disease: beyond cholinesterase inhibitors. *Pharmacol Ther*, 134, 8-25.

Taylor, M., Moore, S., Mayes, J., Parkin, E., Beeg, M., Canovi, M., Gobbi, M., Mann, D. M. A., & Allsop, D. (2010). Development of a proteolytically stable retro-inverso peptide inhibitor of β-amyloid oligomerization as a potential novel treatment for Alzheimer's disease. *Biochemistry*, 49, 3261-3272.

Thies, W., & Bleiler, L. (2013). 2013 Alzheimer's disease facts and figures. *Alzheimers Dement*, 9, 208-245.

Tjernberg, L. O., Näslund, J., Lindqvist, F., Johansson, J., Karlström, A. R., Thyberg, J., Terenius, L., & Nordstedt, C. (1996). Arrest of-amyloid fibril formation by a pentapeptide ligand. *Journal of Biological Chemistry*, 271, 8545-8548.

Tjernberg, L. O., Callaway, D. J., Tjernberg, A., Hahne, S., Lilliehöök, C., Terenius, L., Thyberg, J., & Nordstedt, C. (1999). A molecular model of Alzheimer amyloid β-peptide fibril formation. *J Biol Chem*, 274, 12619-12625.

Tycko, R. (2004). Progress towards a molecular-level structural understanding of amyloid fibrils. *Curr Opin Struct Biol*, 14, 96-103.

Vassar, R., Kovacs, D. M., Yan, R., & Wong, P. C. (2009). The β-secretase enzyme BACE in health and Alzheimer's disease: regulation, cell biology, function, and therapeutic potential. *J Neurosci*, 29, 12787-12794.

Walsh, D. M., Klyubin, I., Fadeeva, J. V., Cullen, W. K., Anwyl, R., Wolfe, M. S., Rowan, M. J., & Selkoe, D. J. (2002). Naturally secreted oligomers of amyloid β protein potently inhibit hippocampal long-term potentiation in vivo. *Nature*, 416, 535-539.

Walsh, D. M., & Selkoe, D. J. (2007). Aβ oligomers–a decade of discovery. *J Neurochem*, 101, 1172-1184.

Wan, X. Z., Li, B., Li, Y. C., Yang, X. L., Zhang, W., Zhong, L., & Tang, S. J. (2012). Activation of NMDA receptors upregulates a disintegrin and metalloproteinase 10 via a Wnt/MAPK signaling pathway. *J Neurosci*, 32, 3910-3916.

Wang, H. Y., Li, W., Benedetti, N. J., & Lee, D. H. (2003). α7 nicotinic acetylcholine receptors mediate β-amyloid peptide-induced tau protein phosphorylation. *J Biol Chem*, 278, 31547-31553.

Wang, H. Y., Bakshi, K., Shen, C., Frankfurt, M., Trocmé-Thibierge, C., & Morain, P. (2010). S 24795 Limits β-Amyloid–α7 Nicotinic Receptor Interaction and Reduces Alzheimer's Disease-Like Pathologies. *Biol Psychiatry*, 67, 522-530.

Wang, Z. C., Zhao, J., & Li, S. (2013). Dysregulation of synaptic and extrasynaptic N-methyl-D-aspartate receptors induced by amyloid-β. *Neurosci Bull*, 29, 752-760.

Webster, S. J., Bachstetter, A. D., Nelson, P. T., Schmitt, F. A., & Van Eldik, L. J. (2014). Using mice to model Alzheimer's dementia: an overview of the clinical disease and the preclinical behavioral changes in 10 mouse models. *Front Genet*, 5, 88.

Wei, B., Wei, Y., Zhang, K., Wang, J., Xu, R., Zhan, S., Lin, G., Wang, W., Liu, M., Wang, L. and Zhang, R., (2009). Development of an antisense RNA delivery system using conjugates of the MS2 bacteriophage capsids and HIV-1 TAT cell penetrating peptide. *Biomed Pharmacother*, *63*, 313-318.

Weingarten, M. D., Lockwood, A. H., Hwo, S. Y., & Kirschner, M. W. (1975). A protein factor essential for microtubule assembly. *Proc Natl Acad Sci USA*, 72, 1858-1862.

Welden, S., & Yesavage, J. A. (1982). Behavioral improvement with relaxation training in senile dementia. *Clin Gerontol*, 1, 45-49.

Westermark, P., Andersson, A., & Westermark, G. T. (2011). Islet amyloid polypeptide, islet amyloid, and diabetes mellitus. *Physiol Rev*, 91, 795-826.

Winblad, B., Jones, R. W., Wirth, Y., Stöffler, A., & Möbius, H. J. (2007). Memantine in moderate to severe Alzheimer's disease: a meta-analysis of randomised clinical trials. *Dement Geriatr Cogn Disord*, 24, 20-27.

Wolfe, M. S. (2008). Inhibition and modulation of γ-secretase for Alzheimer's disease. *Neurotherapeutics,* 5, 391-398.

Xu, R., Feng, X., Xie, X., Zhang, J., Wu, D. and Xu, L. (2012). HIV-1 Tat protein increases the permeability of brain endothelial cells by both inhibiting occludin expression and cleaving occludin via matrix metalloproteinase-9. *Brain Res*, *1436*, 13-19.

Yan, Z., & Feng, J. (2004). Alzheimer's disease: interactions between cholinergic functions and β-amyloid. *Curr Alzheimer Res*, 1, 241-248.

Yiannopoulou, K. G., & Papageorgiou, S. G. (2013). Current and future treatments for Alzheimer's disease. *Ther Adv Neurol Disord*, 6, 19-33.

Zec, R. F., & Burkett, N. R. (2008). Non-pharmacological and pharmacological treatment of the cognitive and behavioral symptoms of Alzheimer disease. *NeuroRehabilitation*, 23, 425-438.

Zhao, Y., & Zhao, B. (2013). Oxidative stress and the pathogenesis of Alzheimer's disease. *Oxid Med Cell Longev*, 316523.

Zhang, M., Katzman, R., Salmon, D., Jin, H., Cai, G., Wang, Z., Qu, G., Grant, I., Yu, E., Levy, P., Klauber, M. R., & Liu, W. T. (1990). The prevalence of dementia and Alzheimer's disease in Shanghai, China: impact of age, gender, and education. *Ann Neurol*, 27, 428-437.

Zhang, L., Song, J., Newhouse, Y., Zhang, S., Weisgraber, K. H., & Ren, G. (2010). An optimized negative-staining protocol of electron microscopy for apoE4• POPC lipoprotein. *J Lipid Res,* 51, 1228-1236.

Ziegler, A., & Seelig, J. (2004). Interaction of the protein transduction domain of HIV-1 TAT with heparan sulfate: binding mechanism and thermodynamic parameters. *Biophys J*, 86, 254-263.

Zlokovic, B. V. (2004). Clearing amyloid through the blood–brain barrier. *J Neurochem,* 89, 807-811.